

# CO-Sources for the Liberation of Cellular Messenger Molecules

## Dissertation

Zur Erlangung des akademischen Grades doctor rerum naturalium  
(Dr. rer. nat.)



---

seit 1558

vorgelegt dem Rat der Chemisch-Geowissenschaftlichen Fakultät  
der Friedrich-Schiller-Universität Jena

von Master-Chem. Taghreed Jazzazi  
geboren am 16.07.1985  
in Amman/Jordan

1. Gutachter: Prof. Dr. Matthias Westerhausen, FSU Jena  
2. Gutachter: Prof. Dr. Rainer Beckert, FSU Jena  
Tag der öffentlichen Verteidigung: 12. June 2013

# ***DEDICATIONS***

***To***

***Candles of my life, my husband***

***Father and Mother***

***My Brother and Sisters***

***All my Family***

***With Love***

# Table of Contents

Dedication.....	i
Table of Contents.....	ii
List of Figures.....	v
List of Schemes.....	ix
List of Tables.....	xi

## Chapter One

<b>1. Introduction</b>	<b>1</b>
1.1 Carbon monoxide (CO).....	1
1.2 Carbonyl chemistry .....	2
1.2.1 Metal carbonyl complexes .....	2
1.2.2 Preparation of metal carbonyl complexes .....	4
1.2.3 Reaction of metal carbonyl complexes .....	5
1.2.4 Coordination modes of carbonyl ligands in metal carbonyl complexes.....	8
1.3 Carbon monoxide (CO) releasing molecules (CORMs).....	10
1.3.1 CORMs in general .....	10
1.3.2 Some selected CORMs .....	11
1.3.2.1 Molybdenum CORMs.....	11
1.3.2.2 Manganese CORMs.....	13
1.3.2.3 Rhenium CORMs.....	16
1.3.2.4 Iron CORMs.....	17
1.3.2.5 Ruthenium CORMs.....	25
1.3.2.6 Cobalt CORMs.....	25
1.3.2.7 Iridium CORMs.....	26
1.3.2.8 Non-transition-metal CORMs.....	27
1.4 Myoglobin assay.....	29

## Chapter Two

<b>2. Results and Discussions</b>	<b>33</b>
2.1 N/S- iron-based CORMs.....	33
2.1.1 Synthesis.....	34
2.1.2 Molecular structures.....	36
2.1.3 CO-release properties.....	45
2.2 N/P- iron-based CORMs.....	50
2.2.1 Synthesis.....	50
2.2.2 Molecular structures.....	52
2.2.3 CO-release properties.....	57
2.4 P- iron-based CORMs.....	64
2.4.1 Synthesis.....	65
2.4.2 Molecular structures.....	67
2.4.3 CO-release properties.....	72

## Chapter Three

<b>3. Experimental</b>	<b>78</b>
3.1 Synthesis of $[\text{Fe}(\text{CO})_2(\text{SCH}_2\text{CH}_2\text{NH}_2)_2]$ (CORM-S1) (1).....	78
3.2 Synthesis of $[\text{Fe}(\text{CO})_2(\text{SC}_6\text{H}_4\text{-2-NH}_2)_2]$ (CORM-S2) (2).....	79
3.3 Synthesis of trans- $[\text{Fe}(\text{NC-Me})_2(\text{H}_2\text{NCH}_2\text{CH}_2\text{PPh}_2)_2]$ $[\text{BF}_4]_2$ (5).....	80
3.4 Synthesis of trans- $[\text{Fe}(\text{NC-Me})_2(\text{H}_2\text{NC}_6\text{H}_4\text{-2-PPh}_2)_2]$ $[\text{BF}_4]_2$ (6).....	81
3.5 Synthesis of $[\text{Fe}(\text{CO})(\text{NC-Me})(\text{H}_2\text{NCH}_2\text{CH}_2\text{PPh}_2)_2]$ $[\text{BF}_4]_2$ (CORM-P1) (7).....	82
3.6 Synthesis of $[\text{Fe}(\text{CO})(\text{NC-Me})(\text{H}_2\text{NC}_6\text{H}_4\text{-2-PPh}_2)_2]$ $[\text{BF}_4]_2$ (CORM-P2) (8).....	83
3.7 Synthesis of $[\text{Fe}(\text{CO})_4(\text{PCl}_3)]$ (CORM-P3) (9).....	84
3.8 Synthesis of $[\text{Fe}_2(\text{CO})_6(\text{PCl}_2)_2]$ (CORM-P6) (12).....	85
3.9 Synthesis of $[\text{Fe}_2(\text{CO})_6\{\text{PCl}(\text{C}_6\text{H}_4\text{-CF}_3)\}_2]$ (CORM-P7) (13).....	86
3.10 Synthesis of $[(\text{thf})_4\text{Ca}\{\text{Fe}_2(\text{CO})_6(\mu\text{-CO})(\mu\text{-PPh}_2)\}_2]$ (CORM-CF) (14).....	87
3.11 Myoglobin Assay.....	88
3.12 X-Ray Structure Determinations.....	89
<b>4. Summary</b> .....	<b>90</b>
<b>5. Zusammenfassung</b> .....	<b>93</b>
<b>6. References</b> .....	<b>96</b>
<b>8. Acknowledgment</b> .....	<b>107</b>
<b>9. Declaration of Originality</b> .....	<b>109</b>
<b>10. Curriculum Vitae</b> .....	<b>110</b>
<b>11. List of Publications</b> .....	<b>112</b>

## List of Figures

1.1	Energy-level diagram for CO can be refined by inclusion of s, p mixing. Crucial to the discussions on M-CO bonding properties are the frontier orbitals $\sigma^*$ (HOMO) and $\pi^*$ (LUMO).....	3
1.2	Bonding of carbonyl to a metal: $\sigma$ -donor bonding (left) and $\pi$ -acceptor bonding (right).....	3
1.3	Most important coordination modes of carbonyl ligands in mononuclear (left), bi-nuclear (middle), and tri-nuclear (right) metal carbonyl complexes.....	8
1.4	Examples of $\sigma/\pi$ -bridging carbonyl ligands.....	9
1.5	IR stretching frequencies for CO as free molecule, terminal ligand, doubly bridging ligand, and triply bridging ligand.....	10
1.6	Structures of Mo-based CORMs (2-pyrone carbonyl complexes).....	12
1.7	Structures of CORMs investigated by the Romão group.....	12
1.8	Chemical structure of $\text{Mo}(\text{CO})_3(\text{CNC}(\text{CH}_3)_2\text{COOH})_3$ CORM-ALF794...	13
1.9	Structures of CORMs investigated theoretically and by Motterlini and coworkers.....	14
1.10	Structures of CORMs investigated theoretically and experimentally by the Mascharak group.....	15
1.11	The molecular structure of $[\text{Mn}(\text{CO})_3(\text{tpm})]^+$ , (tpm = tris(pyrazolyl)methane).....	15
1.12	Manganese complexes with different imidazolylphosphane ligands...	16
1.13	Rhenium complexes used as photo-CORMs.....	16
1.14	Water soluble rhenium CORM investigated theoretically and experimentally by the Ford group.....	17
1.15	Chemical structure of irontricarbonyl-2-pyrone complexes.....	18
1.16	Structures of iron CORMs with cyclopentadienyl ligands.....	19
1.17	Structures of iron CORMs with phosphite ligands.....	19
1.18	Structures of iron CORMs with indenyl ligands.....	20
1.19	Structures of iron CORM with multidentate pyridyl ligands.....	20
1.20	Chemical structures of pentadentate polypyridine ligands.....	21
1.21	Structures of the acyloxybutadiene iron tricarbonyl complexes.....	22

1.22	Structures of the phosphoryloxy-substituted (cyclohexadiene) iron tricarbonyl complexes.....	23
1.23	Structures of iron CORMs investigated experimentally and theoretically.....	24
1.24	Structures of iron CORMs with allyl moiety.....	24
1.25	Most important ruthenium CORMs up to now, CORM-2 [Ru <sub>2</sub> (CO) <sub>6</sub> Cl <sub>4</sub> ] (left), and CORM-3 [Ru(CO) <sub>3</sub> Cl-(glycinate)] (right), which was first synthesized as CORM by the Motterlini group.....	25
1.26	μ <sub>2</sub> -Alkyne dicobalt(0)hexacarbonyl complexes investigated by Fairlamb and Motterlini.....	26
1.27	Structures of iridium-based CORMs investigated theoretically and experimentally.....	27
1.28	Boranocarbamate derivatives of Na[H <sub>3</sub> BCO <sub>2</sub> H].....	28
1.29	Absorption spectra of deoxy-myoglobin and carboxy-myoglobin in the range of 500-600 nm (phosphate buffer, pH 7.4, 37 °C, [Mb] = 100 μM)	30
1.30	UV/Vis spectral changes in the Q band region of myoglobin solution (75 mmol/L) with [Mn(CO) <sub>3</sub> (tpm)] <sup>+</sup> (20 mmol/L) in 0.1 M phosphate buffer upon irradiation at 365 nm (t = 0 to 100 min).....	31
2.1	Molecular structure and numbering scheme of [Fe(CO) <sub>2</sub> (SCH <sub>2</sub> CH <sub>2</sub> NH <sub>2</sub> ) <sub>2</sub> ] <b>1</b> .....	38
2.2	Molecular structure and numbering scheme of [Fe(CO) <sub>2</sub> (SC <sub>6</sub> H <sub>4</sub> -2-NH <sub>2</sub> ) <sub>2</sub> ] <b>2</b> .....	39
2.3	Structure models of [Fe(CO) <sub>2</sub> (SCH <sub>2</sub> CH <sub>2</sub> NH <sub>2</sub> ) <sub>2</sub> ]·THF <b>1</b> (top) and [Fe(CO) <sub>2</sub> (SC <sub>6</sub> H <sub>4</sub> -2-NH <sub>2</sub> ) <sub>2</sub> ]·THF <b>2</b> (bottom) adduct with THF molecule.....	40
2.4	Molecular structure and numbering scheme of <b>3</b> (left) and the structure of <b>3</b> ·THF with the coordination of THF through a hydrogen bridge (right).....	41
2.5	Molecular structure and numbering scheme of [Ru(CO) <sub>2</sub> (SC <sub>6</sub> H <sub>4</sub> -2-NH <sub>2</sub> ) <sub>2</sub> ] <b>4</b> (top) and the structure of <b>4</b> ·DMF.....	42
2.6	IR spectra of the carbonyl region of [Ru(CO) <sub>2</sub> (SC <sub>6</sub> H <sub>4</sub> -2-NH <sub>2</sub> ) <sub>2</sub> ] ( <b>4</b> ).....	45
2.7	Light dependence of CO release. Absorption spectra of [Ru(CO) <sub>2</sub> (SCH <sub>2</sub> CH <sub>2</sub> NH <sub>2</sub> ) <sub>2</sub> ] (left) and [Ru(CO) <sub>2</sub> (SC <sub>6</sub> H <sub>4</sub> -2-NH <sub>2</sub> ) <sub>2</sub> ] (right)..	46



2.8	Light dependence of CO release. Absorption spectra for compounds [Fe(CO) <sub>2</sub> (SCH <sub>2</sub> CH <sub>2</sub> NH <sub>2</sub> ) <sub>2</sub> ] CORM-S1 (left) and [Fe(CO) <sub>2</sub> (SCH <sub>2</sub> CH <sub>2</sub> NH <sub>2</sub> ) <sub>2</sub> ] CORM-S2 (right).....	46
2.9	Absorbance at 540 nm for compounds CORM-S1 and CORM-S2.....	47
2.10	IR spectra of the carbonyl region of; [Fe(CO) <sub>2</sub> (SCH <sub>2</sub> CH <sub>2</sub> NH <sub>2</sub> ) <sub>2</sub> ] (CORM-S1) (top) and [Fe(CO) <sub>2</sub> (SCH <sub>2</sub> CH <sub>2</sub> NH <sub>2</sub> ) <sub>2</sub> ] (CORM-S2) (bottom) after irradiation.....	49
2.11	Molecular structure and numbering scheme of the cation <i>trans</i> -[Fe(NC-Me) <sub>2</sub> (H <sub>2</sub> NC <sub>6</sub> H <sub>4</sub> -2-PPh <sub>2</sub> ) <sub>2</sub> ] <sup>2+</sup> of <b>6</b> .....	53
2.12	Molecular structure and numbering scheme of the cation [Fe(CO)(NC-Me)(H <sub>2</sub> NCH <sub>2</sub> CH <sub>2</sub> PPh <sub>2</sub> ) <sub>2</sub> ] <sup>2+</sup> ( <b>7</b> , CORM-P1) (top) and dimer formation via a N-H...F network of [Fe(CO)(NC-Me)(H <sub>2</sub> NCH <sub>2</sub> CH <sub>2</sub> PPh <sub>2</sub> ) <sub>2</sub> ] [BF <sub>4</sub> ] <sub>2</sub> (bottom).....	54
2.13	Molecular structure and numbering scheme of the cation [Fe(CO)(NC-Me)(H <sub>2</sub> NC <sub>6</sub> H <sub>4</sub> -2-PPh <sub>2</sub> ) <sub>2</sub> ] <sup>2+</sup> of ( <b>8</b> , CORM-P2) (top).....	55
2.14	Time-dependent degradation of <b>7</b> (CORM-P1) upon irradiation with visible light in a 23-mM solution of <b>7</b> in [D <sub>6</sub> ]DMSO followed by <sup>31</sup> P{ <sup>1</sup> H} NMR spectroscopy.....	57
2.15	<sup>31</sup> P{ <sup>1</sup> H} NMR spectra of the degradation of a 23-mM solution of CORM-P1 ( <b>7</b> ) in [D <sub>3</sub> ]acetonitrile during irradiation with visible light....	59
2.16	Light-induced degradation of <b>7</b> (circles, CORM-P1) in a 23-mM [D <sub>3</sub> ]acetonitrile solution.....	60
2.17	Absorption spectra for 100 μM CORM-P1 (left) and CORM-P2 (right) irradiated with white light for 10 min in PBS + 0.1% sodium dithionite + 100 μM deoxymyoglobin (Mb).....	61
2.18	Absorption spectra in the range of 380-450 nm for 5 μM of the indicated CORMs and 10 μM deoxymyoglobin upon 10-min irradiation with 420-nm light.....	62
2.19	Absorbance changes at 422 nm (□A <sub>422</sub> ) as a function of time for the indicated wavelengths.....	63
2.20	CO release is not dependent on dithionite. CO release by CORM-P1 and CORM-P2 during 10-min preincubation without Mb in the	

	presence (“+”) or absence (“–”) of dithionite, with (open bars) or without (grey bars) illumination with white light.....	64
2.21	Molecular structure and numbering scheme of $[\text{Fe}_2(\text{CO})_6(\text{PCl}_2)_2]$ ( <b>12</b> , CORM-P6).....	70
2.22	CO-releasing properties of CORM-P3, CORM-P4, and CORM-P5.....	73
2.23	Absorbance of deoxy-myoglobin solutions (100 $\mu\text{M}$ ) at 540 nm was measured at a frequency of 0.1 Hz.....	74
2.24	Myoglobin assay of CORM-P6 and CORM-P7 compounds.....	75
2.25	Myoglobin assay of CORM-FC.....	76
2.26	Absorption of CORM-FC.....	77

## List of Schemes

1.1	Degradation of heme and liberation of CO in the presence of iron(II) cations during the formation of biliverdin.....	2
1.2	Carbonyl substitutions at 18 VE complexes proceed by a dissociative mechanism (D), via an intermediate of lower coordination number.....	6
1.3	Carbonyl substitutions at 17 VE complexes proceed by associative mechanism (A), via an intermediate of higher coordination number.....	6
1.4	The mixed-metal molybdenum-titanium complex exhibits the very rare coordination mode for bridging carbonyl ligands via the oxygen atom ( $\mu\text{-}\eta^2\text{-CO}$ ).....	9
1.5	Work strategy used to study CO releasing mechanisms in these CORMs series: (Step I) dissociation of an axial CO molecule ( $\text{CO}_{\text{ax}}$ ) cis to L from the Mn center, where L=donor atom of mono- or bidentate ligand groups, (Step II) attack of any putative ligand (L') from the buffer solution at the Mn vacant site; (Step III) dissociation of an equatorial CO molecule ( $\text{CO}_{\text{eq}}$ ), trans to L, from the Mn center.....	14
1.6	Proposed mode of action of enzyme-triggered CO-releasing molecules (ET-CORMs) of type <b>3</b> .....	22
1.7	pH dependency of CO release from $[\text{H}_3\text{BCO}_2\text{H}]^-$ (CORM-A1).....	28
1.8	Proposed mechanisms of CO release from the boranocarbamate derivatives. Step (1): the amides of the compounds are protonated in a rapid, amide $pK_a$ -dependent equilibrium; step (2): the rate-limiting step for this mechanism is the elimination of the amine ( $k_1$ ) yielding $\text{H}_3\text{BCO}$ ; step (3): $\text{H}_3\text{BCO}$ decomposes rapidly to release CO.....	29
2.1	Biogenic ligands derived from cysteamine.....	31
2.2	Synthesis of $[\text{Fe}(\text{CO})_2(\text{SCH}_2\text{CH}_2\text{NH}_2)_2]$ (CORM-S1) and $[\text{Fe}(\text{CO})_2(\text{SC}_6\text{H}_4\text{-2-NH}_2)_2]$ (CORM-S2) starting from $\text{FeSO}_4$ .....	34
2.3	Synthesis of a ruthenium complex with $\text{Ru}(\text{CO})_2\text{N}_2\text{S}_2$ coordination pattern.....	35
2.4	Synthesis of $[\text{Fe}(\text{CO})_2(\text{SCH}_2\text{CH}_2\text{NH}_2)_2]$ (CORM-S1) and $[\text{Fe}(\text{CO})_2(\text{SC}_6\text{H}_4\text{-2-NH}_2)_2]$ (CORM-S2) starting from metal carbonyls $[\text{Fe}_3(\text{CO})_{12}]$ .....	36

2.5	Synthesis of $[\text{Fe}(\text{CO})_2(\text{SCH}_2\text{CH}_2\text{NH}_2)_2]$ (CORM-S1) and $[\text{Fe}(\text{CO})_2(\text{SC}_6\text{H}_4\text{-2-NH}_2)_2]$ (CORM-S2) starting from metal carbonyls $[\text{Fe}_3(\text{CO})_{12}]$ .....	36
2.6	Synthesis of the CO-releasing molecules <b>7</b> (CORM-P1) and <b>8</b> (CORM-P2), starting from $[\text{Fe}(\text{H}_2\text{O})_6][\text{BF}_4]_2$ .....	51
2.7	Synthesis of tetracarbonyl[trichlorophosphine]iron(0) <b>9</b> (CORM-P3)...	65
2.8	Synthesis of $[\text{Fe}_2(\text{CO})_6(\text{PCl}_2)_2]$ ( <b>12</b> , CORM-P4), and $[\text{Fe}_2(\text{CO})_6\{\text{PCl}(\text{C}_6\text{H}_4\text{-CF}_3)\}_2]$ ( <b>13</b> , CORM-P5) starting from diironnonacarbonyl.....	66
2.9	Synthesis of $[(\text{thf})_4\text{Ca}\{\text{Fe}_2(\text{CO})_6(\mu\text{-CO})(\mu\text{-PPh}_2)\}_2]$ ( <b>14</b> , CORM-FC) starting from diironnonacarbonyl.....	66
2.10	Berry pseudorotation of trigonal bipyramidal compounds, the five bonds to the central atom E being represented as $e^1$ , $e^2$ , $e^3$ , $a^1$ and $a^2$ . Two equatorial bonds move apart and become apical bonds at the same time as the apical bonds move together to become equatorial...	68

## List of Tables

2.1	Comparison of physical data of the iron(II) complexes [Fe(CO) <sub>2</sub> (SCH <sub>2</sub> CH <sub>2</sub> NH <sub>2</sub> ) <sub>2</sub> ] ( <b>1</b> , CORM-S1) and [Fe(CO) <sub>2</sub> (SC <sub>6</sub> H <sub>4</sub> -2-NH <sub>2</sub> ) <sub>2</sub> ] ( <b>2</b> , CORM-S2), as well as the homologous Ru-based derivatives [Ru(CO) <sub>2</sub> (SCH <sub>2</sub> CH <sub>2</sub> NH <sub>2</sub> ) <sub>2</sub> ] ( <b>3</b> ) and [Ru(CO) <sub>2</sub> (SC <sub>6</sub> H <sub>4</sub> -2-NH <sub>2</sub> ) <sub>2</sub> ] ( <b>4</b> ) (average values for bond lengths [pm] and angles [deg.]... 43	43
2.2	Comparison of and IR frequencies [cm <sup>-1</sup> ] data of the complexes ( <b>9</b> , CORM-P3), ( <b>10</b> , CORM-P4), and ( <b>11</b> , CORM-P5)..... 67	67
2.3	Comparison of and IR frequencies [cm <sup>-1</sup> ] data of the complexes ( <b>12</b> , CORM-P6), ( <b>13</b> , CORM-P7), and [Fe <sub>2</sub> (CO) <sub>6</sub> (PC <sub>6</sub> H <sub>5</sub> Cl) <sub>2</sub> ]..... 71	71

# 1. Introduction

## 1.1 Carbon monoxide (CO)

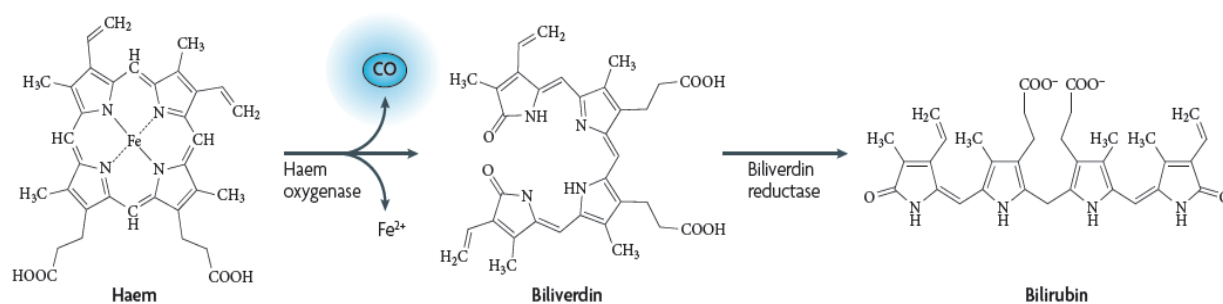
Carbon monoxide (CO) is a colorless, odorless, and tasteless gas which is slightly lighter than air; it is toxic to humans and animals when encountered in higher concentrations. CO consists of one carbon atom and one oxygen atom, connected by a triple bond. It is the simplest oxocarbon, and isoelectronic with the cyanide ion and molecular nitrogen [1].

CO is produced from the partial oxidation of carbon-containing compounds; it forms when there is not enough oxygen to produce carbon dioxide (CO<sub>2</sub>), such as when operating a stove or an internal combustion engine in an enclosed space [2]. In addition, a temperature-dependent equilibrium converts CO<sub>2</sub> and C into CO (Boudouard equilibrium).

Worldwide, the largest source of CO is natural in origin; photochemical reactions in the troposphere layer generate about  $5 \times 10^{12}$  kilograms per year [3]. Other natural sources of CO include volcanoes, forest fires, and other forms of combustion.

The degradation process of hemoglobin which is shown in Scheme 1.1 represents the source of CO in biological systems. The catalytically active centers of hemoglobin are the iron-containing heme groups. Their degradation to biliverdin is accompanied by the liberation of CO in the presence of iron(II) cations. Biliverdin decomposes to bilirubin which is degraded to oxidized decomposition end products (so-called BOXes) [4, 5].

CO is a highly toxic gas; it mainly causes pernicious effects in humans by combining with hemoglobin to form carboxyhemoglobin (HbCO) in the blood. This prevents oxygen binding to hemoglobin, reducing the oxygen-carrying capacity of the blood, leading to hypoxia and even death at the end [6]. Nevertheless, CO is increasingly being accepted as a cytoprotective and homeostatic molecule with important signalling capabilities in physiological and pathophysiological situations [7-12], and due to the high toxicity of CO if inhaled sophisticated strategies have to be developed in order to use these gaseous messenger molecules in cellular tissues. The most promising strategies include the use of carbonyl complexes of transition metals (CO-releasing molecules, CORMs).



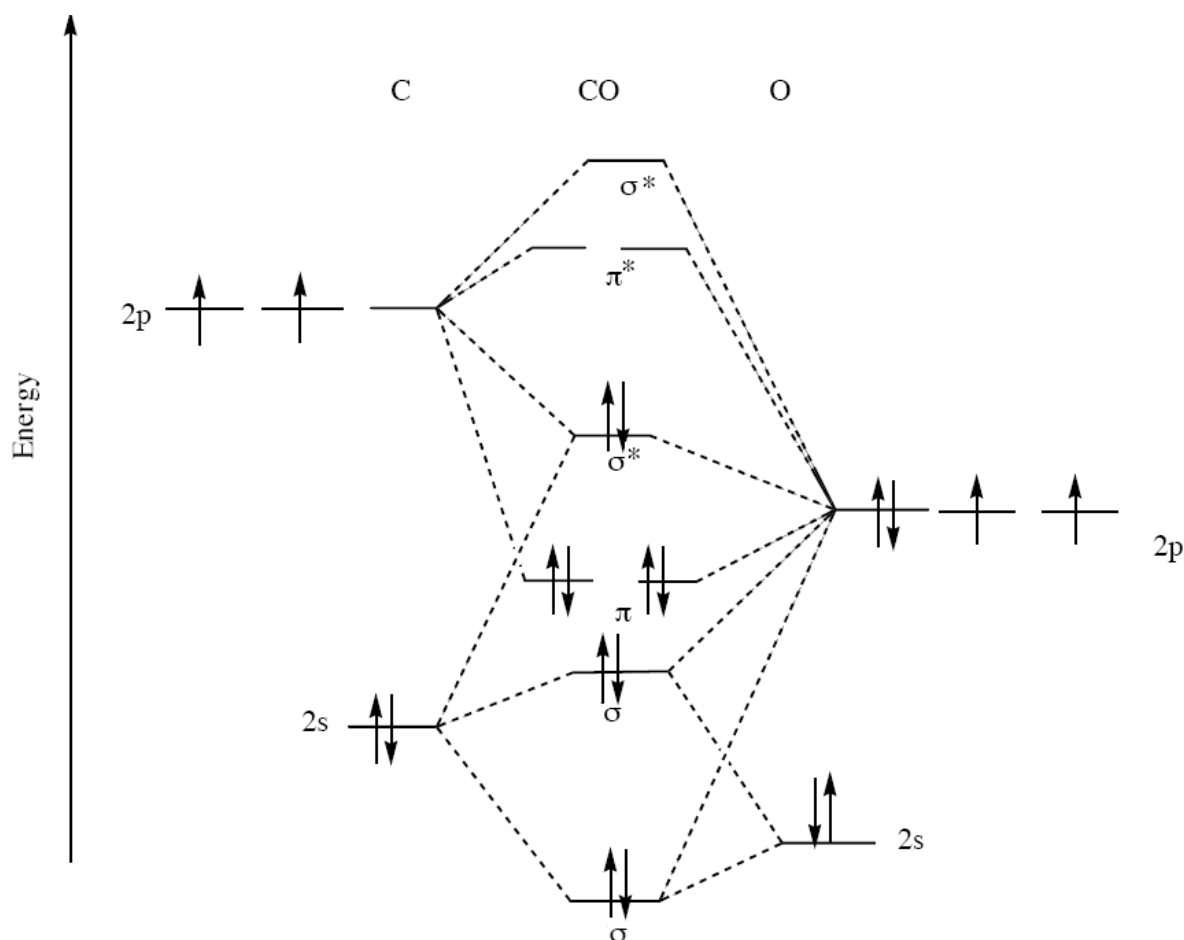
**Scheme 1.1:** Degradation of heme and liberation of CO in the presence of iron(II) cations during the formation of biliverdin.

## 1.2 Carbonyl chemistry

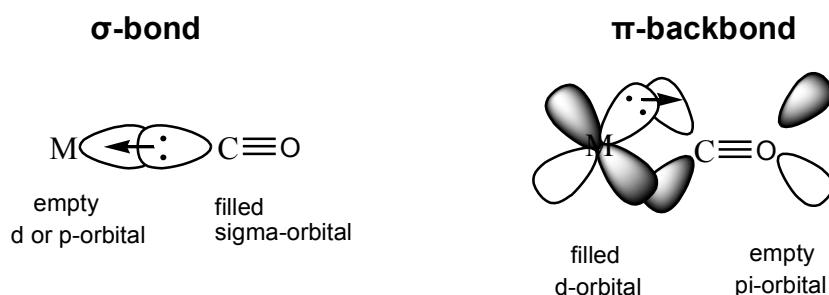
### 1.2.1 Metal carbonyl complexes

Metal carbonyl complexes are compounds that contain carbon monoxide as a coordinated ligand. CO is a common ligand in transition metal chemistry and it is called carbonyl when it coordinates to the metal. Transition metal carbonyl complexes are among the longest known classes of organometallic compounds [13]. These complexes may be homoleptic (complexes consisting of a metal(0) center and carbon monoxide molecules such as  $\text{Fe}(\text{CO})_5$ ), but more commonly metal carbonyl complexes are heteroleptic and contain diverse ligands [13].

To describe the bonding between a carbonyl ligand and a transition metal we have to explain at first the energy level diagram for CO (figure 1.1). The atomic orbitals (AO) of carbon and oxygen combine to form the molecular orbitals (MO) of CO. Carbonyl ligands can donate two electrons from the highest occupied molecular orbital (HOMO- $\sigma^*$ ) and accept electrons from the electron rich metal in the lowest unoccupied molecular orbital (LUMO- $\pi^*$ ). Due to the bonding of the carbonyl ligand to the metal, CO acts as a  $\sigma$ -donor and a  $\pi$ -accepter ligand (figure 1.2). Carbon monoxide donates electron density (HOMO- $\sigma^*$ ) into a vacant metal d-orbital (figure 1.2 (left)). This electron donation makes the metal more electron rich, and in order to compensate for this increased electron density, a filled metal d-orbital may interact with the empty LUMO-  $\pi^*$  orbital on the carbonyl ligand, the so-called  $\pi$ -backdonation (figure 1.2 (right)). The latter kind of binding requires that the metal has d-electrons. A relatively low oxidation state makes the backdonation of electron density favorable. As electrons from the metal fill the  $\pi$ -antibonding orbital of CO, they weaken the carbon-oxygen bond compared with free carbon monoxide, while the metal-carbon bond is strengthened [13].



**Fig 1.1:** Energy-level diagram for CO can be refined by inclusion of s, p mixing. Crucial to the discussions on M-CO bonding properties are the frontier orbitals  $\sigma^*$ (HOMO) and  $\pi^*$ (LUMO).



**Fig 1.2:** Bonding of carbonyl to a metal:  $\sigma$ -donor bonding (left) and  $\pi$ -acceptor bonding (right).

Metal carbonyl complexes occur as neutral complexes, as positively charged metal carbonyl cations or as negatively charged metal carbonylate anions. An increase of negative charge leads to expansion, whereas an increase of positive charge results in contraction of the metal d-orbitals influencing the  $M(d)$ - $CO(\pi^*)$  overlap. Thus the strength of C-O and M-CO bonds depends on the back bonding into the antibonding  $CO(\pi^*)$  orbital.



The C-O bond becomes stronger and at the same time the M-CO bond becomes weaker in the positively charged metal carbonyl cations due to decreased  $\pi$ -backdonation, and vice versa in negatively charged metal carbonylate anions. This fact means that the CO releasing properties become easier in the more positively charged metal carbonyl complexes [13]. These properties play an important role in the mechanisms of CO liberation from the metal carbonyl complexes. Therefore these mechanisms will be explained in detail in the later chapters.

### **1.2.2 Preparation of metal carbonyl complexes**

Initially the synthesis of metal carbonyl complexes was carried out by Justus von Liebig in 1834. By passing CO over molten potassium, he prepared a substance having the empirical formula KCO, which he called Kohlenoxidkalium [14]. As demonstrated later, the compound was not a metal carbonyl, but the potassium salt of hexahydroxy benzene and the potassium salt of dihydroxy acetylene [15]. The synthesis of the first true metal carbonyl complex was performed by Paul Schützenberger in 1868 by passing chlorine and CO over platinum black yielding dicarbonyldichloroplatinum ( $\text{Pt}(\text{CO})_2\text{Cl}_2$ ) [16]. Nowadays the synthesis of metal carbonyl complexes is subject of intense organometallic research. A lot of procedures have been developed for the preparation of mononuclear metal carbonyl complexes as well as homo- and heterometallic carbonyl clusters [15]. Several methods for the preparation of metal carbonyl complexes are possible [13].

- **Direct synthesis**

In this method the direct reaction of metal with CO leads to the formation of homoleptic metal carbonyls. Preparation of iron pentacarbonyl represents an example of this method, which can be prepared according to the following equation 1 [17].



- **Reduction of metal salts**

Some metal carbonyl complexes are prepared by the reduction of metal halides in the presence of high pressure of CO gas. A variety of reducing agents are employed, including copper, aluminum, hydrogen, as well as metal alkyls such as triethylalane. One example of this method is the formation of chromium hexacarbonyl from anhydrous chromium(III) chloride with aluminum as a reducing agent, which is shown in the following equation 2 [17].



- **Photolysis and thermolysis**

Photolysis or thermolysis of mononuclear carbonyl complexes generate bi- and multi-metallic carbonyls such as diironnonacarbonyl ( $\text{Fe}_2(\text{CO})_9$ ) as shown in the following equation 3 [18, 19].



Another example for this method is the thermal decomposition of triosmium dodecacarbonyl ( $\text{Os}_3(\text{CO})_{12}$ ) which provides higher-nuclear osmium carbonyl clusters such as  $\text{Os}_4(\text{CO})_{13}$ ,  $\text{Os}_6(\text{CO})_{18}$  up to  $\text{Os}_8(\text{CO})_{23}$  [20].

- **Preparation of metal carbonyl cations and metal carbonylate anions**

The synthesis of ionic metal carbonyl complexes is possible by oxidation or reduction of the neutral complexes. Anionic metal carbonylates can be obtained for example *via* reduction of dinuclear complexes with sodium or sodium amalgam to give carbonylmetalate anions such as e.g. the reaction of dimanganese decacarbonyl with metallic sodium (equation 4) [21].



The cationic hexacarbonyl salts of manganese, technetium and rhenium can be prepared from the carbonyl halides under CO pressure by reaction with a Lewis acid such as aluminum chloride as depicted in the following equation 5 [22].



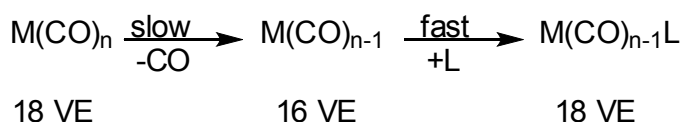
### 1.2.3 Reaction of metal carbonyl complexes

Metal carbonyl complexes are important precursors for the synthesis of other organometallic complexes. The main reactions include substitution of carbonyl by other Lewis basic ligands, oxidation or reduction reactions of the metal center, and reactions at the carbon monoxide ligand itself.

- **Substitution**

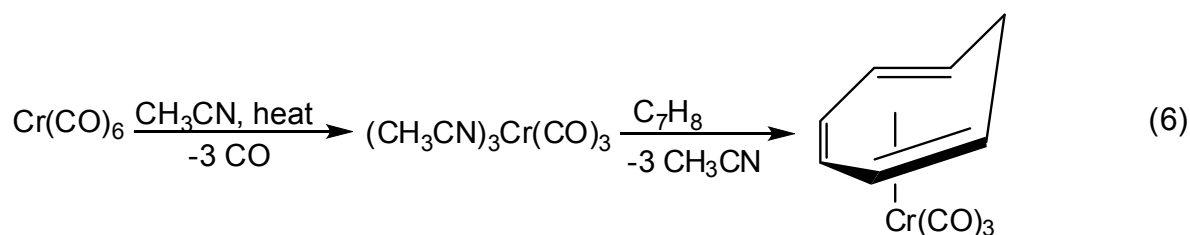
Substitution of CO ligands can be induced thermally or photochemically by donor ligands. The range of ligands is large and includes phosphanes, cyanide, nitrogen donors, and even ethers, especially chelating ones. Olefins, especially diolefins, are effective ligands that yield synthetically useful derivatives. Substitution at 18-electron

complexes generally follows a dissociative mechanism, involving 16-electron intermediates as shown in Scheme 1.2 [13, 23].

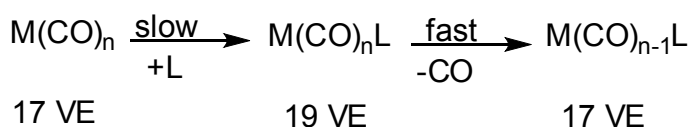


**Scheme 1.2:** Carbonyl substitutions at 18 VE complexes proceed by a dissociative mechanism (D), via an intermediate of lower coordination number.

Substitution of CO in chromiumhexacarbonyl by acetonitrile represents a good example of carbonyl substitutions at 18 VE complexes. As shown in the following equation 6 the acetonitrile ligand can then be replaced by other ligands under mild conditions, due to its labile bond to the metal [23].



Substitution in 17-electron complexes, which are rare, proceeds via associative mechanisms with a 19-electron intermediate (Scheme 1.3) [13].

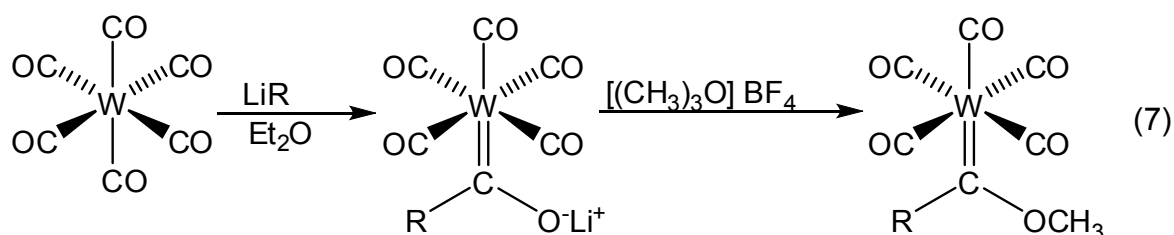


**Scheme 1.3:** Carbonyl substitutions at 17 VE complexes proceed by associative mechanism (A), via an intermediate of higher coordination number.

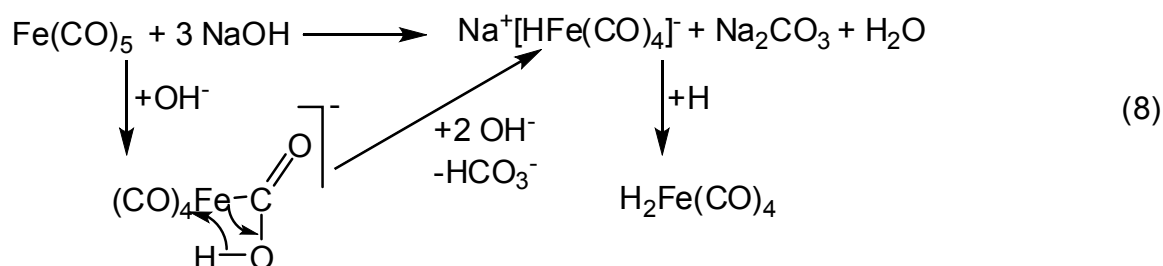
An example of 17 VE complex is  $\text{V(CO)}_6$  which reacts  $10^{10}$  times faster than the 18 VE complexes  $\text{Cr(CO)}_6$ . The acceleration induced by the transition from 18 VE to a 17 VE complex is utilized in electron-transfer (ET) catalysis. This principle was exploited by Kochi in 1983 for the case of ET catalysis, initiated by oxidation of 18 VE complexes and conversion into 17 VE complexes [24].

- **Nucleophilic attack at CO**

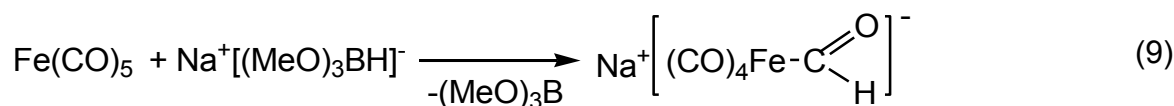
The CO ligand is often susceptible to attack by nucleophiles. This fact is in agreement with quantum-chemical calculations which were made by Fenske in 1968. These calculations showed that the carbon atom in coordinated CO carries a larger positive charge than in free CO [13]. For example, the addition of alkyl lithium to metal carbonyls leads to formation of *Fischer* carbene complexes as shown in the following equation 7 [13].



In the "Hieber base reaction", the CO ligand was attacked by the strong base OH<sup>-</sup>. As shown in the following equation 8 the initial addition product decomposes, presumably by β-elimination, to give carbonyl metalate [13].



The nucleophilic attack at the carbonyl ligand could also lead to formation of *Casey* formyl complexes such as in the following equation 9 [13].



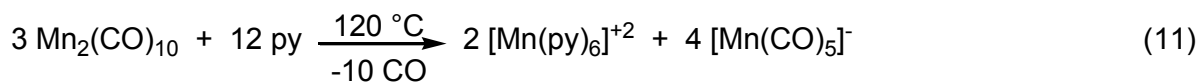
- **Oxidative decarbonylation**

The most famous example of this reaction is the halogenation of metal carbonyl complexes. Iron pentacarbonyl forms ferrous carbonyl halides as shown in the following equation 10 [13].



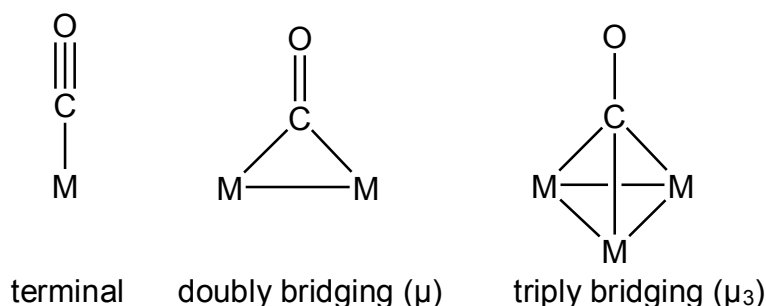
- **Disproportionation**

Disproportionation, also known as dismutation, is a specific type of redox reaction in which a species is simultaneously reduced and oxidized to form two different products. An example of this reaction is shown in the following equation 11 [13].



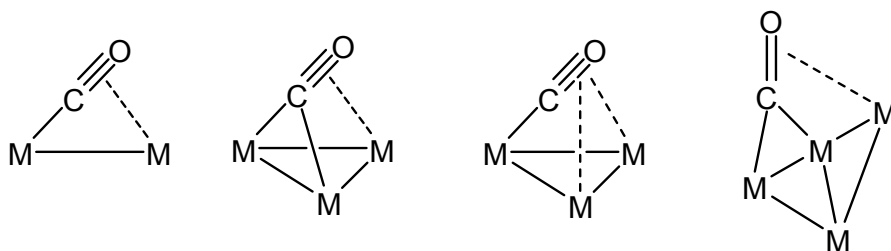
### 1.2.4 Coordination modes of carbonyl ligands in metal carbonyl complexes

The carbonyl ligand shows various bonding modes in metal carbonyl complexes. The most prominent two modes are terminal and bridging carbonyl ligands which exist in metal carbonyl dimers and clusters [13]. In the most common bridging mode, the CO ligand bridges a pair of metals. This bonding mode is observed in the commonly available metal carbonyl complexes such as,  $\text{Co}_2(\text{CO})_8$ ,  $\text{Fe}_2(\text{CO})_9$ ,  $\text{Fe}_3(\text{CO})_{12}$ , and  $\text{Co}_4(\text{CO})_{12}$ . In certain oligo-nuclear clusters, CO bridges faces of three or even four metal atoms [23, 25]. The most important coordination modes of carbonyl ligands are shown in figure 1.3 which represent the symmetrical mode for the bridging carbonyl ligand [13].



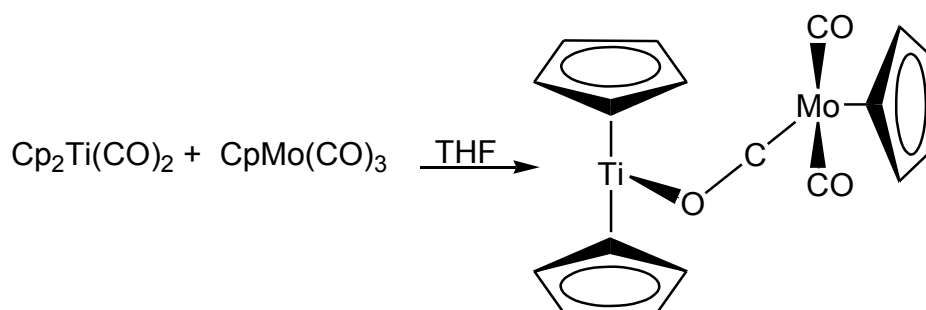
**Fig 1.3:** Most important coordination modes of carbonyl ligands in mononuclear (left), bi-nuclear (middle), and tri-nuclear (right) metal carbonyl complexes.

The bridging carbonyl ligand could also exhibit asymmetric coordination modes in oligo-nuclear metal carbonyl complexes. In these forms the carbonyl ligands act as four or six electron donors by  $\sigma/\pi$ -bridge coordination (figure 1.4). Here, also side-on coordination may occur, which has never been observed in mononuclear carbonyl complexes [13].



**Fig 1.4:** Examples of  $\sigma/\pi$ -bridging carbonyl ligands.

The bridging form  $M-C-O-M'$  occurs very rarely and is subject to certain requisites with respect to the fragments  $M$  and  $M'$ . An example of this form is shown in Scheme 1.4, in this complex we can consider the  $Cp_2Ti^+$  species as Lewis acid and  $CpMo(CO)_3^-$  species as Lewis base [13].


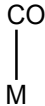
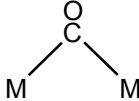
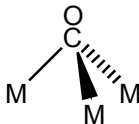


**Scheme 1.4:** The mixed-metal molybdenum-titanium complex exhibits the very rare coordination mode for bridging carbonyl ligands *via* the oxygen atom ( $\mu\text{-}\eta^2\text{-CO}$ ).

Preferred analytical techniques used to characterize metal carbonyl complexes include IR and  $^{13}\text{C}$ -NMR spectroscopy, and mass spectrometry. The most important technique for characterization of metal carbonyls is infrared spectroscopy [26]. The C-O vibration, typically denoted  $\nu_{\text{CO}}$ , occurs at  $2143\text{ cm}^{-1}$  for CO gas. The energies of the  $\nu_{\text{CO}}$  band for the metal carbonyls correlate with the strengths of the carbon-oxygen bonds, and are inversely correlated with the strength of the  $\pi$ -backbonding between the metals and the carbon atoms [13].

The number of vibrational modes of a metal carbonyl complex can be determined by group theory and the number of observable IR transitions can thus be predicted [27, 28, 29]. For example, the CO ligands of octahedral complexes, e.g.  $\text{Cr}(\text{CO})_6$ , transform as  $a_{1g}$ ,  $e_g$ , and  $t_{1u}$ , but only the  $t_{1u}$  mode (asymmetric stretching vibration of the apical carbonyl ligands) is IR-active. Thus, only a single  $\nu_{\text{CO}}$  band is observed in the IR spectra of the octahedral metal hexacarbonyls. Spectra for complexes of lower symmetry are more complex. For example, the IR spectrum of  $\text{Fe}_2(\text{CO})_9$  displays CO

bands at 2082, 2019, 1829  $\text{cm}^{-1}$  [26]. The IR-active stretching frequencies for metal carbonyl complexes are found in the following region (figure 1.5) [13].

	Free	Terminal	$\mu_2$ -CO	$\mu_3$ -CO
				
$\nu_{\text{CO}}$ ( $\text{cm}^{-1}$ )	2143	1850-2120	1750-1850	1620-1730

**Fig 1.5:** IR stretching frequencies for CO as free molecule, terminal ligand, doubly bridging ligand, and triply bridging ligand.

### **1.3 Carbon monoxide (CO) releasing molecules (CORMs)**

#### **1.3.1 CORMs in general**

Reactive oxygen species (ROS) play an important role in intra- and intermolecular communication processes. One of the most prominent examples is carbon monoxide (CO) which also represents an important signalling molecule. Furthermore, intense research efforts are related to CO as potentially valuable therapeutic agent and as pharmaceutical [7,11,12,30-39]. Many physiological effects are documented for controlled application of CO, such as anti-inflammatory effects, regulation of blood pressure, modulation of vascular smooth muscle tone, protection against ischemia and septic shock as well as hyperoxia. In addition CO suppresses organ graft rejection and arteriosclerotic lesions [9,40].

Due to the fact that CO is an extremely toxic gas volumetric dosing in therapeutic applications is very challenging. Therefore for conceivable applications CO-releasing molecules (CORMs) are needed as carriers to supply a definite amount of CO at a predetermined location. For that purpose, CORMs should fulfill specific requirements such as solubility in aqueous solutions, low toxicity of the CORMs and their degradation products, and CO release that can be triggered (e.g. *via* change of pH, ligand substitution, or light irradiation). As we mentioned before the most promising perspective is the use of metal carbonyl complexes as CO releasing molecules (CORMs). The most important CORMs up to now are water-insoluble  $[\text{Mn}_2(\text{CO})_{10}]$  (CORM-1, CO-release light-dependent) and  $[\text{Ru}(\mu\text{-Cl})(\text{CO})_3]_2$  (CORM-2, CO-release *via* ligand substitution) as well as water-soluble  $[\text{Ru}(\text{Cl})(\text{CO})_3\{\text{N}(\text{H}_2)\text{CH}_2\text{COO}\}]$  (CORM-3, CO release *via* ligand substitution),  $\text{Na}_2[\text{H}_3\text{B-COO}]$  (CORM-A1, CO-

release pH-controlled) [11,12], and  $[\text{Mn}(\text{CO})_3(\text{tpm})]\text{Br}$  (CO-release light-dependent, tpm = tris(pyrazolyl)methane) [30,31].

For these metal carbonyl complexes the kinetic measurements are rather straightforward. The common test is based on the transformation of deoxy-myoglobin with CO to carboxy-myoglobin [41]. Therefore this myoglobin assay will be explained in detail in the later chapters. CO liberation from these complexes can be initiated by strategies:

- **Thermal dissociation**

In this mechanism the CO ligand can thermally dissociate from the metal complex while being replaced for instance by another ligand such as ether, water or phosphane [4].

- **Photochemical substitution**

In this procedure the CO ligand is released from the metal complex by photochemical cleavage of the M-CO bonds often leading to a complete decomposition of the metal compounds [4].

In these two mechanisms, liberation of CO becomes easier if the carbonyl ligand have high  $\nu(\text{CO})$  stretching frequencies in the IR spectra because this fact indicates that the M-CO bond is weaker due to a lower back donation of charge from the metal to the  $\pi^*(\text{CO})$  ligand orbitals [4].

- **Associatively supported substitution**

This mechanism can occur in coordinating solvents such as water and is not necessarily dependent on the strength of the M-CO bond. This kind of CO release might be strongly pH dependent, for example the release of carbon monoxide from CORM-A1 is a strongly pH dependent CO releasing process [11].

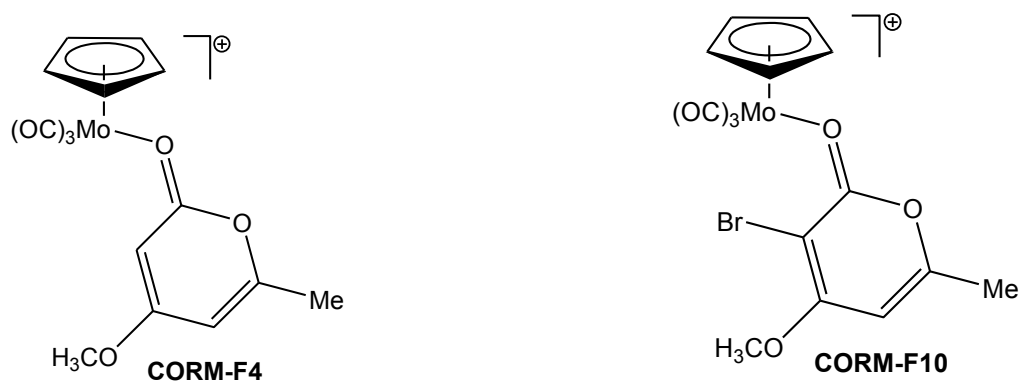
### **1.3.2 Some selected CORMs**

#### **1.3.2.1 Molybdenum CORMs**

Some molybdenum carbonyl complexes were used as carbon monoxide releasing molecules. The compounds reported range from  $[\text{Mo}(\text{CO})_5\text{Br}]^-$  [42,43] to derivatives with a  $\text{Mo}(\text{CO})_3$  fragment; for example, CORM-F4 and CORM-F10 [44], which were synthesized as ligand substitution CORMs, are shown in figure 1.6. CORM-F10

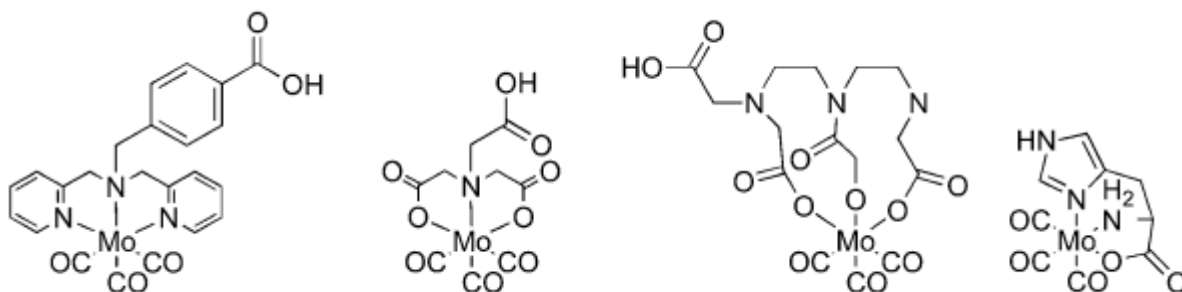


represents one of the most rapid CO releasers reported to date; it also released more than one mole of CO per mole of metal.



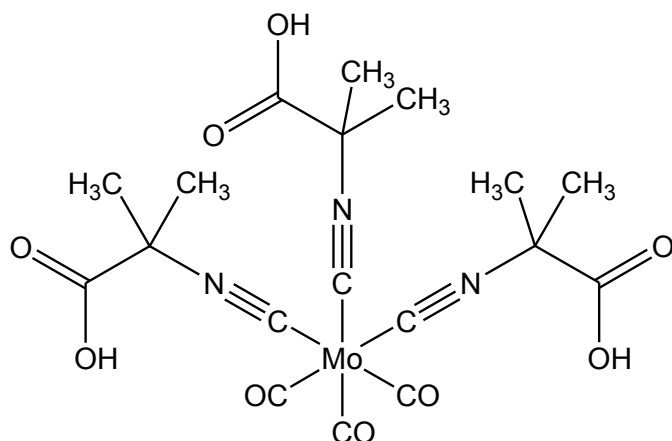
**Fig 1.6:** Structures of Mo-based CORMs (2-pyrone carbonyl complexes) [44].

The Romão group submitted many patents on molybdenum CORMs. Most of their work focused on molybdenum carbonyl derivatives for a wide range of medical applications, including inflammation, infection, and vasorelaxation [7,45]. These compounds are derivatives containing the Mo(CO)<sub>3</sub> moiety with oxygen and nitrogen ligands (figure 1.7) [46,47].



**Fig 1.7:** Structures of CORMs investigated by the Romão group [46,47].

The formation of molybdenum tricarbonyl complexes with lithium isocyanoacetate ligands that had a small molecular size was described by the Beck group [48]. These complexes appeared to be soluble and stable in water under ambient conditions, therefore derivatives of isocyanoacetate ligands were explored for the formation of molybdenum carbonyl CORMs for the treatment of liver diseases [49]. Figure 1.8 shows ALF794 as an example of these molybdenum CORMs, which is the first compound that delivers CO in a targeted manner to an organ in vivo with such a high level of specificity [49].

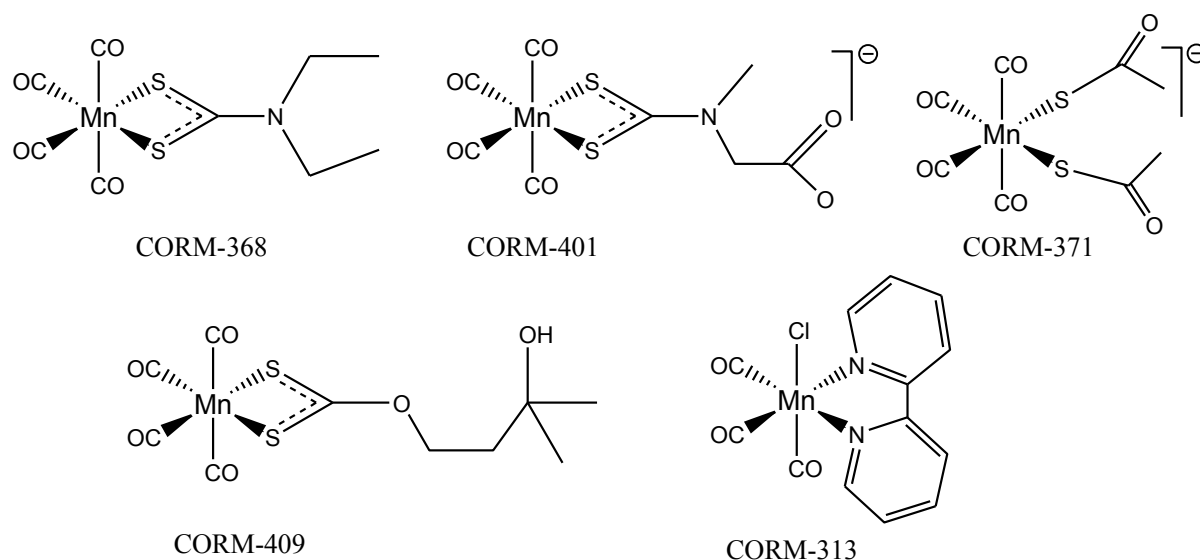


**Fig 1.8:** Chemical structure of Mo(CO)<sub>3</sub>(CNC(CH<sub>3</sub>)<sub>2</sub>COOH)<sub>3</sub> CORM-ALF794 [49].

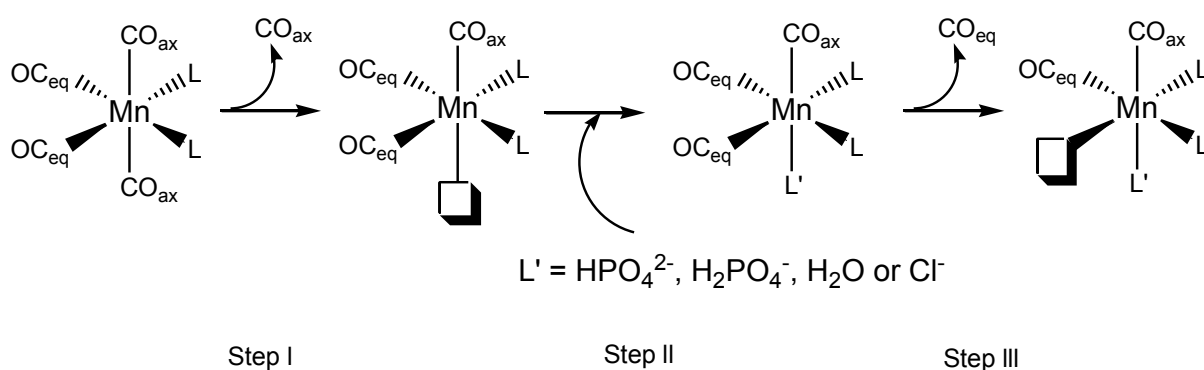
### 1.3.2.2 Manganese CORMs

Manganese carbonyl complexes have been already used as successful carbon monoxide releasing molecules by many groups such as of Motterlini, Mascharak, and Schatzschneider. Initially, a commercially available manganese carbonyl complex like dimanganesedecacarbonyl [Mn<sub>2</sub>(CO)<sub>10</sub>] was studied that requires activation by light to release CO [50]. A series of manganese carbonyls were synthesized by the Motterlini group such as [Mn(CO)<sub>5</sub>Cl] and [Mn(CO)<sub>4</sub>(bpy)]<sup>+</sup> (bpy = 2,2'-bipyridine). These CORMs have t<sub>1/2</sub>(37 °C) values of greater than 900 min for CO release [51]. Thereafter the same group discovered that compounds such as [Mn(CO)<sub>3</sub>X<sub>3</sub>Mn(CO)<sub>3</sub>]<sup>-</sup> (X = Cl, OAc) and [Mn(CO)<sub>4</sub>I<sub>2</sub>]<sup>-</sup> released CO much more rapidly [51].

Recently, many manganese carbonyls have been synthesized by Motterlini coworkers such as CORM-368, CORM-401, CORM-371, CORM-409, and CORM-313 which are shown in figure 1.9 [51-53]. The nature of the Mn-CO bond in these CORMs was characterized by natural bond orbital (NBO) analysis. According to the NBO calculations, the charge transfer is the major source of Mn-CO bond stabilization for this series. On the basis of the nature of the experimental buffers, the nucleophilic attack of putative ligands (L' = HPO<sub>4</sub><sup>-2</sup>, H<sub>2</sub>PO<sub>4</sub><sup>-</sup>, H<sub>2</sub>O, and Cl<sup>-</sup>) at the vacant site of the metal was analyzed by ligand-exchange reaction energies (Scheme 1.5). The analysis revealed that different L'-exchange reactions were spontaneous in all these CORMs.

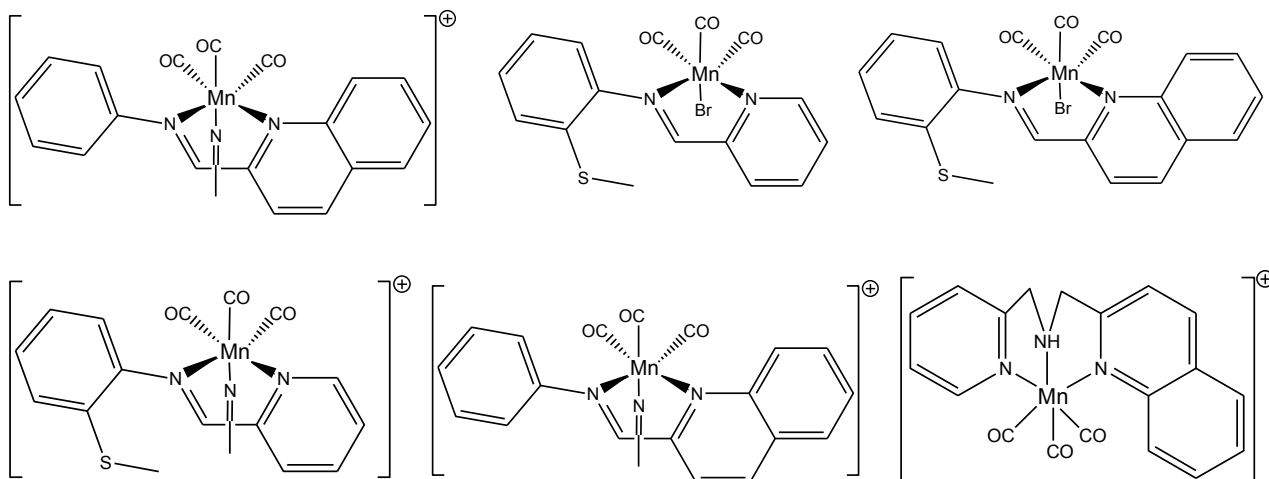


**Fig 1.9:** Structures of CORMs investigated theoretically and by Motterlini and coworkers [53].



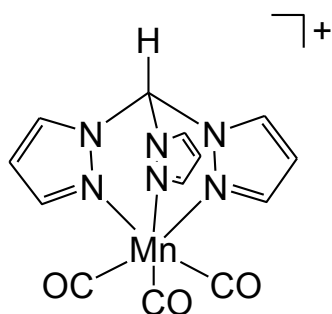
**Scheme 1.5:** Work strategy used to study CO releasing mechanisms in these CORMs series: (Step I) dissociation of an axial CO molecule ( $\text{CO}_{\text{ax}}$ ) *cis* to L from the Mn center, where L=donor atom of mono- or bidentate ligand groups, (Step II) attack of any putative ligand ( $\text{L}'$ ) from the buffer solution at the Mn vacant site; (Step III) dissociation of an equatorial CO molecule ( $\text{CO}_{\text{eq}}$ ), *trans* to L, from the Mn center.

Photolysis has been employed for many manganese carbonyls. The Mascharak and Schatzschneider groups worked in this field and prepared many manganese CORMs that release CO on photolysis with light. Mascharak synthesized a series of manganese carbonyls with ligands that contain extended conjugation and electron-rich donors (figure 1.10) [54,55]. These CORMs readily release CO upon exposure to visible light. In this work density functional theory (DFT) and time dependent DFT (TDDFT) studies indicate that low energy metal to ligand charge transfer (MLCT) transitions from Mn-CO bonding into ligand  $\pi^*$ -orbitals lead to reduction of M-CO( $\pi^*$ ) back-bonding and loss of CO from these photo CORMs [55].



**Fig 1.10:** Structures of CORMs investigated theoretically and experimentally by the Mascharak group [54,55].

Another important success in photo-manganese based CORMs was published by Schatzschneider and coworkers who realized a facial coordination of the tpm (tris(pyrazolyl)methane) ligand to the manganese tricarbonyl unit [56]. The molecular structure for this CORM is shown in figure 1.11.



**Fig 1.11:** The molecular structure of  $[Mn(CO)_3(tpm)]^+$ , (tpm = tris(pyrazolyl)methane) [56].

Furthermore, Kunz and Schatzschneider reported on the synthesis and characterization of a series of manganese photo CORMs with different imidazolylphosphane ligands (figure 1.12) [57]. The substitution pattern of the imidazolylphosphane ligand was found to determine the number of CO molecules released. Whereas the compounds with the imidazol-2-ylphosphane liberate approximately 2 mol of CO per mol of complex, those with the imidazol-4-ylphosphane release only 1 mol of CO per  $Mn(CO)_3$  unit.

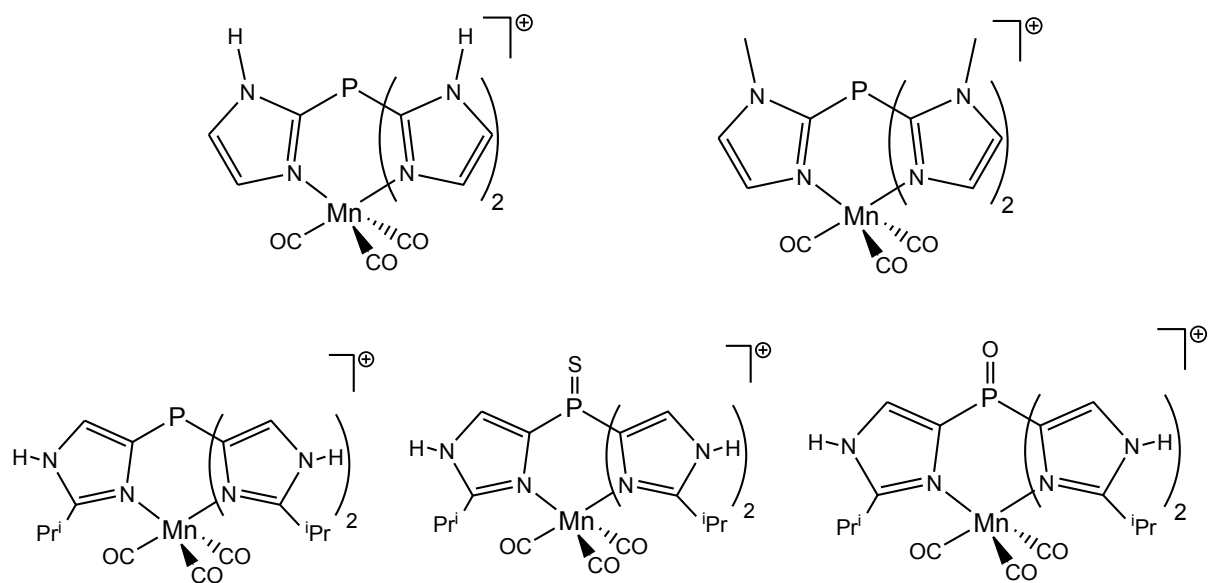


Fig 1.12: Manganese complexes with different imidazolyphosphane ligands [57].

### 1.3.2.3 Rhenium CORMs

A number of rhenium carbonyl complexes were synthesized as CORMs. The Kunz group prepared a series of rhenium photo CORMs which contain the  $\text{Re}(\text{CO})_3$  moiety with imidazolyphosphane ligands (figure 1.13) [57].

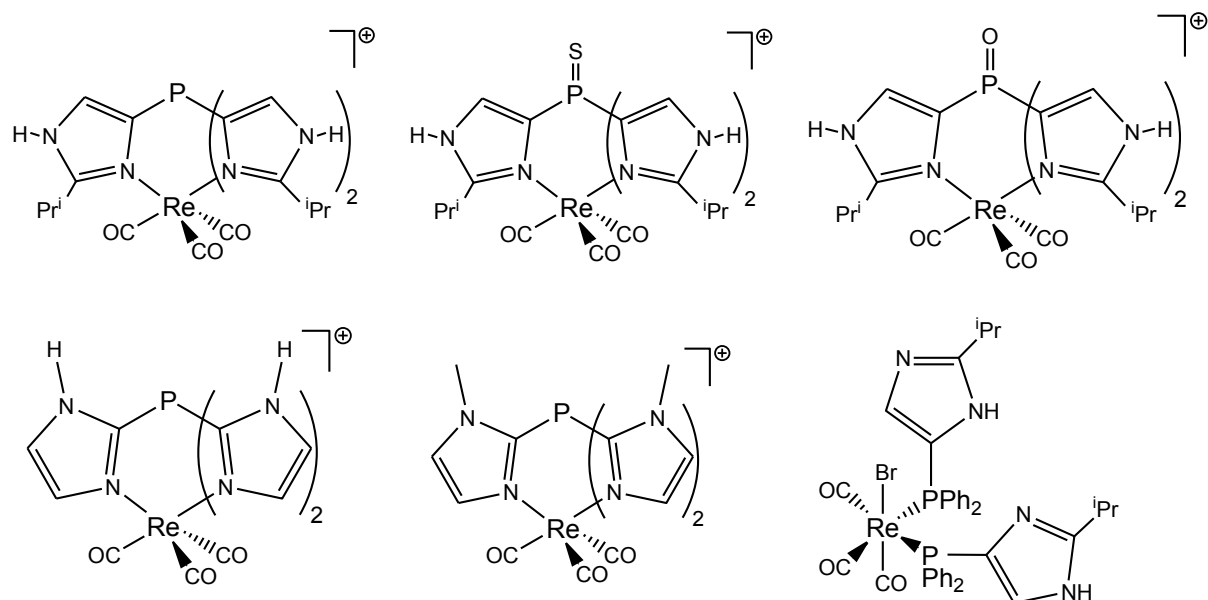
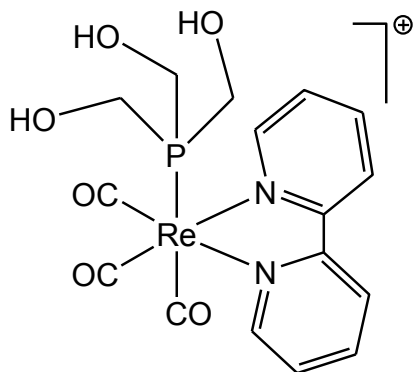


Fig 1.13: Rhenium complexes used as photo-CORMs [57].

Another important rhenium CORM is the water soluble rhenium carbonyl complex  $[\text{Re}(\text{bpy})(\text{CO})_3(\text{thp})]^+$  (bpy = 2,2'-bipyridine, thp = tris(hydroxymethyl)phosphine) as shown in figure 1.14. This complex was prepared by the Ford group in 2012 [58] and is a very promising candidate as photo CORM with potential therapeutic applications.

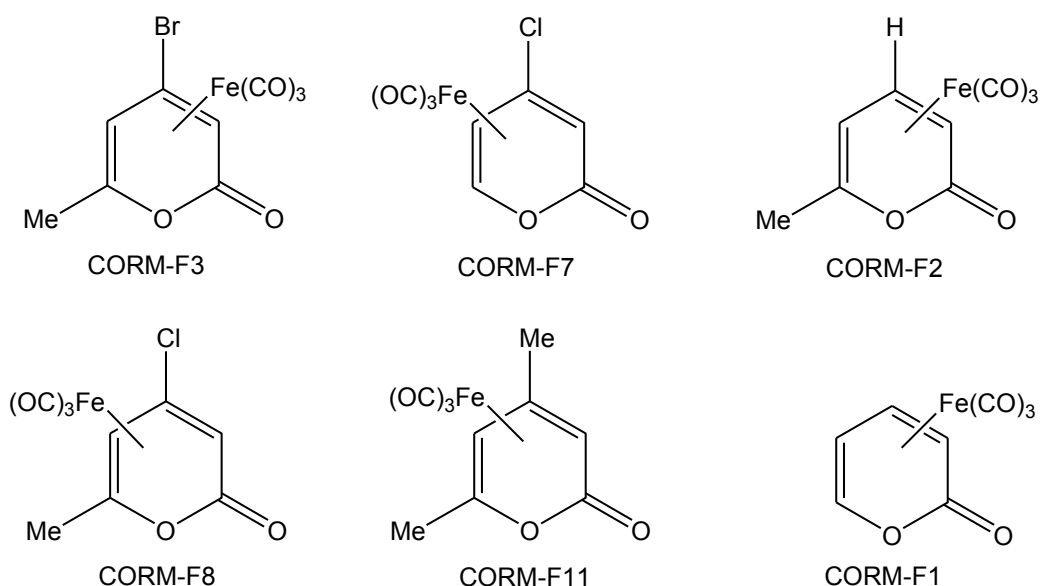


**Fig 1.14:** Water soluble rhenium CORM investigated theoretically and experimentally by the Ford group [58].

Recently a family of 17-electron rhenium complexes containing the  $\text{Re}(\text{CO})_2$ -fragment has been described as ligand substitution rhenium CORMs by the Zobi group [59]. The reaction of  $[\text{Et}_4\text{N}]_2[\text{ReBr}_4(\text{CO})_2]$  (ReCORM-1) with cyanocobalamin ( $\text{B}_{12}$ ) was presented to produce  $\text{B}_{12}\text{-Re}(\text{CO})_2$  derivatives as pharmaceutically acceptable CORMs.

#### 1.3.2.4 Iron CORMs

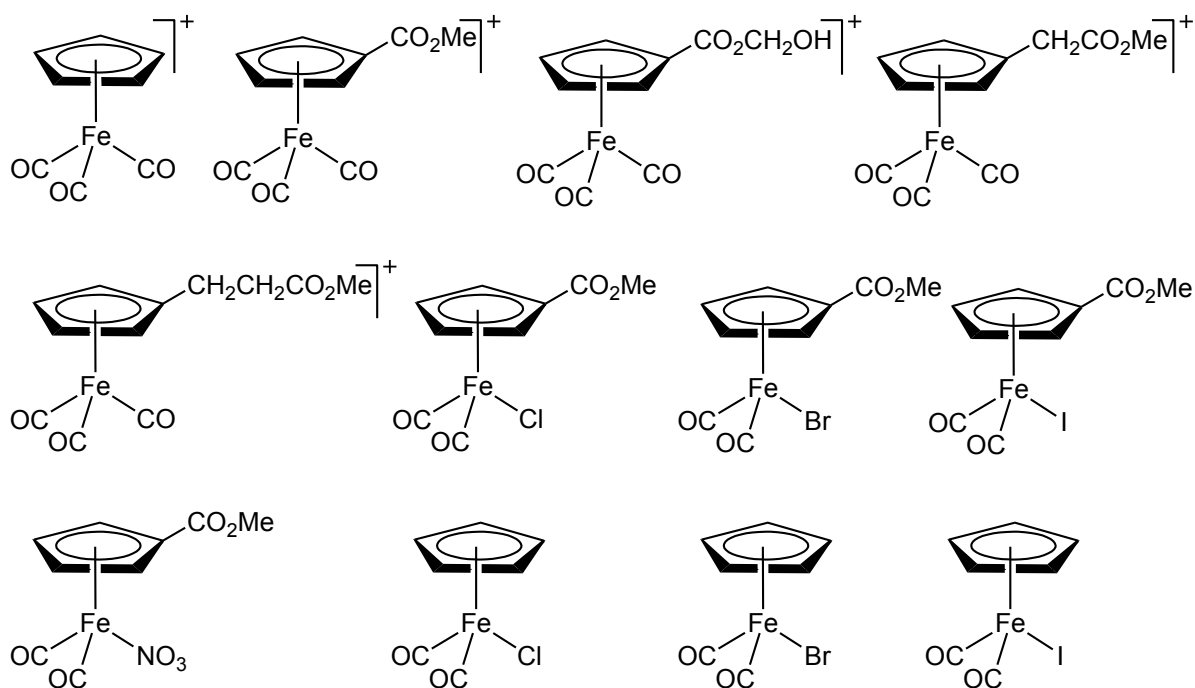
Iron-based carbon monoxide releasing complexes represent a promising target due to the fact that iron is a non toxic 3d metal whose concentration is easily regulated in biological systems because it is naturally present in the body and is a product of heme catabolism by heme oxygenase to produce CO [60]. Therefore it is not surprising that these compounds are under investigation for many years.  $[\text{Fe}(\text{CO})_5]$  represents the first commercially available photo-labile iron CORM [50]. Subsequently a series of irontricarbonyl complexes bearing a 2-pyrone ligand has been evaluated as ligand substitution iron CORMs by the Motterlini group in 2006, these CORMs are shown in figure 1.15 [61-63].



**Fig 1.15:** Chemical structure of irontricarbonyl-2-pyrone complexes [63].

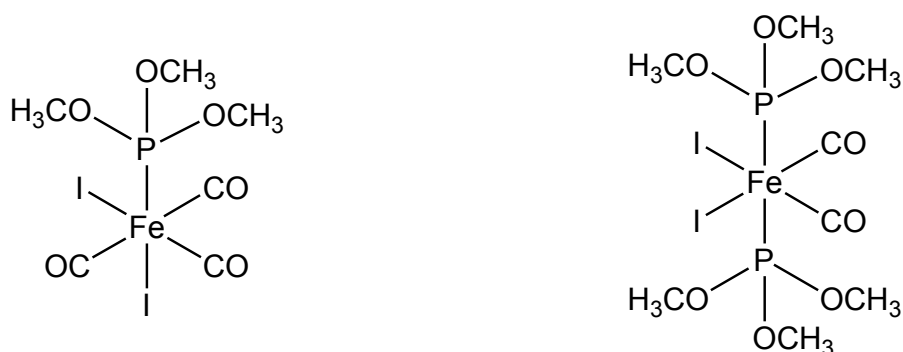
The difference in these complexes is the position of the substituents in the 2-pyrone ring for example 4-bromo and 6-methyl in CORM-F3, 4-chloro and 6-methyl in CORM-F8, 4-chloro and 6-hydrogen in CORM-F7, and 4,6-dimethyl in CORM-F11. The rate of CO release from these CORMs is affected by the presence of a halogen substituent on the 2-pyrone ring [61]; for example a comparison of CORM-F3 and the CORM-F2 demonstrates the importance of the bromide substituent at the 4-position of 2-pyrone. CORM-F3 releases CO while CORM-F2 did not release any detectable amount of CO, this result is in agreement with the qualitative observation that in CDCl<sub>3</sub> solution the CORM-F2 is more stable than CORM-F3 [63].

A year later the same group identified a new group of carbon monoxide releasing molecules based on cyclopentadienyl iron carbonyls [64], as shown in figure 1.16. In this group of ligand substitution iron CORMs, the introduction of a substituent into the cyclopentadienyl ring can be used to control the rate of CO release; for example the introduction of an ester group into the cyclopentadienyl substituent of  $[(\eta\text{-C}_5\text{H}_4\text{CO}_2\text{R})\text{Fe}(\text{CO})_2\text{X}]$  (X= Cl, Br, I) increases the rate of CO loss; this substituent withdraws electron density from the metal weakening the M-CO bond facilitating the CO release process. In addition, introduction of this ester group at the cyclopentadienyl ligand enhances water solubility of this CORM.



**Fig 1.16:** Structures of iron CORMs with cyclopentadienyl ligands [64].

In 2009 the Lynam group incorporated phosphite ligands into the coordination sphere of the iron metal in  $\text{Fe}_2(\text{CO})_4$  to produce iron CORMs which are shown in figure 1.17 [65]. The incorporation of phosphite ligands in this ligand substitution CORMs could modulate the rapid CO release exhibited by  $\text{Fe}_2(\text{CO})_4$  [65]; thus the CO release from these CORMs is slower than from  $\text{Fe}_2(\text{CO})_4$ .

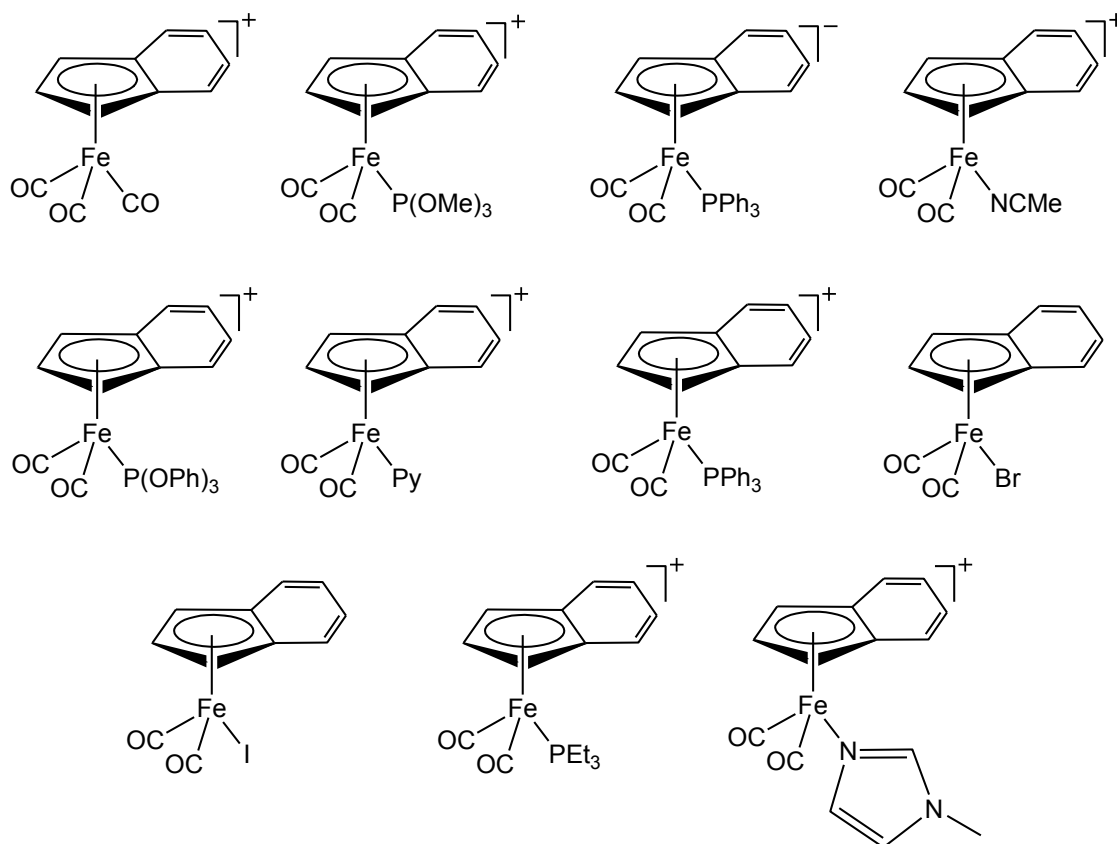


**Fig 1.17:** Structures of iron CORMs with phosphite ligands [65].

In 2010 a paper was published to investigate the effect of enhancement of the  $\pi$ -system on the rate of carbon monoxide release [64], using indenyl ligands as shown in figure 1.18 [66]. The authors expected that these ligand substitution CORMs with indenyl ligands would release CO faster than the corresponding cyclopentadienyl CORMs, however, only  $[\text{Fe}(\eta^5\text{-C}_9\text{H}_7)(\text{CO})_3]^+$  liberates CO faster than the

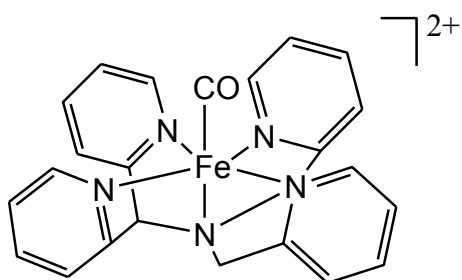


corresponding cyclopentadienyl compound, an unexpected result in this publication [66].



**Fig 1.18:** Structures of iron CORMs with indenyl ligands [66].

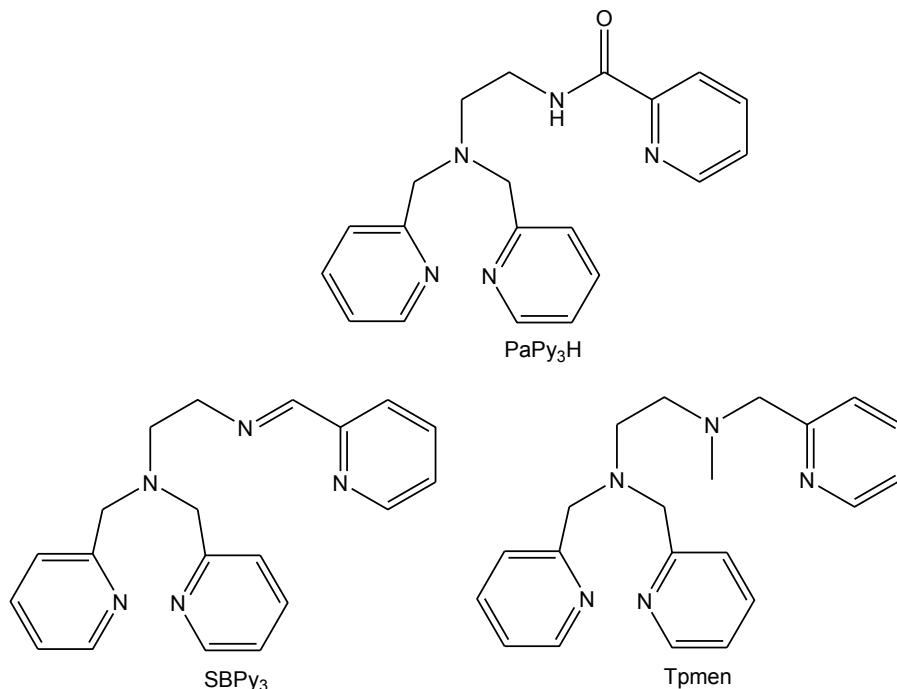
A new iron carbonyl complex was reported in a communication in 2011 [67] as shown in figure 1.19. This compound exhibits exceptional stability in aqueous media due to its slow release of carbon monoxide. Furthermore, CO release can be triggered rapidly by UV light.



**Fig 1.19:** Structures of iron CORM with multidentate pyridyl ligands [67].

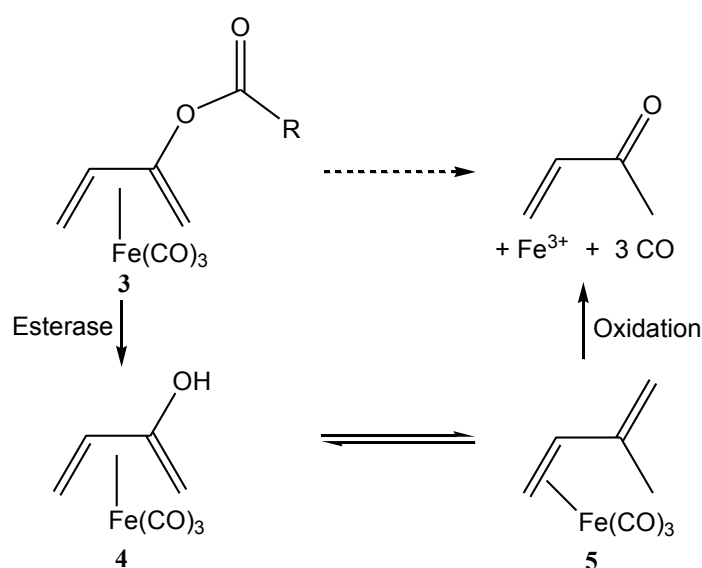
In the same year the Mascharak group investigated three new iron ligand substitution CORMs which had been synthesized from a designed polypyridine ligand [68]. These ligands are expected to stabilize Fe(II) centers and allow CO binding.

Figure 1.20 shows the chemical structures for these polypyridine ligands, the structurally related series for these CORMs being  $[(\text{PaPy}_3)\text{Fe}(\text{CO})]$  ( $\text{ClO}_4$ ),  $[(\text{SBPy}_3)\text{Fe}(\text{CO})](\text{BF}_4)_2$ , and  $[(\text{Tpmen})\text{Fe}(\text{CO})](\text{ClO}_4)_2$  [68,69]. In the structurally related series, the design allowed to arrange carbonyl ligand *trans* to a carboxamido-N (strong  $\sigma$ -donor), an imine-N (moderately  $\pi$ -accepting) and a tertiary amine-N (weak  $\sigma$ -donor) center, respectively. Strong CO stretching vibrations ( $\nu_{\text{CO}}$ ) at 1972, 2010, and 2012  $\text{cm}^{-1}$ , respectively, confirm the presence of three bound CO ligands. The change from a strong  $\sigma$ -donating and negatively charged carboxamido-N donor in the first complex to a neutral (and moderately  $\pi$ -accepting) imine-N or weak tertiary-N donor in the second and third complexes, respectively, increases the  $\nu_{\text{CO}}$  value from the first to the third complex as shown by IR spectroscopy. This increase in  $\nu_{\text{CO}}$  values clearly demonstrates that as more electron density is pushed toward the Fe(II) center, it transfers part of the electron density to the antibonding orbital of the bound CO ligand *trans* to it (as is the case in the first complex). Such transfer strengthens the Fe-CO bond in the first complex more than the other two carbonyls and makes it slow CO-releasing [69].

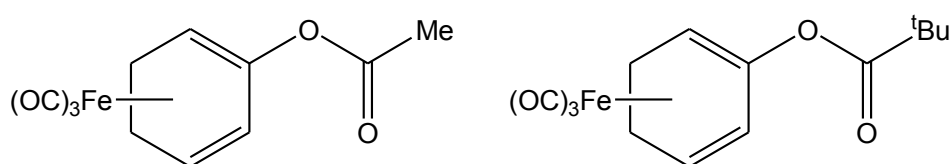


**Fig 1.20:** Chemical structures of pentadentate polypyridine ligands [69].

Enzyme triggered carbon monoxide releasing molecules (ET-CORMs) represents a new concept in the CORMs field. Amslinger and Schmalz introduced acyloxybutadiene- iron tricarbonyl complexes as enzyme-triggered CO-releasing molecules ET-CORMs [77]. The idea resulted from an earlier observation that dienol-iron tricarbonyl complexes like **4** are very labile and readily decompose already under slightly oxidative conditions (presumably *via* a 16-VE intermediate of type **5**), such complexes could potentially act as CORMs, provided that they can be generated under physiological conditions from stable precursors. An appealing possibility would be the use of dienylester complexes of type **3**, which are expected to be sufficiently stable. However, once such complexes have entered a cell they may be cleaved by intracellular esterase. The oxidative decomposition of the resulting dienol-iron tricarbonyl complexes **4** would then be linked to the release of three molecules of CO (Scheme 1.6). To probe this concept, they first had to synthesize some potentially suitable acyloxydiene-iron tricarbonyl complexes, which were prepared from cyclohexenone (figure 1.21) [70].

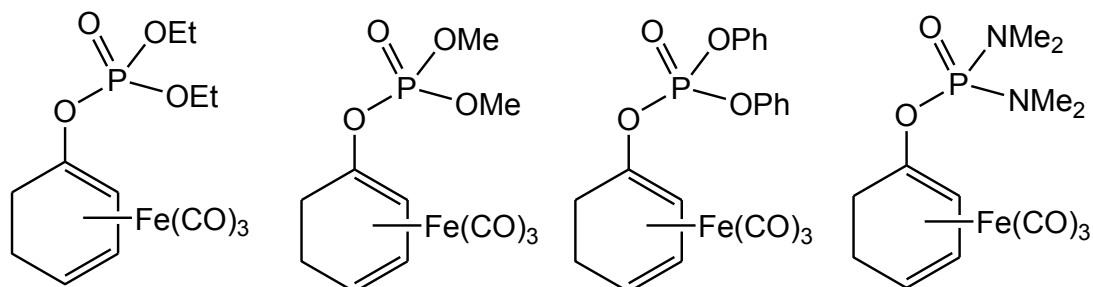


**Scheme 1.6:** Proposed mode of action of enzyme-triggered CO-releasing molecules (ET-CORMs) of type **3**.



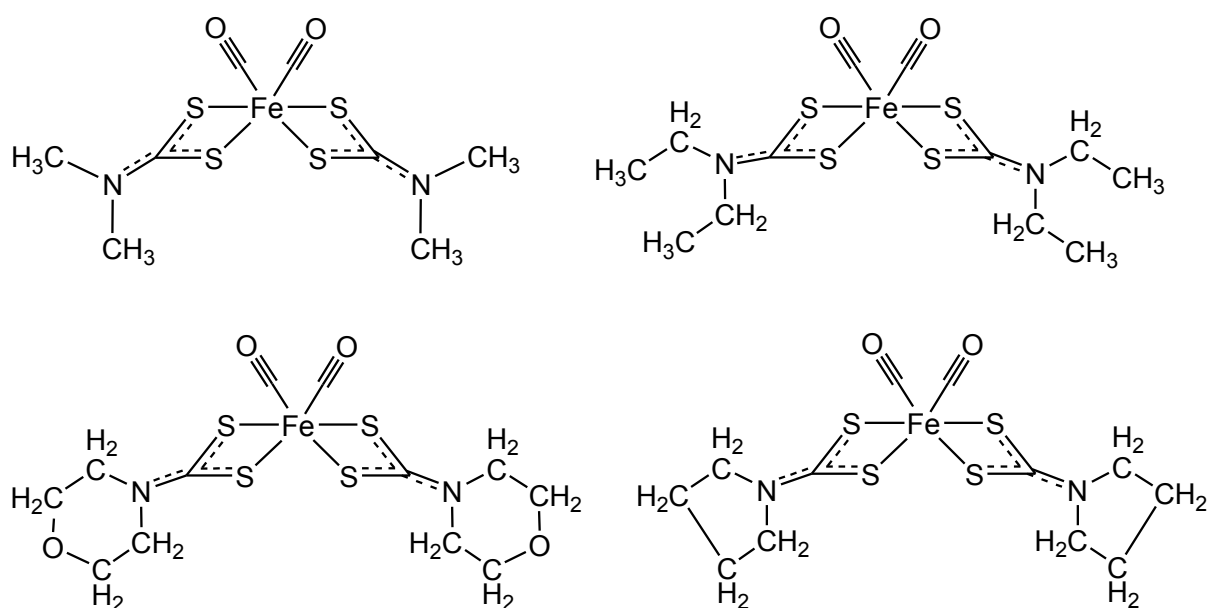
**Fig 1.21:** Structures of the acyloxybutadiene iron tricarbonyl complexes [70].

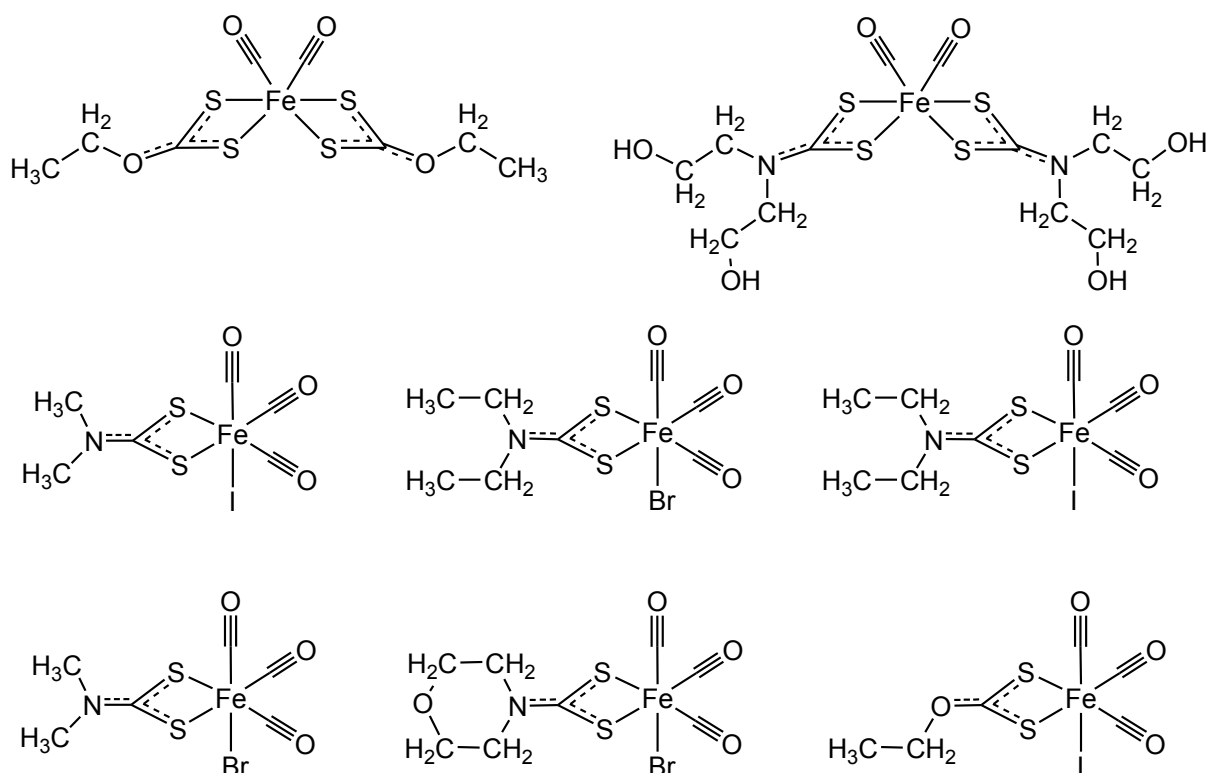
In the search for enzyme triggered CO-releasing molecules (ET-CORMs) with improved properties, the Schmalz group studied and reported phosphoryloxy-substituted (cyclohexadiene)Fe(CO)<sub>3</sub> complexes as the first potentially water soluble compounds as shown in figure 1.22 [71].



**Fig 1.22:** Structures of the phosphoryloxy-substituted (cyclohexadiene) iron tricarbonyl complexes [71-73].

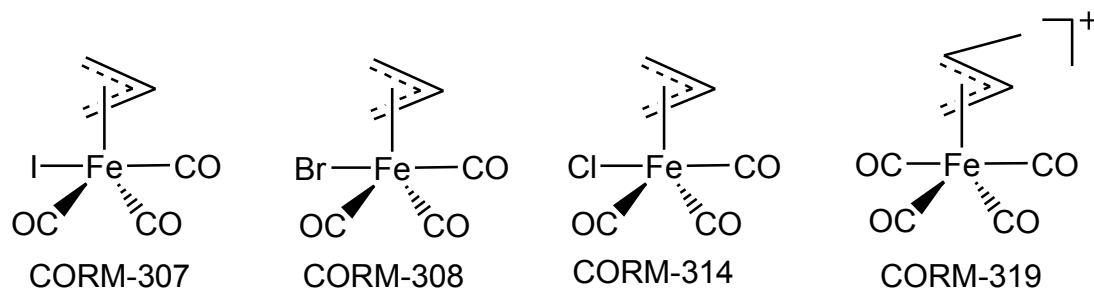
Recently, a new ligand substitution CORMs based on iron metal were reported (figure 1.23) [74]. In this study the information on the mechanism of CO release comes from calculations on the stability of the species involved in sequential CO loss from [Fe(CO)<sub>3</sub>Br(S<sub>2</sub>CNMe<sub>2</sub>)] and [Fe(CO)<sub>2</sub>(S<sub>2</sub>CNMe<sub>2</sub>)<sub>2</sub>]. The complexes of the type [Fe(CO)<sub>3</sub>X(S<sub>2</sub>CNR<sub>2</sub>)] liberate 2 mol of CO very rapidly and the final mole of CO is liberated more slowly. CO loss is much slower from [Fe(CO)<sub>2</sub>(S<sub>2</sub>CNR<sub>2</sub>)<sub>2</sub>] and is not observed from [Fe(CO)<sub>2</sub>(S<sub>2</sub>COEt)<sub>2</sub>]. [Fe(CO)<sub>3</sub>l(S<sub>2</sub>COCH<sub>2</sub>CH<sub>3</sub>)] is an exception, where only 0.4 mol of CO is released. It is probable that the electron-withdrawing ability of O results in stronger CO bonding and less electron density to stabilize the five-coordinate intermediate.





**Fig 1.23:** Structures of iron CORMs investigated experimentally and theoretically [74,75].

Very recently, the Motterlini group studied and reported the effects of newly synthesized CO-RMs containing an iron-allyl moiety by specifically analyzing the CO releasing properties in relation to their biochemical, biological and pharmacological parameters including solubility, cytotoxicity profile as well as vasodilatory and anti-inflammatory activities *in vitro* [76]. The chemical structures for these ligand substitution CORMs are shown in figure 1.24. CORM-307, CORM-308 and CORM-314 that are soluble in DMSO release CO with faster rate than CORM-319 which is soluble in water and liberates CO with a slower rate.



**Fig 1.24:** Structures of iron CORMs with allyl moiety [76].

### 1.3.2.5 Ruthenium CORMs

Photo-labile ruthenium carbonyl complexes represent an important target because these systems are often more air-stable and less labile than the other metal carbonyl complexes such as iron carbonyls.

CORM-2 and CORM-3 which are shown in figure 1.25 represent the most important ruthenium carbonyls well-known as carbon monoxide releasing molecules [50,77].



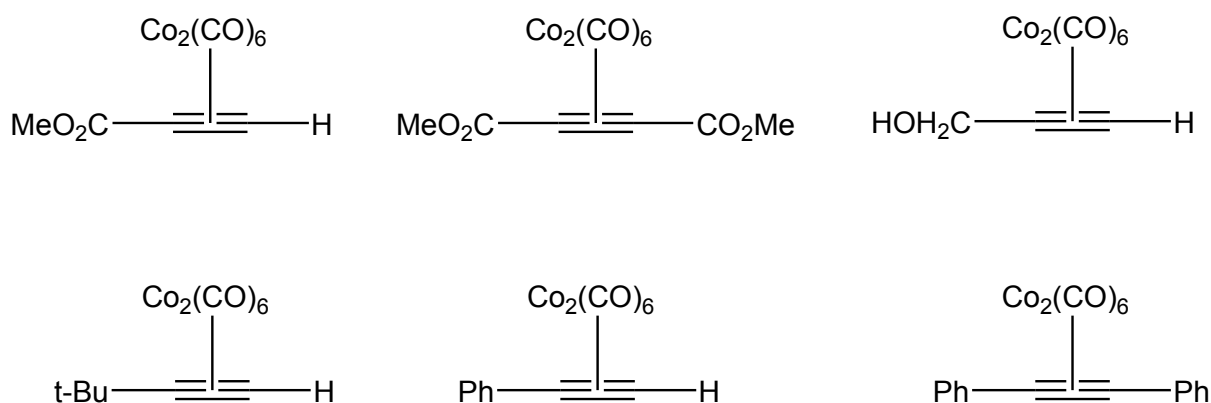
**Fig 1.25:** Most important ruthenium CORMs up to now, CORM-2 [Ru<sub>2</sub>(CO)<sub>6</sub>Cl<sub>4</sub>] (left), and CORM-3 [Ru(CO)<sub>3</sub>Cl-(glycinate)] (right), which was first synthesized as CORM by the Motterlini group.

CORM-2 is a commercially available ruthenium carbonyl complex which firstly had been employed as carbon monoxide releasing molecule in 2002 by the Motterlini group [50]. Although CORM-2 acted as a very efficient substitution CORM, it is insoluble in water and only releases 0.9 mol of CO per mol CORM-2 to myoglobin [78]. In view of the fact that [Ru<sub>2</sub>(CO)<sub>6</sub>Cl<sub>4</sub>] represents an efficient CORM, emphasis was placed on literature compounds and their analogues containing the Ru(II)(CO)<sub>3</sub> fragment. Amino acids were used as one of the most substantial ligands with this fragment because they are naturally present in the body and should not cause toxicity problems [79].

The most promising compound in this family is CORM-3 [Ru(CO)<sub>3</sub>Cl-(glycinate)] which was also synthesized by the Motterlini group in 2003. CORM-3 represents the first known air-stable and water-soluble carbon monoxide releasing molecule, with similarities to CORM-2; it releases CO by ligand substitution as inducing factor for the CO liberation process [33,77]. This compound has become popular as a CORM to study the effect of CO on a wide range of biological systems, and approximately 100 papers have appeared so far on its use.

### 1.3.2.6 Cobalt CORMs

Several cobalt carbonyl complexes were synthesized as CORMs. Fairlamb and Motterlini reported a series of carbon monoxide releasing molecules based on  $\mu_2$ -alkyne dicobalthexacarbonyl complexes in 2009, these complexes are shown in figure 1.26 [41].



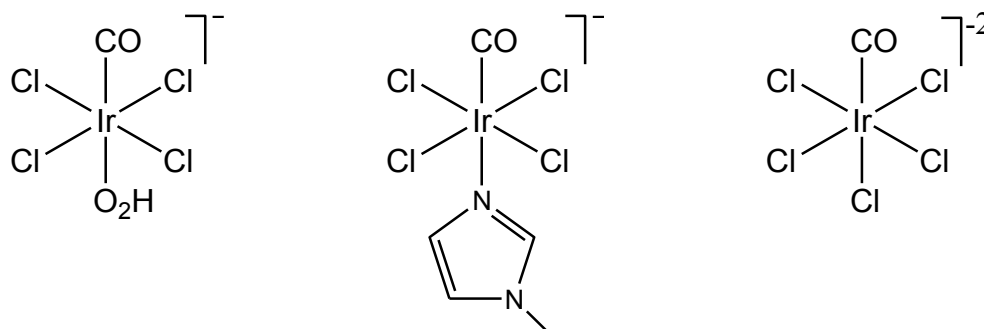
**Fig 1.26:**  $\mu_2$ -Alkyne dicobalt(0)hexacarbonyl complexes investigated by Fairlamb and Motterlini [41].

The rationale for selecting these  $\mu_2$ -alkyne dicobalthexacarbonyl complexes was two-fold: (i) 18-electron cobalt(0) carbonyl complexes possess labile CO ligands; [80] (ii) the alkyne ligand allows the electronic properties of the cobalt(0) center to be modulated, which may, in turn, allow control over the release rate. It is worthy of note that this class of compounds exhibit cytotoxicity towards leukaemia and tumour cells [81-85]. In addition, the first organometallic peptide conjugate was based on a cobalt(0) carbonyl-alkyne enkephalin derivative, which also exhibits toxicity against tumour cells [86].

### 1.3.2.7 Iridium CORMs

Iridium carbonyl complexes represent a new family of compounds as potential carbon monoxide releasing molecules. On the basis of substitution, based on tetrachlorocarbonyliridate(III) derivatives as shown in figure 1.27 [87]. This quite simple moiety has shown to be robust enough to stabilize coordinated S-nitrosothiols, N-nitrosamines, and C-nitroso compounds [88-92]. At the same time, the chloride *trans* to the CO (or N(OR)) moiety is labile enough to be replaced by other ligands

[93]. These compounds are soluble in water and release CO under physiological conditions.



**Fig 1.27:** Structures of iridium-based CORMs investigated theoretically and experimentally [87].

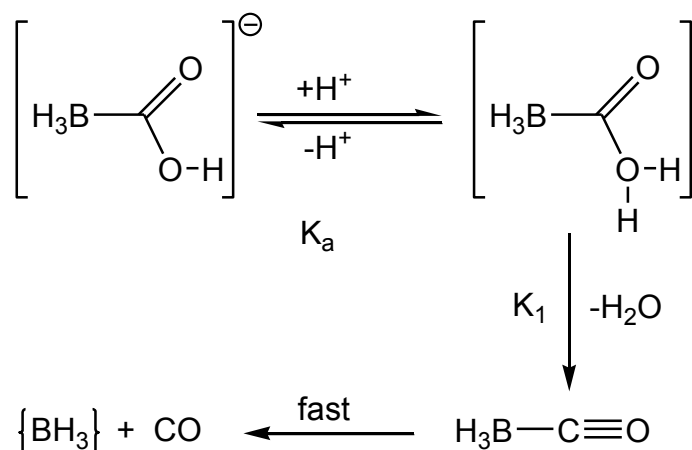
The most interesting feature of these CORMs is the poor backdonation from the iridium center to the CO in favor to the CO releasing properties. This effect can be verified by the calculated population (NPA) of the CO moieties in each one of these complexes [87].

### 1.3.2.8 Non-transition-metal CORMs

There is one group of non-transition-metal compounds which release carbon monoxide, namely  $\text{Na}[\text{H}_3\text{BCO}_2\text{H}]$  (CORM-A1) and  $\text{Na}[\text{H}_3\text{BCONR}_2]$  [94-96]. CORM-A1 represents a water soluble CORM and does not contain a transition metal, in addition it liberates carbon monoxide at a very slow rate under physiological conditions, which may be advantageous in the treatment of chronic conditions that require carbon monoxide to be delivered in a carefully controlled manner. The release of CO from CORM-A1 is both pH- and temperature-dependent; this was demonstrated by using a myoglobin assay and an amperometric carbon monoxide electrode [94]. Interestingly, the time required to completely release CO from CORM-A1 gradually decreased by lowering the pH values [94].

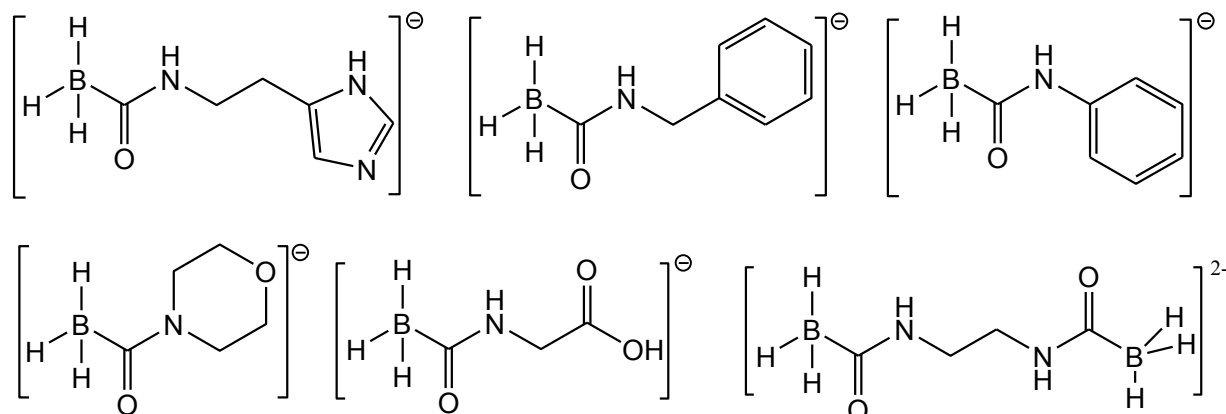
The aqueous solutions of CORM-A1 are alkaline and very stable at room temperature, but in the presence of protons, the compound starts to decompose and to liberate carbon monoxide [97]. CORM-A1 is involved in two acid/base equilibria and loses CO as a result of the reaction with protons at physiological pH values as shown in Scheme 1.7.





**Scheme 1.7:** pH dependency of CO release from  $[\text{H}_3\text{BCO}_2\text{H}]^-$  (CORM-A1).

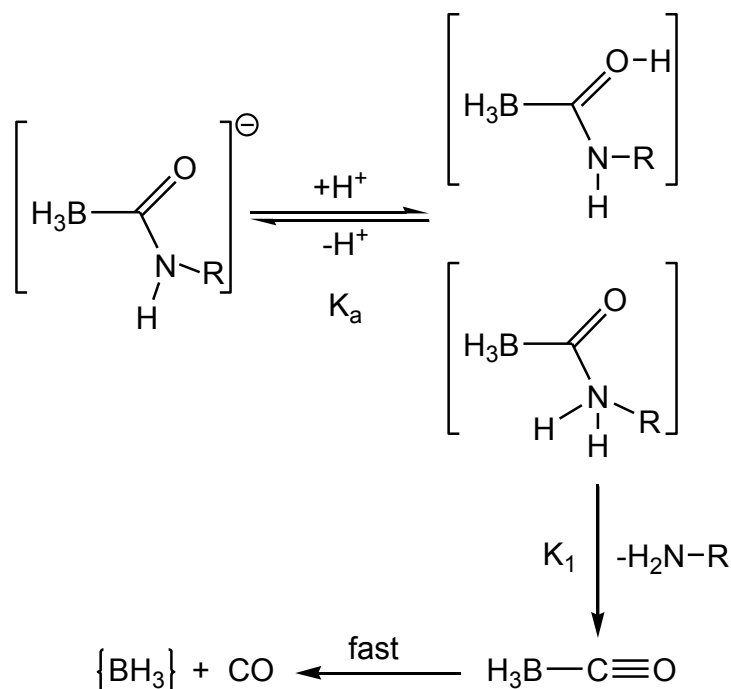
After CORM-A1 a number of boranocarbamates  $[\text{H}_3\text{BCONR}_2]^-$  were prepared from  $[\text{H}_3\text{BCO}_2\text{H}]^-$  in 2010 [96] (figure 1.28). Since protonation of an amide in these compounds is more difficult than of the acid(-COOH) group in CORM-A1, these compounds release CO at a much slower rate than the parent compound and are therefore potential carbon monoxide releasing molecules for biological and medicinal application.



**Fig 1.28:** Boranocarbamate derivatives of  $\text{Na}[\text{H}_3\text{BCO}_2\text{H}]$  [96].

The half lives of these boranocarbamate derivatives were calculated at different pH values [96]. They have the same results as CORM-A1, thus the half life time gradually decreased by lowering the pH values, but the half life values itself are higher than those of CORM-A1; the reason for this finding is based on the fact that

an amide in these compounds is more challenging to protonate than of the carboxylic acid group in CORM-A1. Scheme 1.8 shows the mechanism which has been proposed for the CO release from the boranocarbamate derivatives [96].



**Scheme 1.8:** Proposed mechanisms of CO release from the boranocarbamate derivatives. Step (1): the amides of the compounds are protonated in a rapid, amide  $pK_a$ -dependent equilibrium; step (2): the rate-limiting step for this mechanism is the elimination of the amine ( $k_1$ ) yielding  $H_3BCO$ ; step (3):  $H_3BCO$  decomposes rapidly to release CO.

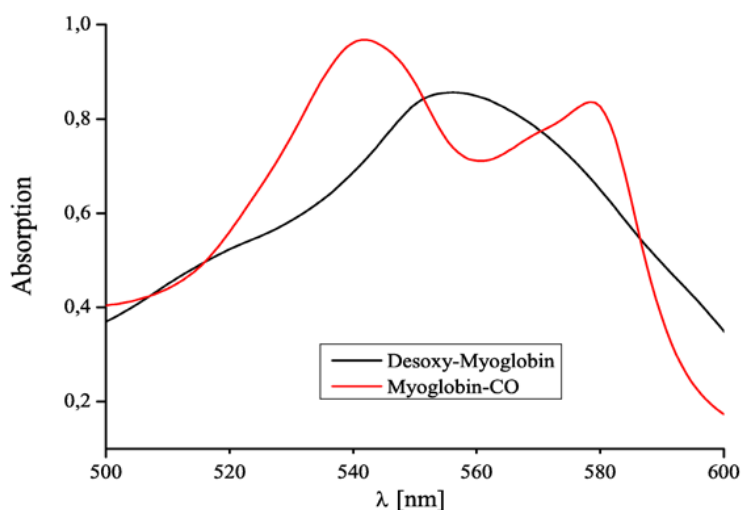
#### 1.4 Myoglobin assay

The most important analytical question concerns quantification of the amount of carbon monoxide released by a CORM during mode of action. In comparable experiments with nitric oxide, NO-specific microelectrodes have been used for such quantitative measurements [98,99]. These are remarkably sensitive but are also notoriously difficult to use with good reproducibility. In this context, it is notable that the use of a CO electrode was reported several years ago [94] to be useful for monitoring CO release from a CORM. In addition, an electrochemical-based gas analyzer has been used for monitoring of exhaled CO from asthmatic and diabetic patients [100,101]. By far the most common analytical method used for this purpose is based on monitoring the conversion of a buffered aqueous solution of deoxy-myoglobin to carboxy-myoglobin at a pH value of 7.4. This technique allows to

evaluate the potential release of CO from CORMs and the myoglobin acts as CO trapping agent in this assay (equation 12) [41].

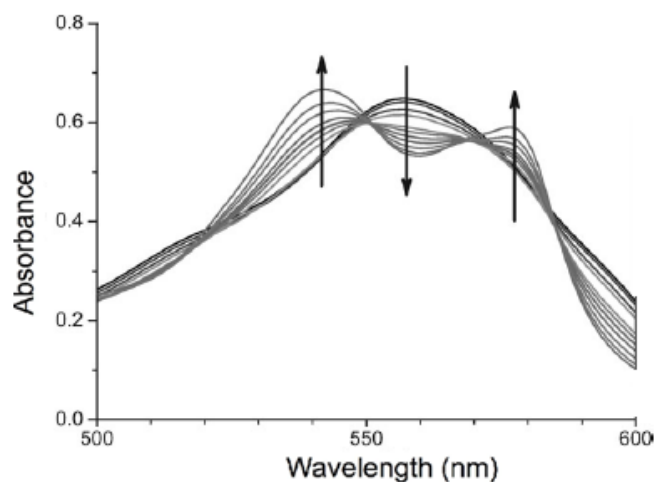


The CORMs are added as a solution in dimethylsulfoxide to a solution of buffered deoxy-myoglobin in water at 37°C (it was mentioned in the CORMs literature, that the final concentration of the CORM in the myoglobin buffered aqueous solution should range between 10-100  $\mu\text{mol/L}$ ), in the presence of sodium dithionite as reducing agent. Deoxy-myoglobin shows an absorption maximum at 560 nm, during the reaction with CO two absorption maxima at 540 and 578 nm are formed, whereas a decreasing intensity for the absorption at 560 nm is observed. At the same time the conversion of deoxy-myoglobin to carboxy-myoglobin shows five isosbestic points at 504, 517, 551, 571, and 586 nm (figure 1.29).



**Fig 1.29:** Absorption spectra of deoxy-myoglobin and carboxy-myoglobin in the range of 500-600 nm (phosphate buffer, pH 7.4, 37°C, [Mb] =100  $\mu\text{M}$ ).

The UV/Vis spectral change in the Q band region after addition of  $[\text{Mn}(\text{CO})_3(\text{tpm})]^+$ , (tpm = tris(pyrazolyl)methane) to deoxy-myoglobin solution and irradiation with light is an example of this myoglobin assay as depicted in figure 1.30 [56].



**Fig 1.30:** UV/Vis spectral changes in the Q band region of myoglobin solution (75 mmol/L) with  $[\text{Mn}(\text{CO})_3(\text{tpm})]^+$  (20 mmol/L) in 0.1 M phosphate buffer upon irradiation at 365 nm ( $t = 0$  to 100 min).

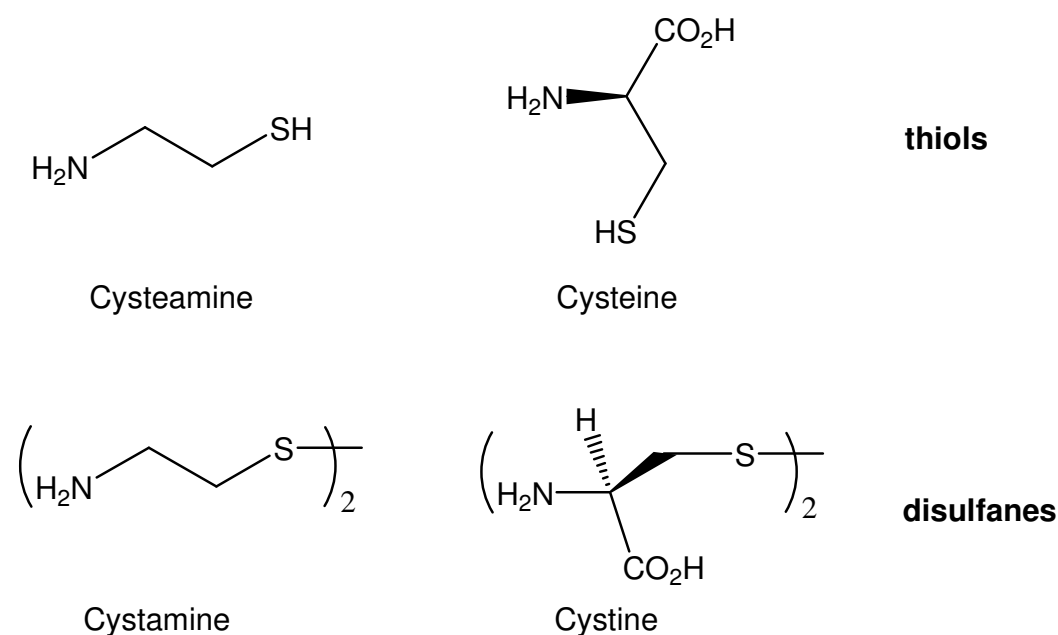
The dissociation constant for carboxy-myoglobin is 37 nM and the changes in the absorption spectra are substantial owing to the strong, distal-ligand sensitive Soret and Q-bands, so the sensitivity of this method for detecting CO released into the medium is quite good [50]. A recent article by Atkin et al. very nicely summarizes the applications of this technique as well as the necessary purification procedures, etc. in order to ensure its accuracy [102]. However, since myoglobin is an oxygen sensor, this methodology is not compatible with photolyses in aerated media, so there is a need to develop quantitative methods that avoid that limitation. Another complication of the myoglobin assay for CO is that this protein is strongly colored in the near UV and visible regions of the spectrum and these absorbances may interfere with photochemical processes *via* inner filter effects if the myoglobin is present in the solution. In this context, Rimmer et al. [103] reported three analytical procedures for determining the quantity of CO released from photoCORMs that leave the spectrum of the photolysis solution unperturbed and that are compatible with studies in aerated media. Moreover Mclean et al. [104] described an oxy-hemoglobin as a convenient assay for CO release from CORMs Instead of myoglobin assay.

In our study we are interested to investigate photo- induced iron(II)-based CORMs with various groups of ligands; N/S ligands such as cysteamine and 2-aminothiophenol in  $[\text{Fe}(\text{CO})_2(\text{SCH}_2\text{CH}_2\text{NH}_2)_2]$  (CORM-S1) and  $[\text{Fe}(\text{CO})_2(\text{SC}_6\text{H}_4\text{-2-NH}_2)_2]$  (CORM-S2), respectively, and N/P ligands such as 2-(diphenylphosphino)ethylamine and 2-(diphenylphosphino)aniline in  $[\text{Fe}(\text{CO})(\text{NC-Me})(\text{H}_2\text{NCH}_2\text{CH}_2\text{PPh}_2)_2]^{2+}$  (CORM-P1) and  $[\text{Fe}(\text{CO})(\text{NC-Me})(\text{H}_2\text{NC}_6\text{H}_4\text{-2-PPh}_2)_2]^{2+}$  (CORM-P2) respectively. Furthermore we will report here the investigation of iron carbonyl complexes with different phosphorus-containing ligands such as trichloro phosphine in  $[\text{Fe}(\text{CO})_4(\text{PCl}_3)]$  (CORM-P3),  $[\text{Fe}_2(\text{CO})_6(\text{PCl}_2)_2]$  (CORM-P6), [*p*-*N,N*-dimethylaminophenyl)dichlorophosphine] in  $[\text{Fe}(\text{CO})_4(\text{PCl}_2\text{C}_6\text{H}_4\text{-}p\text{-NMe}_2)]$  (CORM-P4), [(morpholino)dichlorophosphine] in  $[\text{Fe}(\text{CO})_4(\text{PCl}_2\text{N}(\text{CH}_2\text{CH}_2)_2\text{O})]$  (CORM-P5), [*p*-trifluoromethylphenyl)dichlorophosphine] in  $[\text{Fe}_2(\text{CO})_6\{\text{PCl}(\text{C}_6\text{H}_4\text{-CF}_3)\}_2]$  (CORM-P7), and calciumbis(diphenylphosphanide) in  $[(\text{thf})_4\text{Ca}\{\text{Fe}_2(\text{CO})_6(\mu\text{-CO})(\mu\text{-PPh}_2)\}_2]$  (CORM-FC).

## 2. Results and discussion

### 2.1 N/S-iron-based CORMs

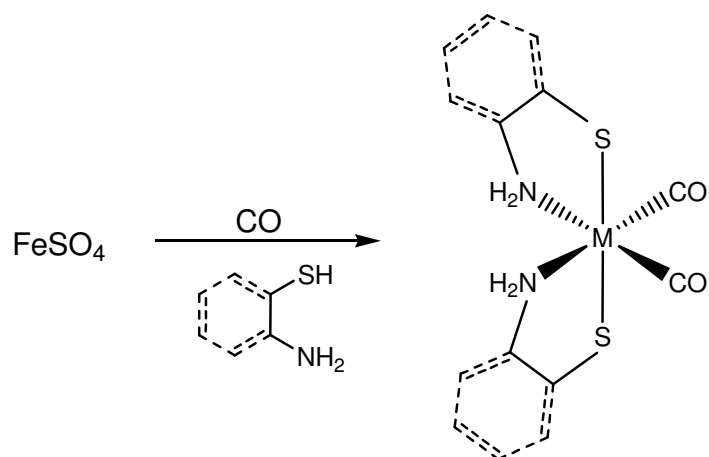
CORMs with medicinal applications have to meet certain preconditions. They and their degradation products must be non-toxic. Therefore we started our investigations with bidentate ligands with N- and S-donors such as cysteine. The iron(II) complexes  $[\text{Fe}(\text{CO})_2(\text{SCH}_2\text{CH}_2\text{NH}_2)_2]$  (CORM-S1) and  $[\text{Fe}(\text{CO})_2(\text{SC}_6\text{H}_4\text{-2-NH}_2)_2]$  (CORM-S2) represent our examples of N/S containing CORMs. Iron complexes with biogenic ligands such as cysteine and isocysteine contain reversibly bound carbon monoxide [105,106]. Twenty years ago a systematic approach verified that iron(II) thiolates generally act as CO carriers with reversibly bound carbon monoxide [107] making these compounds ideal CORMs for medicinal and physiological applications. We focused our research on biogenic ligands derived from cysteamine (Scheme 2.1).



**Scheme 2.1:** Biogenic ligands derived from cysteamine.

### 2.1.1 Synthesis

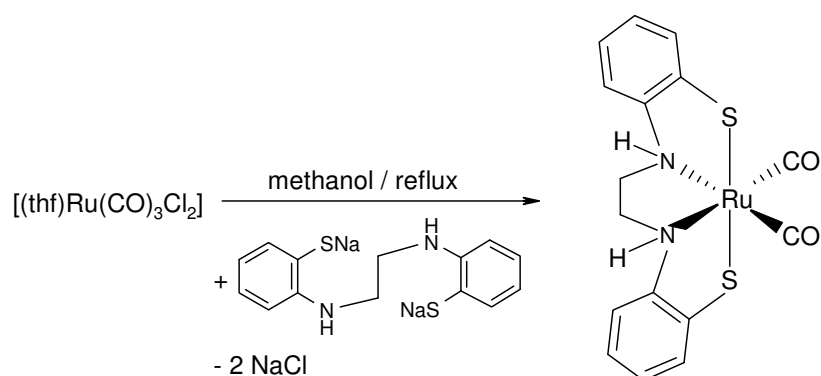
The complexes  $[\text{Fe}(\text{CO})_2(\text{SCH}_2\text{CH}_2\text{NH}_2)_2]$  (**1**) and  $[\text{Fe}(\text{CO})_2(\text{SC}_6\text{H}_4\text{-2-NH}_2)_2]$  (**2**) were prepared earlier from  $\text{FeSO}_4$  and the appropriate thiol in methanol in the presence of  $\text{NEt}_3$  in a CO atmosphere in poor yields (Scheme 2.2) [108].



**Scheme 2.2:** Synthesis of  $[\text{Fe}(\text{CO})_2(\text{SCH}_2\text{CH}_2\text{NH}_2)_2]$  (CORM-S1) and  $[\text{Fe}(\text{CO})_2(\text{SC}_6\text{H}_4\text{-2-NH}_2)_2]$  (CORM-S2) starting from  $\text{FeSO}_4$ .

A similar procedure using KOH as a base was published for the synthesis of **2** in 43% yield [109] which crystallized as **2**·THF with the THF molecule bridging the amino functionalities *via* hydrogen bridges. However, the bridging THF clamp does not influence the coordination pattern of iron(II) because in complexes of the type  $[\text{Fe}(\text{CO})_2(\text{SR})_2(\text{en})]$  (en = ethylenediamine), the thiolate ligands also show a *trans* arrangement and the two carbonyl ligands a *cis* alignment. We have shown in physiological studies that THF-free **1** is an ideal CORM with a similar coordination sphere of the iron(II) center that releases CO upon irradiation with visible light. In addition, **2** was prepared from the reaction of bis(2-aminophenyl)disulfane with the  $[\text{HFe}(\text{CO})_4]^-$  anion [110]. Mechanistically, the first step was proposed as the addition of the Fe-H bond to the disulfane moiety to give intermediate  $[(\text{OC})_4\text{Fe}(\text{SC}_6\text{H}_4\text{-2-NH}_2)]^-$  with the liberation of 2-aminothiophenol. The oxidative addition of another equivalent of disulfane to this iron(0) anion yielded  $[(\text{OC})_3\text{Fe}(\text{SR})_3]^-$ . Subsequent loss of a 2-aminothiophenolate anion and one carbonyl molecule finally gave **2**.

Ruthenium-based CORMs (e.g. CORM-2 and CORM-3) release CO upon ligand substitution. The orange-brown diamagnetic complex  $[\text{Ru}(\text{CO})_2(\text{SC}_6\text{H}_4\text{-2-NH}_2)_2]$  (**4**) was prepared in 30% yield by the reduction of  $\text{RuCl}_3$  with CO in ethanol and subsequent addition of 2-aminothiophenol [111]. The IR spectrum of **4** shows CO stretching vibrations at 2035 and 1970  $\text{cm}^{-1}$ . Iron and ruthenium complexes with comparable metal environments have been studied by Sellmann and coworkers [112-116] who showed that these complexes are thermally stable but release one CO ligand upon UV irradiation, which leads to subsequent ligand substitution. These compounds were prepared from the reaction of  $[(\text{thf})\text{Ru}(\text{CO})_3\text{Cl}_2]$  with the sodium salt of 1,2-bis(2-mercaptoanilino)-ethane and 2,3-bis(2-mercaptoanilino)butane (Scheme 2.3) [112] and show coordination spheres similar to the related iron(II) compounds.

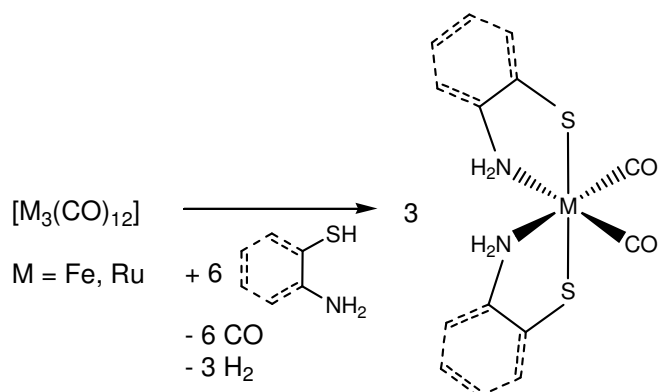


**Scheme 2.3:** Synthesis of a ruthenium complex with  $\text{Ru}(\text{CO})_2\text{N}_2\text{S}_2$  coordination pattern.

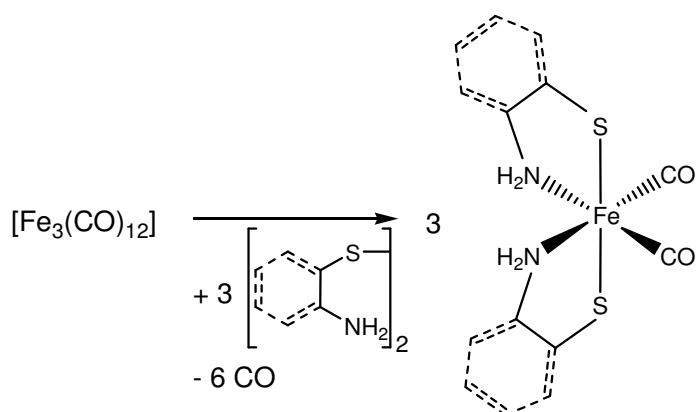
The promising properties of **1** and the possibility to activate the Sellmann complexes with UV light led to an expansion of our investigations with respect to photosensitive CORMs. We prepared and reported  $[\text{Fe}(\text{CO})_2(\text{SCH}_2\text{CH}_2\text{NH}_2)_2]$  (CORM-S1) (**1**) [126] and  $[\text{Fe}(\text{CO})_2(\text{SC}_6\text{H}_4\text{-2-NH}_2)_2]$  (CORM-S2) (**2**). The homologous Ru-based derivatives  $[\text{Ru}(\text{CO})_2(\text{SCH}_2\text{CH}_2\text{NH}_2)_2]$  (**3**) and  $[\text{Ru}(\text{CO})_2(\text{SC}_6\text{H}_4\text{-2-NH}_2)_2]$  (**4**) were also reported here [117] with good yields *via* the direct metalation of the appropriate thiol with iron carbonyls (Scheme 2.4) or *via* the oxidative addition of cystamine ( $\text{H}_2\text{N-CH}_2\text{-CH}_2\text{-S}$ )<sub>2</sub> to iron carbonyls (Scheme 2.5). These approaches ease the work up because gaseous



byproducts are easily removed and no salt-like byproducts enforce purification by fractional crystallization.



**Scheme 2.4:** Synthesis of  $[Fe(CO)_2(SCH_2CH_2NH_2)_2]$  (CORM-S1) and  $[Fe(CO)_2(SC_6H_4-2-NH_2)_2]$  (CORM-S2) as well as of the homologous ruthenium complexes  $[Ru(CO)_2(SCH_2CH_2NH_2)_2]$  (**3**) and  $[Ru(CO)_2(SC_6H_4-2-NH_2)_2]$  (**4**) starting from metal carbonyls.



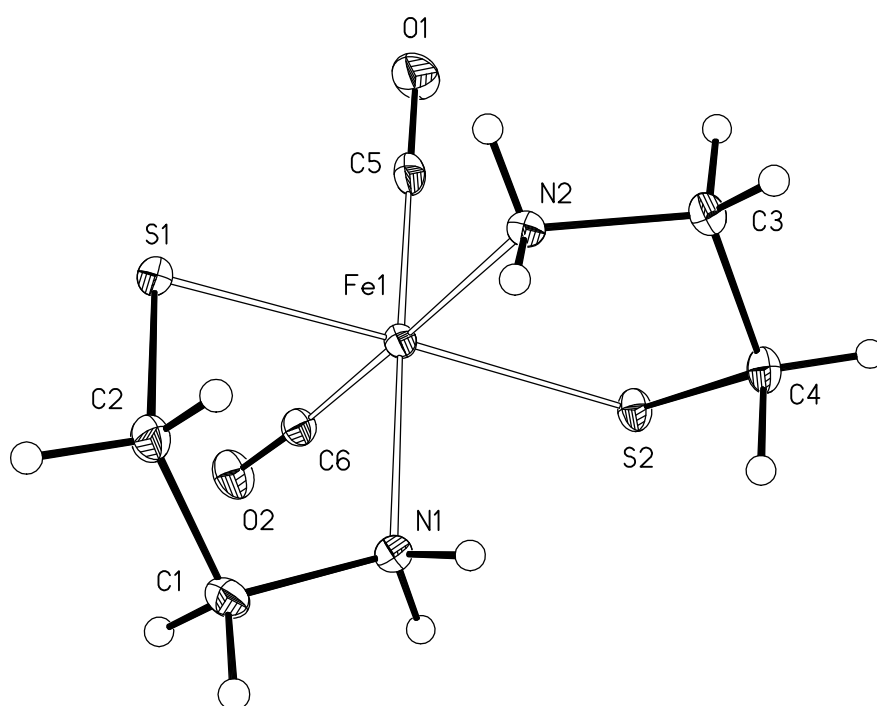
**Scheme 2.5:** Synthesis of  $[Fe(CO)_2(SCH_2CH_2NH_2)_2]$  (CORM-S1) and  $[Fe(CO)_2(SC_6H_4-2-NH_2)_2]$  (CORM-S2) starting from  $[Fe_3(CO)_{12}]$ .

### 2.1.2 Molecular structures

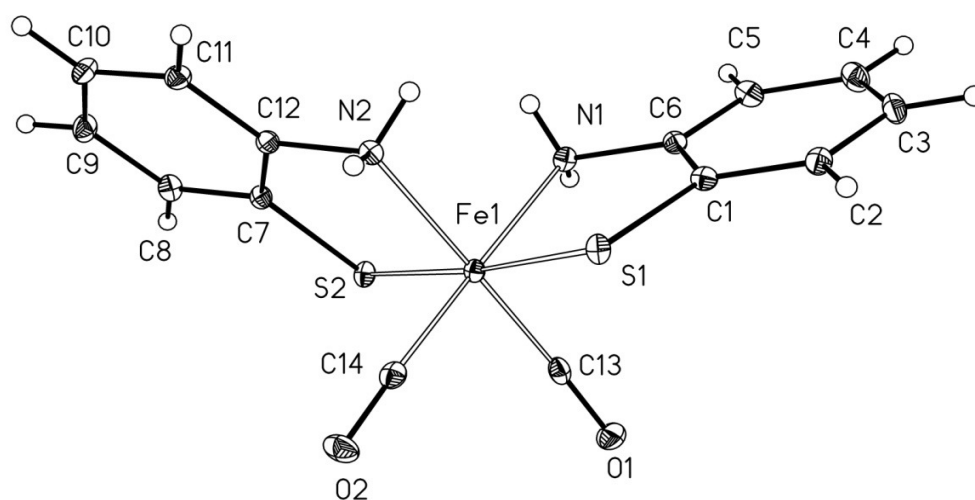
The molecular structures of  $[Fe(CO)_2(SCH_2CH_2NH_2)_2]$  (**1**) [126] and  $[Fe(CO)_2(SC_6H_4-2-NH_2)_2]$  (**2**) [117] are shown in figures 2.1 and 2.2 respectively. The N/S iron-based CORMs **1** and **2** form THF adducts through hydrogen bridges, and these adducts are displayed in figure 2.3. Although the environments of the iron(II) centers are very similar in CORM-S1 and CORM-S2, additional THF molecules show different coordination modes. In **2**, the THF molecule occupies a bridging position between the two amino

functionalities [108], whereas the THF molecule is only bound to one amino group in **1**. The molecular structures of homologous  $[\text{Ru}(\text{CO})_2(\text{SCH}_2\text{CH}_2\text{NH}_2)_2]$  (**3**) and  $[\text{Ru}(\text{CO})_2(\text{SC}_6\text{H}_4\text{-2-NH}_2)_2]$  (**4**) [117] are shown in figures 2.4 and 2.5, respectively, together with representations of their adducts with solvent molecules. Complexes **1** (CORM-S1) and **3** precipitate from THF with isotopic crystal structures, which both show a THF molecule bound to one of the amino functionalities. Complex **4** was recrystallized from *N,N*-dimethylformamide (DMF) and a DMF adduct formed during crystallization. Nevertheless, the adduct formation of **4** shows far-reaching similarities with that of CORM-S2. The coordination spheres of the metal centers in all these complexes are very similar with *cis*-arranged carbonyl ligands. Due to electrostatic repulsion, the thiolato anions show a *trans*-arrangement. Selected physical parameters are summarized in table 2.1. The structural parameters are very similar and the metal atoms have only a weak influence on the structural data. Due to the fact that the Ru-S and Ru-N bonds are longer than the corresponding Fe-S and Fe-N bonds of CORM-S1 and CORM-S2, a small N...S distance (bite) of the chelate ligands leads to endocyclic S-Ru-N bond angles, which are smaller than the corresponding values of the iron compounds.

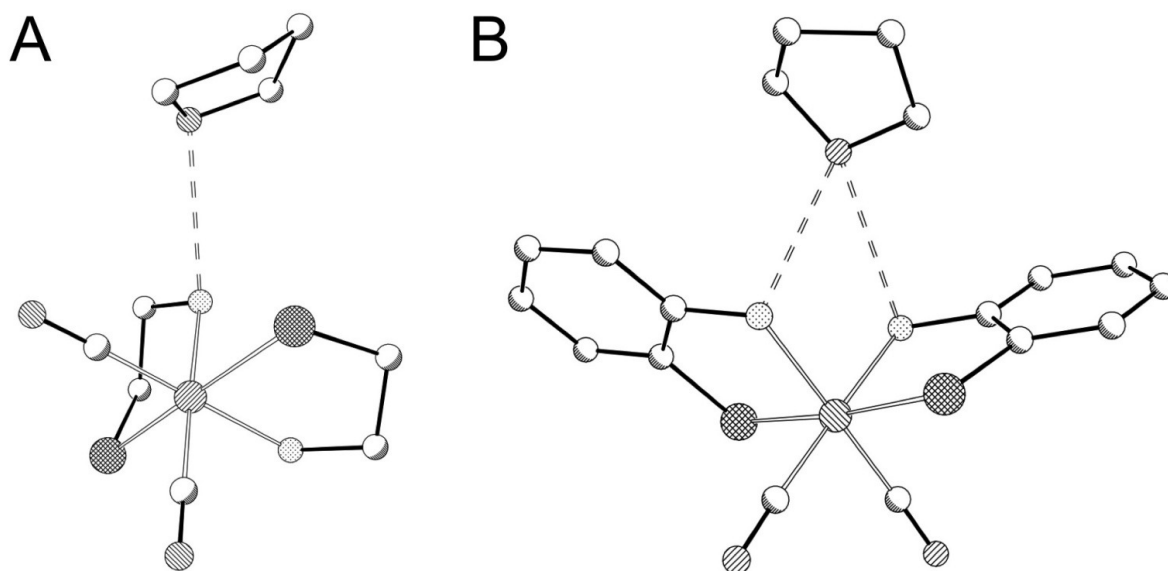
**Fig 2.1:** Molecular structure and numbering scheme of **1**. The ellipsoids represent a probability of 50%. Selected bond lengths (pm): Fe-C5 176.9(2), Fe-C6 176.7(2), Fe-S1 230.53(6), Fe-S2 230.66(6), Fe-N1 204.4(2), Fe-N2 204.4(2), C5-O1 114.7(2), C6-O2 114.9(2); selected bond angles [°]: C5-Fe-C6 90.71(9), C5-Fe-S1 94.73(7), C5-Fe-S2 90.32(7), C5-Fe-N1 178.88(9), C5-Fe-N2 90.42(8), C6-Fe-S1 88.48(7), C6-Fe-S2 96.43(7), C6-Fe-N1 89.83(8), C6-Fe-N2 177.64(8), S1-Fe-S2 172.92(2), S1-Fe-N1 86.26(5), S1-Fe-N2 89.35(5), S2-Fe-N1 88.64(5), S2-Fe-N2 85.64(5).



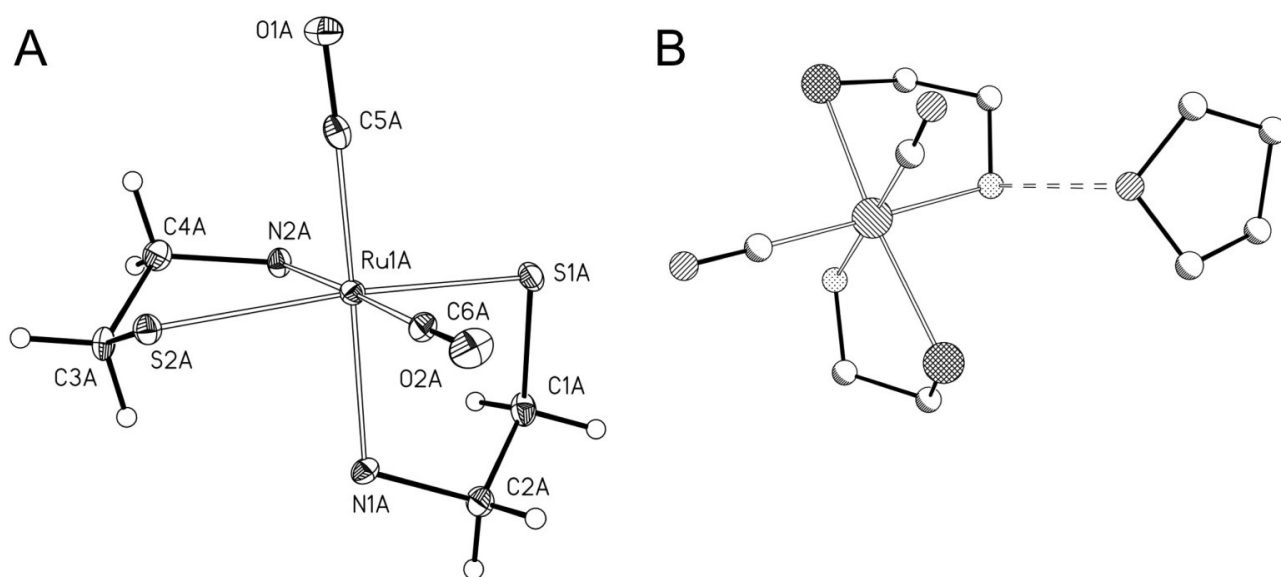
**Fig 2.2:** Molecular structure and numbering scheme of **2**. The ellipsoids represent a probability of 40%. Selected bond lengths (pm): Fe-C13 177.8(2), Fe-C14 178.1(2), Fe-S1 229.25(5), Fe-S2 229.40(5), Fe-N1 204.16(18), Fe-N2 203.64(17), C13-O1 114.1(3), C14-O2 113.8(3); selected bond angles [°]: C13-Fe-C14 88.31(10), C13-Fe-S1 89.67(7), C13-Fe-S2 94.12(7), C13-Fe-N1 91.13(9), C13-Fe-N2 178.95(10), C14-Fe-S1 93.48(7), C14-Fe-S2 90.22(7), C14-Fe-N1 178.83(10), C14-Fe-N2 90.69(8), S1-Fe-S2 174.78(2), S1-Fe-N1 85.49(5), S1-Fe-N2 90.07(5), S2-Fe-N1 90.85(5), S2-Fe-N2 86.20(5).



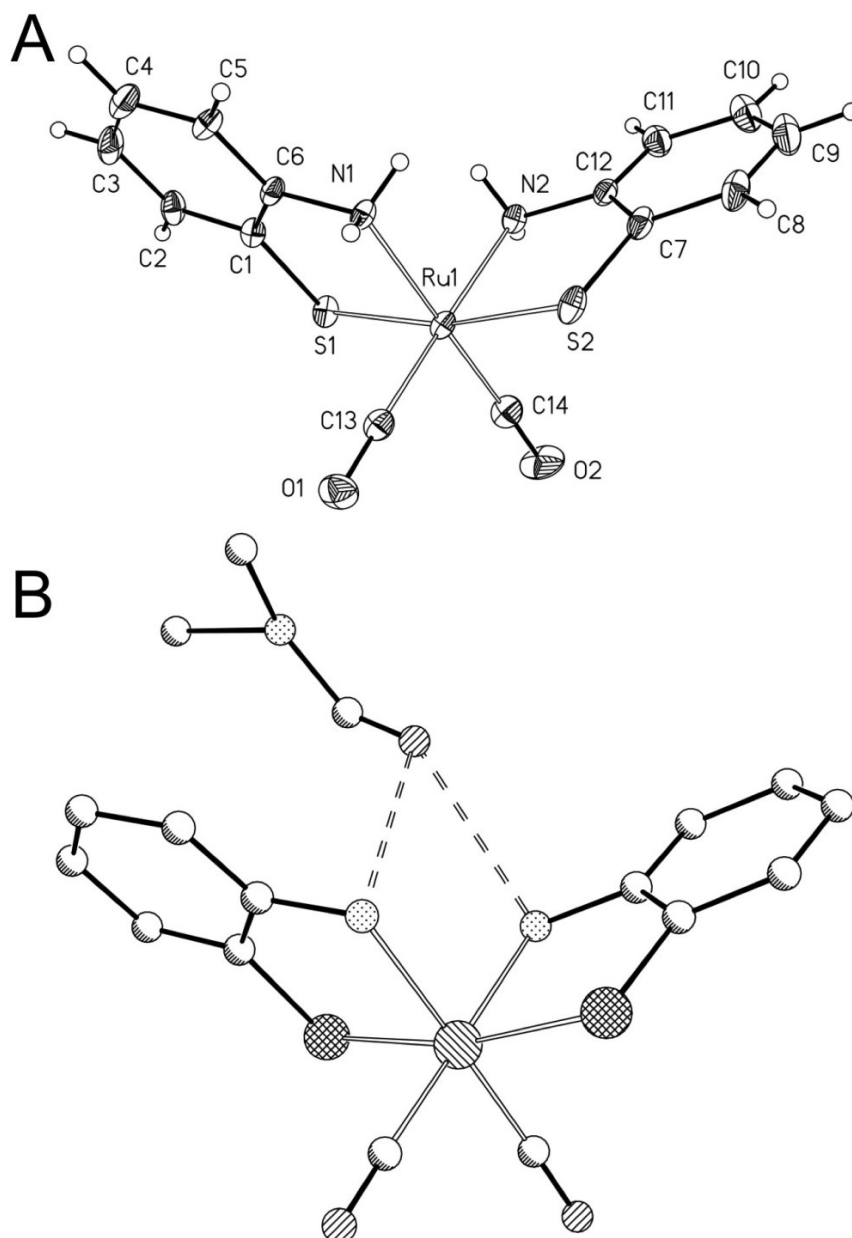
**Fig 2.3:** Structure models of  $[\text{Fe}(\text{CO})_2(\text{SCH}_2\text{CH}_2\text{NH}_2)_2]\cdot\text{THF}$  (A) and  $[\text{Fe}(\text{CO})_2(\text{SC}_6\text{H}_4\text{-2-NH}_2)_2]\cdot\text{THF}$  (B). The heavy atoms are shown with arbitrary radii, and H atoms are omitted for clarity. The THF molecules are bound by  $\text{N-H}\cdots\text{O}_{\text{thf}}$  hydrogen bridges.



**Fig 2.4:** Molecular structure and numbering scheme of **3** (A). The asymmetric unit contains two molecules but only one is displayed. H atoms are drawn with arbitrary radii. (B) The structure of **3**-THF with the coordination of THF through a hydrogen bridge. Selected bond lengths [pm]: Ru1A-S1A 241.7(2), Ru1A-S2A 240.7(1), Ru1A-N1A 216.8(4), Ru1A-N2A 217.2(4), Ru1A-C5A 186.1(6), Ru1A-C6A 187.1(6), C5A-O1A 114.3(7), C6A-O2A 114.6(7); selected bond angles [°]: S1A-Ru1A-S2A 167.88(5), N1A-Ru1A-C5A 178.6(2), N2A-Ru1A-C6A 178.2(2), S1A-Ru1A-N1A 83.6(1), S2A-Ru1A-N2A 84.0(1), S1A-Ru1A-N2A 86.2(1), S2A-Ru1A-N1A 88.8(1), S1A-Ru1A-C5A 97.5(2), S2A-Ru1A-C5A 90.0(2), S1A-Ru1A-C6A 94.9(2), S2A-Ru1A-C6A 94.7(2), C5A-Ru1A-C6A 89.2(2).



**Fig 2.5:** Molecular structure and numbering scheme of **4** (A; the ellipsoids represent a probability of 40%, and H atoms are shown with arbitrary radii) and the structure of **4-DMF** (B; atoms drawn with arbitrary radii, H atoms omitted for clarity). Selected bond lengths [pm]: Ru1-S1 239.4(1), Ru1-S2 239.3(1), Ru1-N1 214.9(4), Ru1-N2 215.5(4), Ru1-C13 186.7(5), Ru1-C14 187.6(5), C13-O1 114.2(6), C14-O2 114.3(6); selected bond angles [°]: S1-Ru1-S2 168.54(5), N1-Ru1-C14 177.5(2), N2-Ru1-C13 178.7(2), S1-Ru1-N1 83.8(1), S2-Ru1-N2 83.4(1), S1-Ru1-N2 89.0(1), S2-Ru1-N1 87.4(1), S1-Ru1-C13 92.2(2), S2-Ru1-C14 94.2(2), S1-Ru1-C14 94.3(2), S2-Ru1-C13 95.5(2), C13-Ru1-C14 89.2(2).



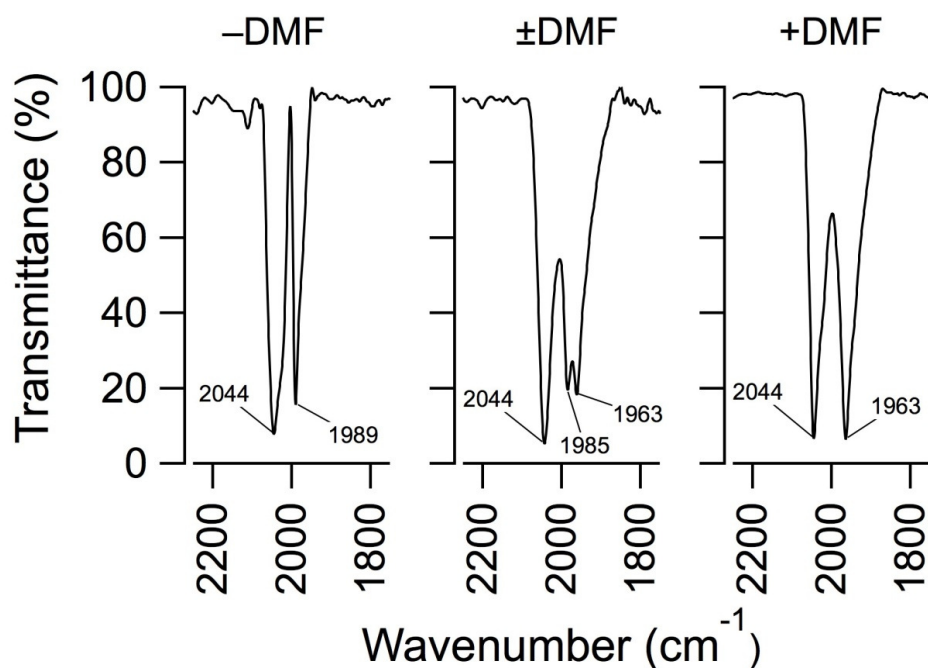
**Table 2.1:** Comparison of physical data of the iron(II) complexes  $[\text{Fe}(\text{CO})_2(\text{SCH}_2\text{CH}_2\text{NH}_2)_2]$  (**1**, CORM-S1) and  $[\text{Fe}(\text{CO})_2(\text{SC}_6\text{H}_4\text{-2-NH}_2)_2]$  (**2**, CORM-S2) as well as the homologous Ru-based derivatives  $[\text{Ru}(\text{CO})_2(\text{SCH}_2\text{CH}_2\text{NH}_2)_2]$  (**3**) and  $[\text{Ru}(\text{CO})_2(\text{SC}_6\text{H}_4\text{-2-NH}_2)_2]$  (**4**) (average values for bond lengths [pm] and angles [deg.]).

Compound	<b>1</b> (CORM-S1)	<b>2</b> (CORM-S2)	<b>3</b>	<b>4</b>
M	Fe	Fe	Ru	Ru
$\nu_{\text{as}}(\text{CO})$	2014	2035	2023	2044
$\nu_{\text{s}}(\text{CO})$	1945	1976	1950	1989
$\delta(^{13}\text{C})$	215.0	213.6	201.3	189.3
M-C <sub>CO</sub>	176.8	178.0	186.6	187.2
M-N	204.4	203.9	217.4	215.2
M-S	230.6	229.3	241.2	239.4
C-M-C	90.7	88.3	89.8	89.2
S-M-S	172.9	174.8	168.5	168.5
N-M-N	89.1	89.9	87.0	87.9
S-M-N <sub>endo</sub>	86.0	85.8	83.8	83.6
S-M-N <sub>exo</sub>	89.0	90.5	87.9	88.2
S-M-C	92.5	91.9	94.1	94.1
N-M-C <sub>trans</sub>	178.0	178.9	178.3	178.1
N-M-C <sub>cis</sub>	89.8	90.9	91.6	91.5



Larger differences with respect to the metal center and substitution pattern of the chelate base are evident for the CO stretching frequencies and the  $^{13}\text{C}$  chemical shifts of the carbonyl ligands in the IR and NMR spectra, respectively. Takács et al. [108] reported identical stretching frequencies of 2020 and 1963  $\text{cm}^{-1}$  for **1** and **2** in methanol solution. Nujol suspensions of pure compounds, however, gave another picture, which is in agreement with the trend of the parameters of **3** and **4**. The aromatic backbone of the chelate base leads to higher wavenumbers by 20  $\text{cm}^{-1}$  for the asymmetric and ca. 30  $\text{cm}^{-1}$  for the symmetric stretching vibrations. In addition, substitution of iron(II) by ruthenium(II) causes a shift to higher wavenumbers. In agreement with the expectation that the anionic charge on the sulfur atom in **2** and **4** might be partially delocalized into the arene backbone, the  $\pi$ -backdonation from the metal center into the  $\pi^*(\text{CO})$  orbital is lower than in complexes with an aliphatic backbone. This situation leads to a shift of the  $^{13}\text{C}$  NMR resonances to lower frequencies for the complexes with bidentate 2-thiolatoaniline bases.

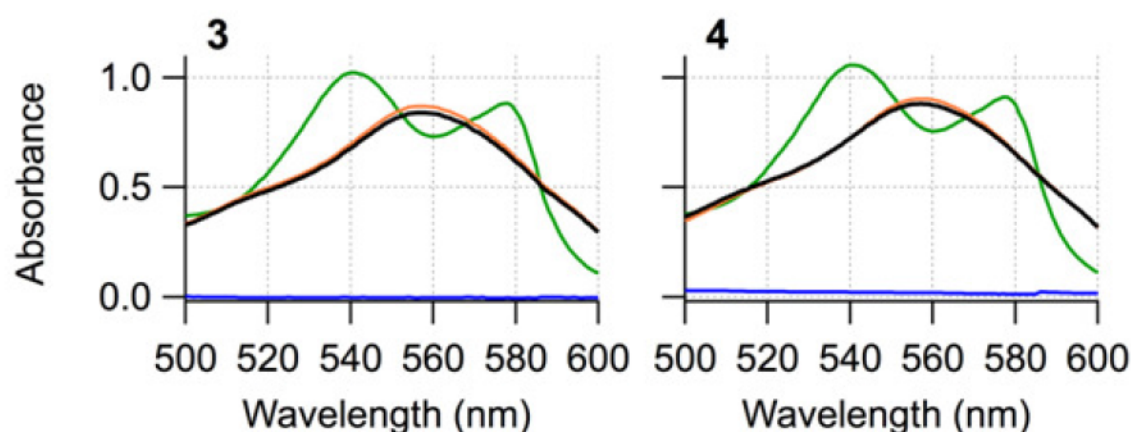
The IR spectrum of DMF-free **4** [117] shows characteristic vibrations at 3243 and 3235  $\text{cm}^{-1}$  for the  $\text{NH}_2$  group and at 2044 and 1989  $\text{cm}^{-1}$  in the carbonyl region. Upon formation of a DMF adduct, the  $\text{NH}_2$  vibrations shifted to lower wavenumbers and two bands at 2044 and 1963  $\text{cm}^{-1}$  were observed in the carbonyl region (figure 2.6). Recrystallization of **4** from DMF yielded the DMF adduct, however, storage at room temperature led to partial loss of DMF and deterioration of the crystals. Due to the fixed geometry of the bidentate chelating ligands, the protons at the nitrogen atoms are chemically nonequivalent, which leads to significantly different chemical shifts in the  $^1\text{H}$  NMR spectra of 3.85 and 5.00 ppm for **3** and of 5.75 and 6.83 ppm for **4**.



**Fig 2.6:** IR spectra of the carbonyl region of  $[\text{Ru}(\text{CO})_2(\text{SC}_6\text{H}_4\text{-2-NH}_2)_2]$  (**4**) [117]. The DMF-free compound exhibits IR absorption bands at 2044 and 1989  $\text{cm}^{-1}$  (left panel), while the DMF adduct  $[\text{Ru}(\text{CO})_2(\text{SC}_6\text{H}_4\text{-2-NH}_2)_2]\cdot\text{DMF}$  (**4**·DMF) has bands at 2044 and 1963  $\text{cm}^{-1}$  (right panel). Partial loss of DMF leads to an overlay of the spectra of both compounds (center panel).

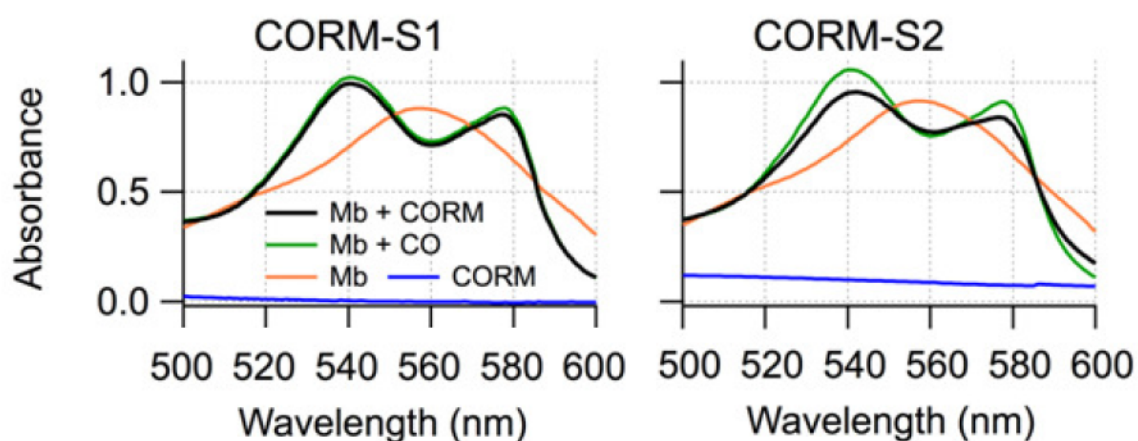
### **2.1.3 CO-release properties**

Light-triggered CORMs are useful therapeutic agents [7,118]. Therefore, CO release during irradiation with visible light in a buffer solution was studied with a myoglobin assay. For neither  $[\text{Ru}(\text{CO})_2(\text{SCH}_2\text{CH}_2\text{NH}_2)_2]$  (**3**) nor  $[\text{Ru}(\text{CO})_2(\text{SC}_6\text{H}_4\text{-2-NH}_2)_2]$  (**4**) [117], even at a concentration of 200  $\mu\text{M}$ , we could observe release of CO upon irradiation with visible light from a cold light source (figure 2.7). Hence, these compounds cannot be used as photo-CORMs in the visible light domain. Sellmann and coworkers [110] have shown that only one CO molecule was liberated during irradiation with a mercury lamp in the presence of triphenylphosphane leading to the formation of complexes with one CO and one phosphane ligand bound to ruthenium. However, the use of UV-light from a mercury source for the activation of metal complexes is limited because of its phototoxicity ultimately damaging cells and tissues.



**Fig 2.7:** Light dependence of CO release. Absorption spectra of [Ru(CO)<sub>2</sub>(SCH<sub>2</sub>CH<sub>2</sub>NH<sub>2</sub>)<sub>2</sub>] (**left**) and [Ru(CO)<sub>2</sub>(SC<sub>6</sub>H<sub>4</sub>-2-NH<sub>2</sub>)<sub>2</sub>] (**right**); compound without myoglobin (blue), myoglobin alone (orange), myoglobin saturated with CO (green), and myoglobin with the compound after irradiation with visible light (black).

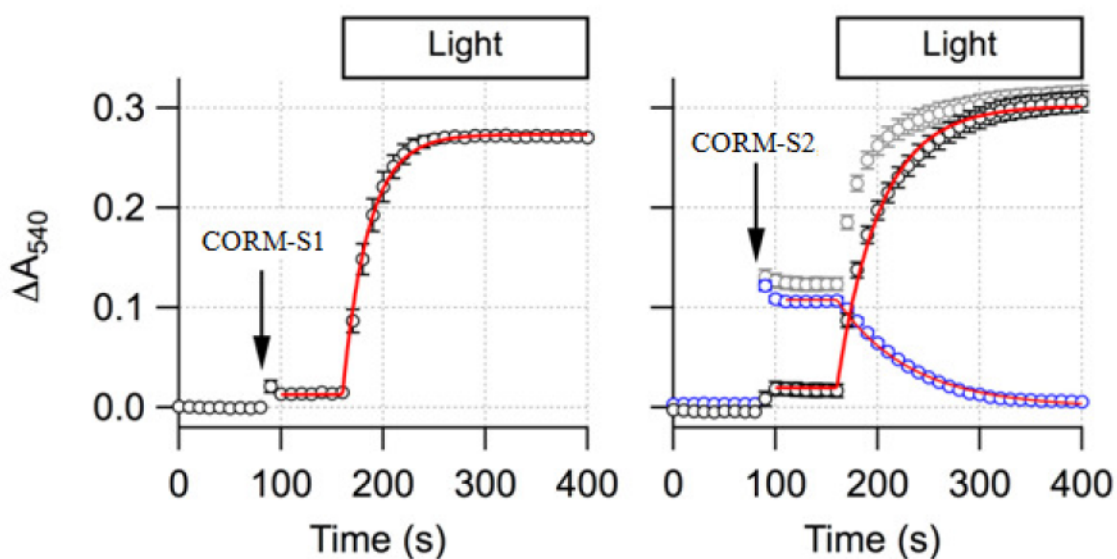
In contrast, 50  $\mu$ M of iron-based [Fe(CO)<sub>2</sub>(SCH<sub>2</sub>CH<sub>2</sub>NH<sub>2</sub>)<sub>2</sub>] (**1**) was sufficient to almost fully convert 100  $\mu$ M deoxy-myoglobin ( $96.5 \pm 2.8\%$ ,  $n = 3$ ) upon irradiation with visible light (figure 2.8(left)). The same concentration of [Fe(CO)<sub>2</sub>(SC<sub>6</sub>H<sub>4</sub>-2-NH<sub>2</sub>)<sub>2</sub>] (**2**) only released  $82.7 \pm 6.3 \mu$ M of CO ( $n = 4$ ), (figure 2.8(right)).



**Fig 2.8:** Light dependence of CO release. Absorption spectra for the indicated compounds: compound without myoglobin (blue), myoglobin alone (orange), myoglobin saturated with CO (green), and myoglobin with the compound after irradiation with visible light (black).

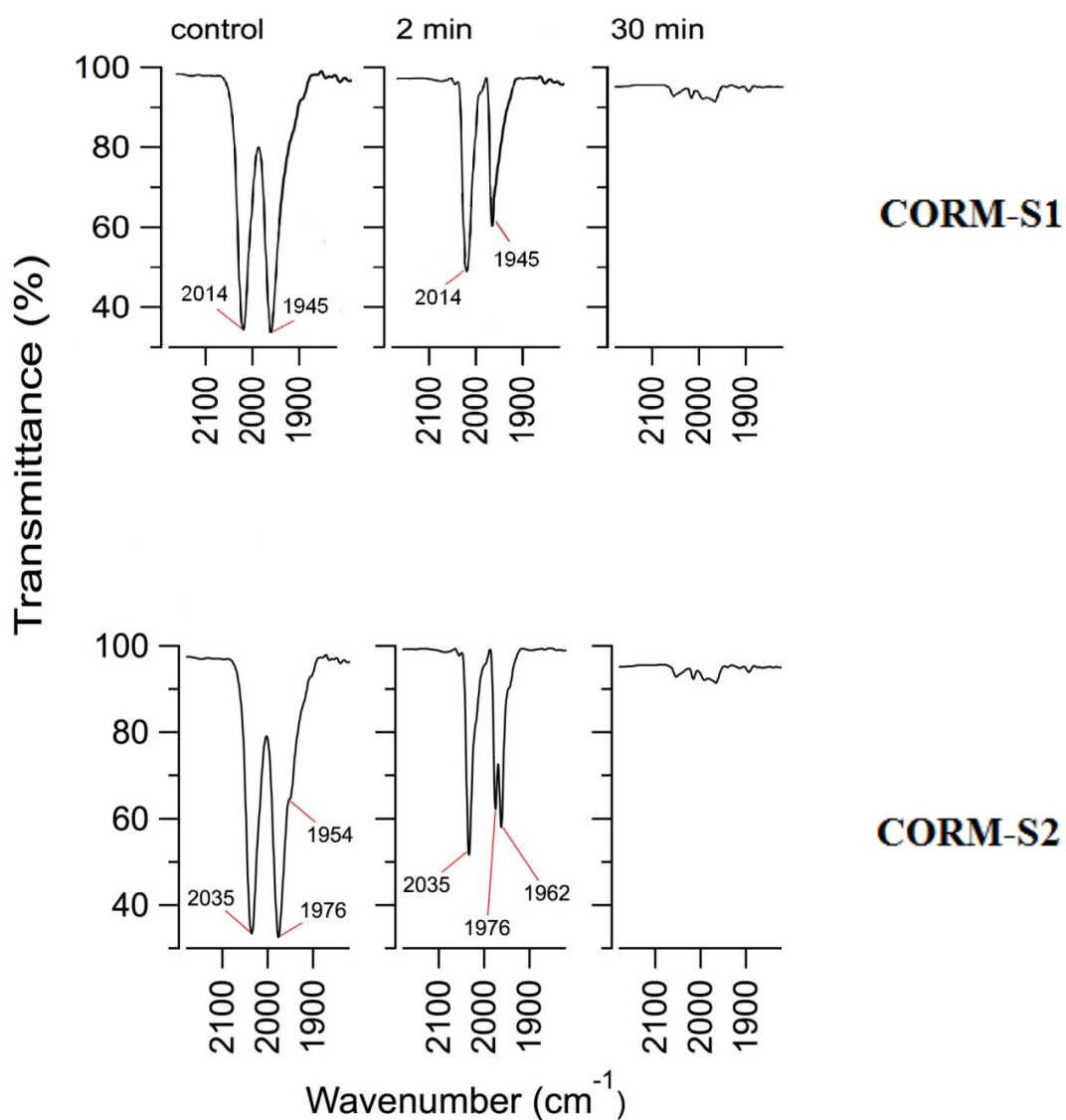
The time constant ( $\tau$ ) was derived from a single-exponential fit to the data shown in figure 2.9. The time course of CO release by [Fe(CO)<sub>2</sub>(SCH<sub>2</sub>CH<sub>2</sub>NH<sub>2</sub>)<sub>2</sub>] (**1**) was fitted

reasonably well by a single exponential function with  $\tau = 26 \pm 4$  s ( $n = 4$ ), which suggests that two molecules CO were released practically simultaneously upon the light-induced breakdown of CORM-S1 (figure 2.8 (left)). The CO release from  $[\text{Fe}(\text{CO})_2(\text{SC}_6\text{H}_4\text{-2-NH}_2)_2]$  (**2**),  $\tau = 43 \pm 2$  s ( $n = 6$ ), was significantly ( $P < 0.05$  based on a two-sided student's *t*-test) slower than for CORM-S1, but faster ( $P < 0.001$ ) than the light-induced breakdown of CORM-S2 in the absence of myoglobin ( $\tau = 71 \pm 2$  s,  $n = 4$ ), indicative of a step-wise release of CO (figure 2.9 (right)).



**Fig 2.9:** Absorbance at 540 nm: Compounds CORM-S1 and CORM-S2 were applied to myoglobin as indicated by the arrows, and the absorbance sharply increased upon irradiation of the samples with visible light. Continuous gray curves are single-exponential fits. On the right, opened data points (blue) show the absorbance of **2** alone, which was subtracted from the raw absorbance data (open symbols, gray) to yield the corrected increase in absorbance (open symbols, black), which indicates CO release. Data points are means  $\pm$  SEM ( $n = 4-6$ ).

As such a step-wise release of CO should result in at least transient occurrence of CO-containing intermediates, IR spectrometry was used to follow the light-triggered degradation of these complexes. The IR spectroscopic monitoring during light-triggered degradation of CORM-S1 didn't show any evidence of CO-containing intermediates, (figure 2.10 (top)). CORM-S1 shows two bands at 2014 and 1945  $\text{cm}^{-1}$ , during irradiation at 470 nm. These bands have a lower intensity without appearance of any new bands in this region, hence, there are no intermediates containing carbonyl ligands which formed during irradiation of CORM-S1. However, the degradation mechanism of CORM-S2 differs significantly, and CO containing intermediates were observed during the irradiation of CORM-S2 at 470 nm (figure 2.10 (bottom)). CORM-S2 shows two bands at 2035 and 1976  $\text{cm}^{-1}$ . Upon irradiation, another band at 1962  $\text{cm}^{-1}$  appeared, indicative of a carbonyl-containing intermediate. This finding supports a one-step and step-wise release of carbon monoxide from CORM-S1 and CORM-S2, respectively, during irradiation. Extended exposure to light led to further degradation of the carbonyl complexes, and the bands of CORM-S1, CORM-S2 and CORM-S2 immediate degradation product vanish to give numerous weak bands in the carbonyl region.



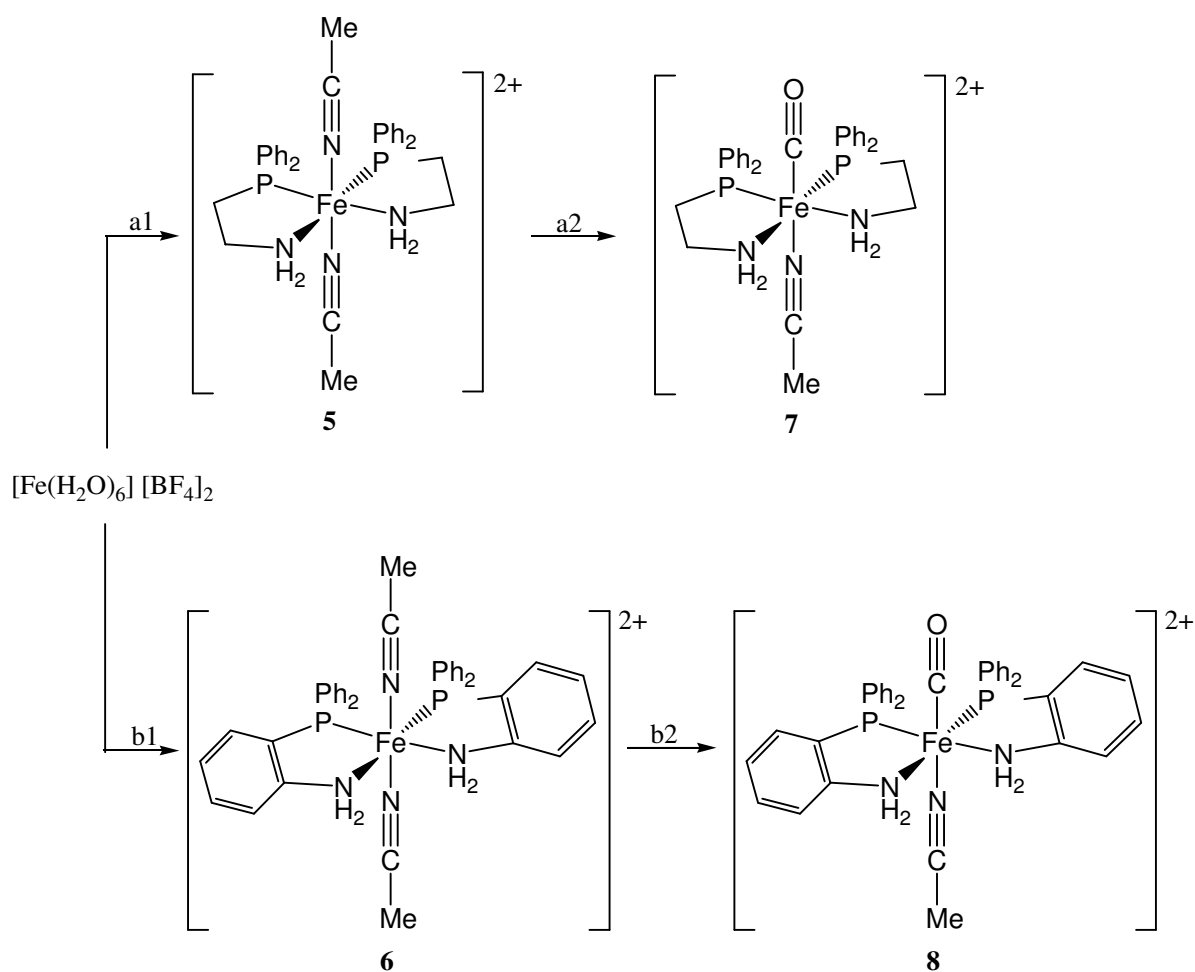
**Fig 2.10:** IR spectra of the carbonyl region of  $[\text{Fe}(\text{CO})_2(\text{SCH}_2\text{CH}_2\text{NH}_2)_2]$  (CORM-S1) (top panel, left), after 2 min of irradiation no any new band can be recognized in the carbonyl region (center) (**top**).  $[\text{Fe}(\text{CO})_2(\text{SC}_6\text{H}_4\text{-2-NH}_2)_2]$  (CORM-S2) (bottom panel, left), after 2 min of irradiation another band at 1962  $\text{cm}^{-1}$  can be recognized (center) (**bottom**). After 30 min of irradiation complete degradation of CORM-S1 and CORM-S2 occurred (right panel in both **top** and **bottom**)

## **2.2 N/P-iron-based CORMs**

In the course of our investigations on iron(II)-based CORMs we compared dicarbonyl-bis(cysteaminato)iron(II) (CORM-S1) and dicarbonyl-bis(ortho-aminothiophenolato)iron(II) (CORM-S2). In CORM-S2, a step-wise CO release was observed upon irradiation with visible light whereas both carbon monoxide molecules were liberated at the same time from CORM-S1 [117]. We intended to investigate an iron(II)-based photo-CORM with only one CO ligand coordinated to the metal atom in order to avoid interference between two CO-releasing steps as obviously detected for CORM-S2. In addition, an NMR probe should be introduced enabling the observation not only of CO release but also of the degradation of the metal complex. This procedure allows direct comparison of the analytical methodologies and at best validation of the myoglobin assay for photo-CORMs. Therefore, we investigated and reported complexes of N/P iron-based CORMs  $[\text{Fe}(\text{CO})(\text{NC-Me})(\text{H}_2\text{NCH}_2\text{CH}_2\text{PPh}_2)_2]^{2+}$  (CORM-P1) and  $[\text{Fe}(\text{CO})(\text{NC-Me})(\text{H}_2\text{NC}_6\text{H}_4\text{-2-PPh}_2)_2]^{2+}$  (CORM-P2), the counter anions being tetrafluoroborate, with the  $^{31}\text{P}$  nucleus being a very sensitive NMR probe [119].

### **2.2.1 Synthesis**

The reactions of  $[\text{Fe}(\text{H}_2\text{O})_6] [\text{BF}_4]_2$  with aminoethyl-diphenylphosphane and 2-(diphenylphosphino)aniline in acetonitrile solvent yielded the complexes *trans*- $[\text{Fe}(\text{NC-Me})_2(\text{H}_2\text{NCH}_2\text{CH}_2\text{PPh}_2)_2] [\text{BF}_4]_2$  (**5**) [120] and *trans*- $[\text{Fe}(\text{NC-Me})_2(\text{H}_2\text{NC}_6\text{H}_4\text{-2-PPh}_2)_2] [\text{BF}_4]_2$  (**6**). Exposing these complexes, dissolved in  $\text{CH}_2\text{Cl}_2$ , to a CO atmosphere led to substitution of one acetonitrile molecule by a carbon monoxide ligand under maintenance of the residual iron(II) environment, yielding  $[\text{Fe}(\text{CO})(\text{NC-Me})(\text{H}_2\text{NCH}_2\text{CH}_2\text{PPh}_2)_2] [\text{BF}_4]_2$  (**7**, CORM-P1) and  $[\text{Fe}(\text{CO})(\text{NC-Me})(\text{H}_2\text{NC}_6\text{H}_4\text{-2-PPh}_2)_2] [\text{BF}_4]_2$  (**8**, CORM-P2) according to scheme 2.6. Substitution of the second acetonitrile did neither occur at longer reaction periods nor at higher carbon monoxide pressure or higher temperature. Therefore, very pure iron(II) complexes were easily obtained and isolated with high yields. Iron(II) complexes with two or three monoxide ligands usually show *cis* or facial arrangements of these molecules due to the strong *trans*-influence of carbon monoxide. Exceptions are described in mixed cyano/carbonyl iron(II) complexes [121] which can be explained by the isoelectronic nature of CO and CN $^-$ .



**Scheme 2.6:** Synthesis of acetonitrile complexes **5**, **6**, and the CO-releasing molecules **7** (CORM-P1), **8** (CORM-P2), starting from  $[\text{Fe}(\text{H}_2\text{O})_6][\text{BF}_4]_2$ . Reaction conditions: a) 1. Reaction with aminoethyl-diphenylphosphane in acetonitrile, 2. substitution of one acetonitrile by CO; b) 1. Reaction with 2-diphenylphosphinoaniline in acetonitrile, 2. substitution of one acetonitrile by CO.

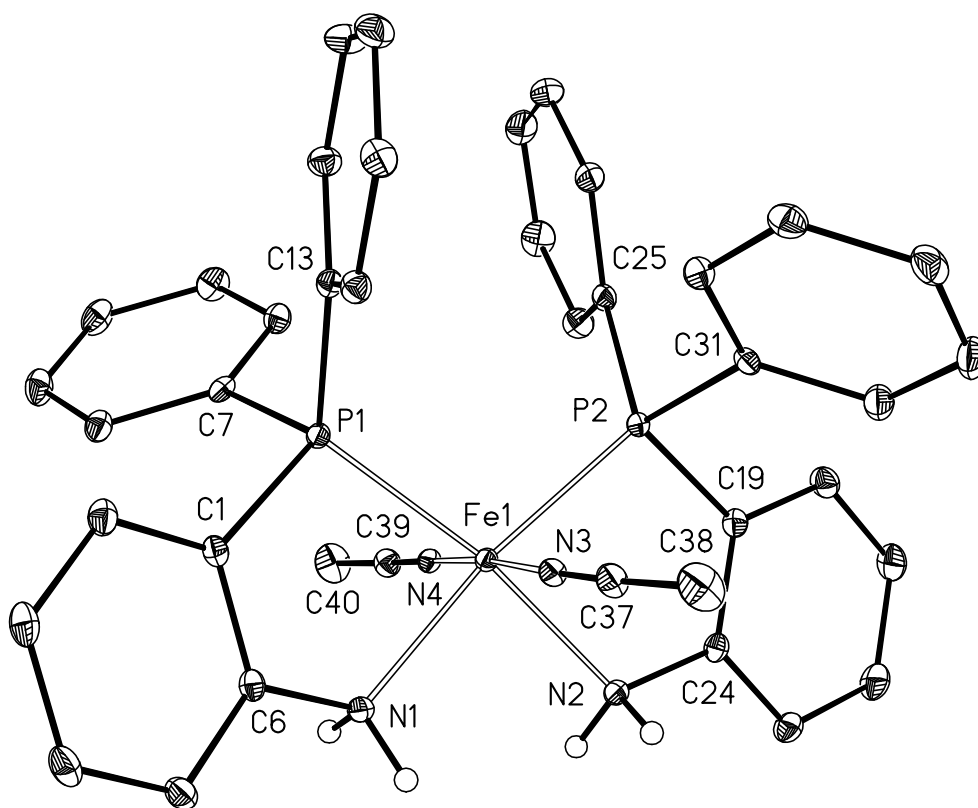
In solution solvent-separated ions are observed. The NMR parameters of the tetrafluoroborate anion of **5** and **6** are very similar and do not depend on the cation, even though in the crystalline state N-H $\cdots$ F bridges are observed.



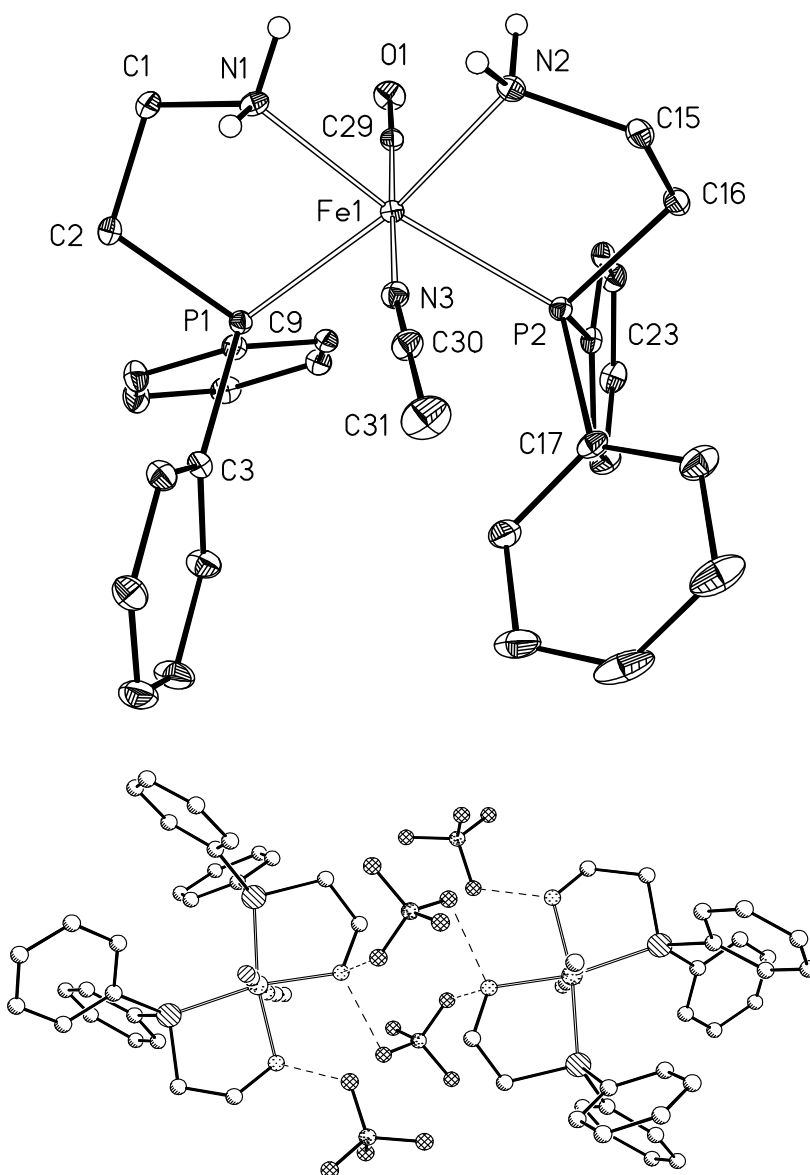
### 2.2.2 Molecular structures

The cations *trans*-[Fe(NC-Me)<sub>2</sub>(H<sub>2</sub>NCH<sub>2</sub>CH<sub>2</sub>PPh<sub>2</sub>)<sub>2</sub>]<sup>2+</sup> (**5**) [120] (counterion [FeBr<sub>4</sub>]<sup>2-</sup>) and *trans*-[Fe(NC-Me)<sub>2</sub>(H<sub>2</sub>NC<sub>6</sub>H<sub>4</sub>-2-PPh<sub>2</sub>)<sub>2</sub>]<sup>2+</sup> (**6**) (figure 2.11, counterions [BF<sub>4</sub>]<sup>-</sup> not displayed for clarity reasons) show very similar geometries which deviate only slightly from C<sub>2v</sub> symmetry. The iron(II) centers are in distorted octahedral environments with the acetonitrile ligands *trans* to each other. The diphenylphosphanyl groups are *cis*-arranged as are the amino groups. The difference between these cations is the more rigid benzo-backbone of the cation of **6** leading to smaller bites of the bidentate ligands and, hence, to slightly smaller P1-Fe1-N1 and P2-Fe1-N2 bond angles. The structural changes, however, are insignificant and even the P1-Fe1-P2 and N1-Fe1-N2 bond angles are very much alike. The nearly linear acetonitrile molecules show very short C≡N bond lengths. Whereas the more flexible ethylene backbone of *trans*-[Fe(NC-Me)<sub>2</sub>(H<sub>2</sub>NCH<sub>2</sub>CH<sub>2</sub>PPh<sub>2</sub>)<sub>2</sub>]<sup>2+</sup> allows to align to steric necessities, the more rigid benzo unit of **6** suffers more severe distortions. Thus, the P1-C1-C2/6 and P2-C19-C20/24 angles differ by approximately 10° due to the bulky phenyl substituents at P1 and P2. For the small amino groups N1 and N2 the difference between proximal and distal N1-C6-C1/5 and N2-C24-C19/23 angles is much smaller. Substitution of one acetonitrile ligand by a carbon monoxide reduces the symmetry of the cation and only the mirror plane containing the CO and NC-Me ligands is maintained. Figure 2.12 shows [Fe(CO)(NC-Me)(H<sub>2</sub>NCH<sub>2</sub>CH<sub>2</sub>PPh<sub>2</sub>)<sub>2</sub>] [BF<sub>4</sub>]<sub>2</sub> (**7**, CORM-P1) and figure 2.13 displays the molecular structure of [Fe(CO)(NC-Me)(H<sub>2</sub>NC<sub>6</sub>H<sub>4</sub>-2-PPh<sub>2</sub>)<sub>2</sub>] [BF<sub>4</sub>]<sub>2</sub> (**8**, CORM-P2) clarifying also the stabilization by N-H...F hydrogen bridges to the tetrafluoroborate anions.

**Fig 2.11:** Molecular structure and numbering scheme of the cation  $trans\text{-}[\text{Fe}(\text{NC-Me})_2(\text{H}_2\text{NC}_6\text{H}_4\text{-2-PPh}_2)_2]^{2+}$  of **6**. The ellipsoids represent a probability of 40%. H atoms with the exception of the amino groups are neglected for clarity reasons. Selected bond lengths (pm): Fe1-P1 223.72(5), Fe1-P2 222.66(5), Fe1-N1 206.0(2), Fe1-N2 205.8(2), Fe1-N3 192.0(2), Fe1-N4 191.5(2), N1-C6 145.2(2), N2-C24 145.7(2), N3-C37 114.1(2), N4-C39 114.0(2), P1-C1 182.1(2), P1-C7 182.8(2), P1-C13 182.4(2), P2-C19 181.3(2), P2-C25 182.0(2), P2-C31 183.1(2); selected bond angles [°]: N3-Fe1-N4 175.99(6), P1-Fe1-P2 104.62(2), N1-Fe1-N2 88.14(6), P1-Fe1-N1 83.25(4), P2-Fe1-N2 84.05(4).

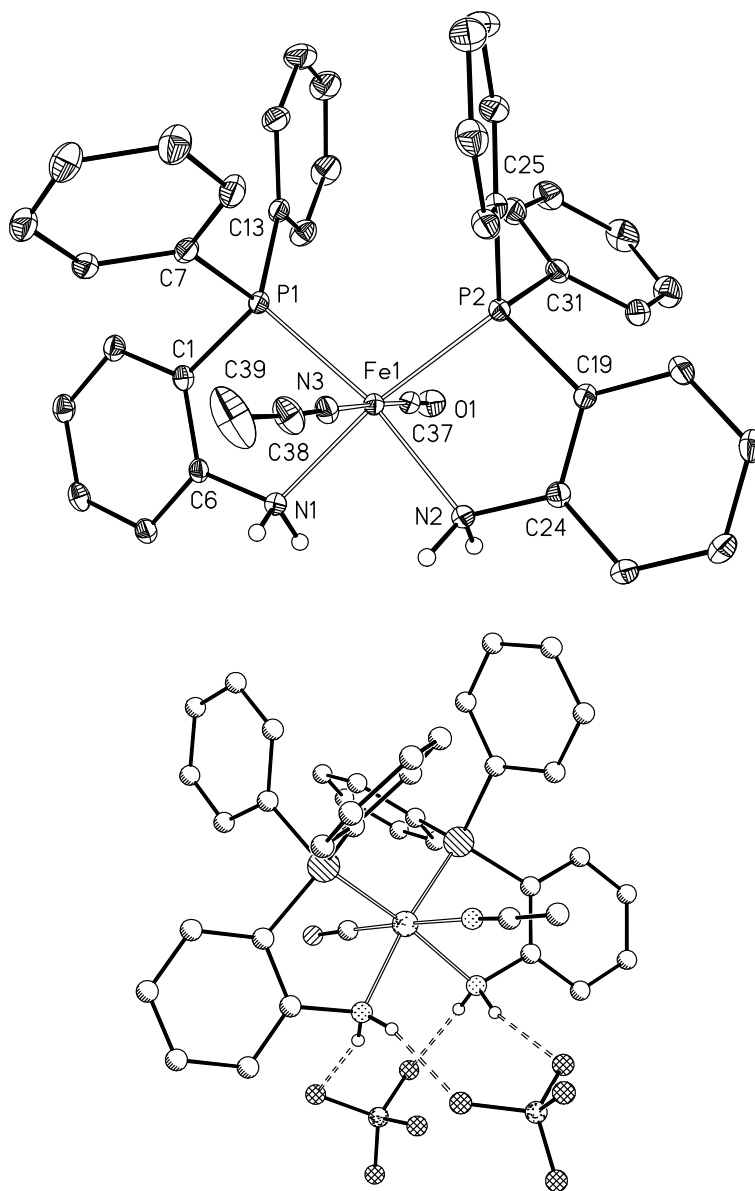


**Fig 2.12:** Molecular structure and numbering scheme of the cation  $[\text{Fe}(\text{CO})(\text{NC-Me})(\text{H}_2\text{NCH}_2\text{CH}_2\text{PPh}_2)_2]^{2+}$  (**7**, CORM-P1) (top). The ellipsoids represent a probability of 40%, all C-bound H atoms are omitted for clarity reasons. At the bottom, dimer formation *via* a N-H $\cdots$ F network of  $[\text{Fe}(\text{CO})(\text{NC-Me})(\text{H}_2\text{NCH}_2\text{CH}_2\text{PPh}_2)_2][\text{BF}_4]_2$  is represented. Here arbitrary radii were chosen for all atoms. Selected bond lengths (pm): Fe1-P1 228.84(5), Fe1-P2 228.55(5), Fe1-N1 204.4(2), Fe1-N2 205.9(2), Fe1-N3 194.7(2), Fe1-C29 176.4(2), C29-O1 114.4(2), N1-C1 148.5(2), N2-C15 149.0(2), N3-C30 114.1(3), P1-C2 185.0(2), P1-C31 83.4(2), P1-C9 182.5(2), P2-C16 183.3(2), P2-C17 181.5(2), P2-C23 182.3(2); selected bond angles [ $^\circ$ ]: N3-Fe1-C29 178.11(8), P1-Fe1-P2 106.85(2), N1-Fe1-N2 86.00(7), P1-Fe1-N1 83.32(5), P2-Fe1-N2 83.68(5), Fe1-C29-O1 178.5(2).



**Fig 2.13:** Molecular structure and numbering scheme of the cation  $[\text{Fe}(\text{CO})(\text{NC-Me})(\text{H}_2\text{NC}_6\text{H}_4\text{-2-PPh}_2)_2]^{2+}$  of (**8**, CORM-P2) (top). The ellipsoids represent a probability of 40%. All C-bound hydrogen atoms are

neglected for clarity reasons. At the bottom, the structure of  $[\text{Fe}(\text{CO})(\text{NC-Me})(\text{H}_2\text{NC}_6\text{H}_4\text{-2-PPH}_2)_2][\text{BF}_4]_2$  (**8**, CORM-P2) is shown, displaying the formation of a contact ion pair *via* N-H $\cdots$ F bridges. The atoms are drawn with arbitrary radii. Selected bond lengths (pm): Fe1-P1 225.50(8), Fe1-P2 225.32(8), Fe1-N1 206.3(2), Fe1-N2 206.0(2), Fe1-N3 195.6(2), Fe1-C37 176.9(3), C37-O1 114.3(4), N1-C6 145.9(4), N2-C24 146.0(4), N3-C38 113.5(4), P1-C1 181.2(3), P1-C7 181.9(3), P1-C13 181.8(3), P2-C19 181.2(3), P2-C25 182.0(3), P2-C31 182.6(3); selected bond angles [ $^\circ$ ]: N3-Fe1-C37 178.4(1), P1-Fe1-P2 103.79(3), N1-Fe1-N2 87.1(1), P1-Fe1-N1 84.32(7), P2-Fe1-N2 84.91(7), Fe1-C37-O1 178.6(3).



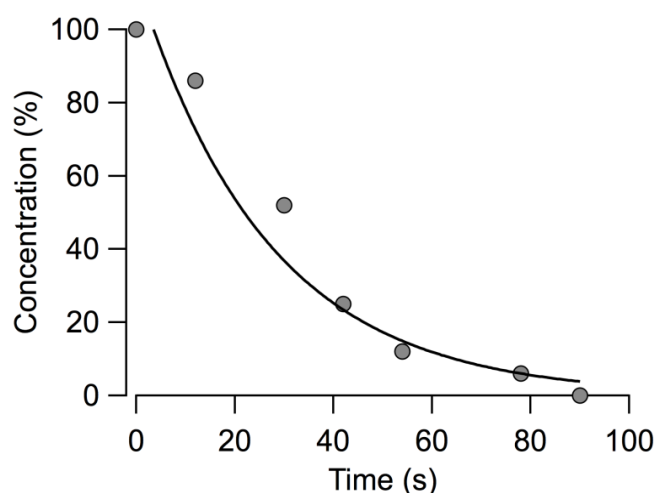
The structural parameters are very similar with respect to the carbonyl fragment. The CO bond lengths and the Fe-C distances with average values of 114.4 and 176.7 pm, respectively, differ only within their estimated standard deviations. Also the Fe-C-O

angles of  $178.6^\circ$  for both cations deviate only insignificantly from linearity. The acetonitrile ligand experiences a significant Fe-N bond elongation due to the *trans*-positioned CO molecule by approximately 4 pm as a consequence of a weakened  $\pi$ -backdonation of electron density from the metal center to the  $\pi^*$  orbitals of the nitrile group. This fact is in agreement with the IR spectroscopic findings. The effect on the C $\equiv$ N bond lengths is much smaller and lies within the standard deviations. However, the presence of the CO ligand also leads to elongation of the Fe-P bonds by approximately 2-3 pm. The tetrafluoroborate anions form hydrogen bridges to the amino groups of the cations. In the compounds **6** and **8** (CORM-P2) the benzo backbone fixes the nearly parallel alignment of the NH bonds of the amino groups. The BF $_4^-$ -anions are able to form two intramolecular N-H $\cdots$ F bridges to the same cation. Contrary to this formation of a contact ion pair due to the flexibility of the ethylene backbone in **7** (CORM-P1), the tetrafluoroborate anions form N-H $\cdots$ F bridges to two different cations leading to the formation of a dimeric contact ion pair.

The symmetric and asymmetric stretching frequencies of the carbon monoxide ligands of CORM-S1 (2014, 1945  $\text{cm}^{-1}$  [117]) and CORM-S2 (2035, 1976  $\text{cm}^{-1}$  [117]) are observed at significantly lower wave numbers than those of free carbon monoxide (2134  $\text{cm}^{-1}$  [122]). The iron(II) complexes CORM-P1 (C $\equiv$ N: 2303, C $\equiv$ O: 1985  $\text{cm}^{-1}$ ) and CORM-P2 (C $\equiv$ N: 2290, C $\equiv$ O: 2001  $\text{cm}^{-1}$ ) also show two bands, in this case due to acetonitrile (free gaseous acetonitrile 2268  $\text{cm}^{-1}$ ) and carbon monoxide stretching vibrations. A shift of the C $\equiv$ N stretching mode to higher wavenumbers upon coordination to Lewis acids represents a very common observation for such complexes [122,123] with acetonitrile acting as a  $\pi$ -donor [124]. The wavenumbers of the C $\equiv$ N stretching modes of the CORMs **7** and **8** are significantly larger than observed for the bis(acetonitrile) iron(II) complexes **5** (2163  $\text{cm}^{-1}$ ) and **6** (2207  $\text{cm}^{-1}$ ) because CO is a strong  $\pi$ -acceptor supporting the  $\pi$ -donor ability of acetonitrile.

### 2.2.3 CO-release properties

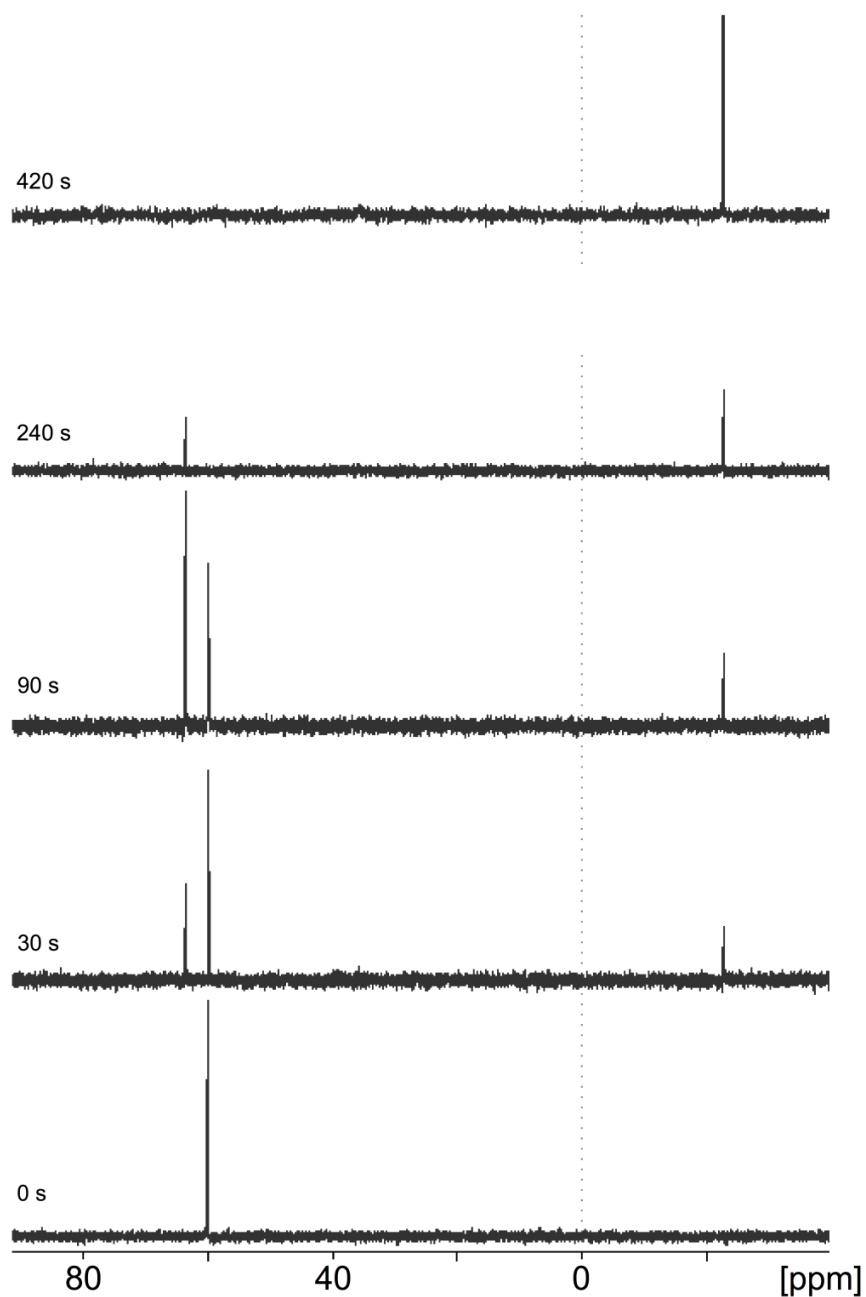
To infer about the mechanism of CO release we studied the light-triggered degradation of the CORMs by  $^{31}\text{P}$  NMR spectroscopy. For this purpose CORM-P1 **7** and CORM-P2 **8** were dissolved in  $[\text{D}_6]$ dimethylsulfoxide (DMSO) at a final concentration of 23 mM. As expected, both CORMs showed no degradation in the dark. In order to quantitatively record the degradation of CORM-P1, the phosphorus-containing reference compound tetraphenylphosphonium chloride  $[\text{Ph}_4\text{P Cl}; \delta(^{31}\text{P}) = 23.2]$  was added. From this solution the degradation was observed in dependency of the irradiation duration (figure 2.14). The free ligand aminoethyl-diphenylphosphane was formed during CO release, and no other intermediates were detected by  $^{31}\text{P}\{^1\text{H}\}$  NMR spectroscopy.



**Fig 2.14:** Time-dependent degradation of **7** (CORM-P1) upon irradiation with visible light in a 23-mM solution of **7** in  $[\text{D}_6]$ DMSO followed by  $^{31}\text{P}\{^1\text{H}\}$  NMR spectroscopy. For quantification reasons  $\text{Ph}_4\text{P Cl}$  was added as a reference compound. The continuous curve is the result of a single-exponential data fit with a time constant of 27 s.

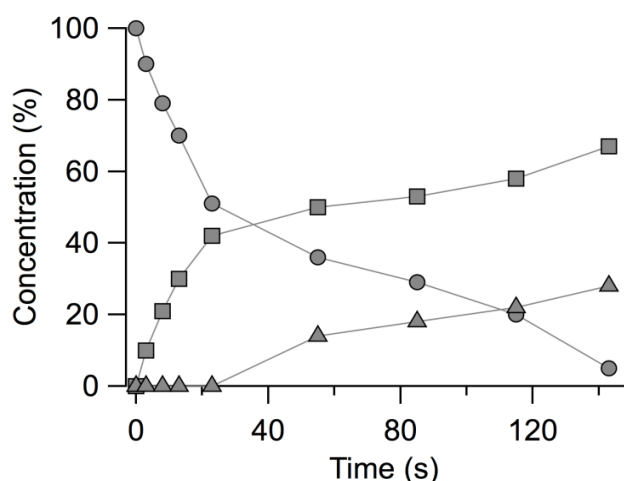
A different picture resulted from a  $[\text{D}_3]$ acetonitrile solution of CORM-P1, again at 23 mM. Already in the dark a very slow decomposition was observed leading to a quantitative conversion to *trans*- $[\text{Fe}(\text{NC-Me})_2(\text{H}_2\text{NCH}_2\text{CH}_2\text{PPh}_2)_2] [\text{BF}_4]_2$  (**5**) and carbon monoxide within two weeks. Irradiation of a freshly prepared solution of **7** in  $\text{D}_3\text{C-C}\equiv\text{N}$  led to CO liberation and formation of **5**. Therefore, initially no free ligand was observed. However, *trans*- $[\text{Fe}(\text{NC-Me})_2(\text{H}_2\text{NCH}_2\text{CH}_2\text{PPh}_2)_2] [\text{BF}_4]_2$  (**5**) also degrades during irradiation but this breakup is slower than the decomposition of CORM-P1 (**7**). The  $^{31}\text{P}\{^1\text{H}\}$  NMR

spectra of this degradation reaction is shown in figure 2.15, the interpretation is depicted in figure 2.16. Here it becomes obvious that there is an induction period for the appearance of  $\text{H}_2\text{NCH}_2\text{CH}_2\text{PPh}_2$  due to the intermediate formation of **5**. A control experiment verified that a solution of *trans*- $[\text{Fe}(\text{NC-Me})_2(\text{H}_2\text{NCH}_2\text{CH}_2\text{PPh}_2)_2] [\text{BF}_4]_2$  (**5**) in  $[\text{D}_3]$ acetonitrile is stable in the dark but that this complex degrades upon irradiation liberating free aminoethyl-diphenylphosphane.



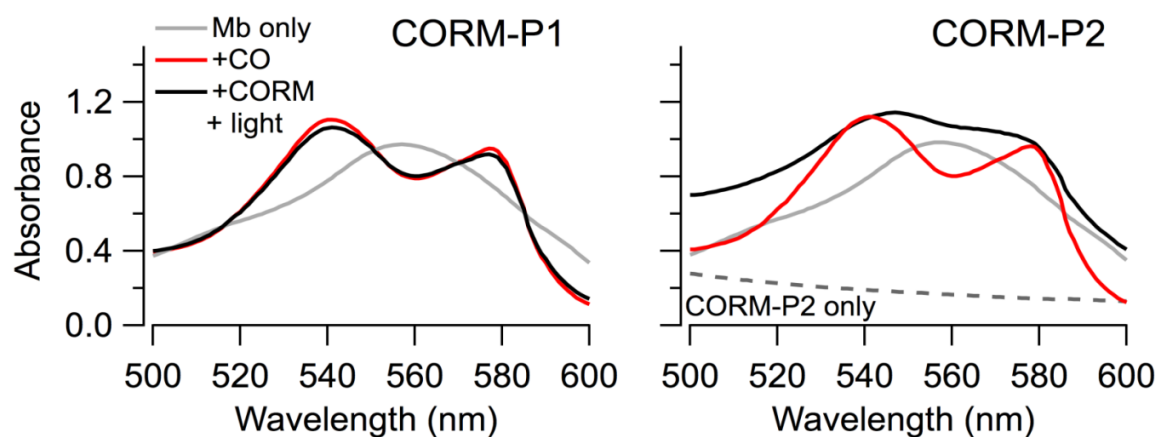
**Fig 2.15:**  $^{31}\text{P}\{^1\text{H}\}$  NMR spectra of the degradation of a 23-mM solution of CORM-P1 (**7**) in  $[\text{D}_3]$ acetonitrile during irradiation with visible light. The bottom spectrum shows the resonance of pure CORM-P1 ( $t = 0$  s,  $\delta = 61.7$ ). The spectra were recorded at the indicated times. During irradiation with light of 470 nm, the signals of *trans*- $[\text{Fe}(\text{NC-Me})_2(\text{H}_2\text{NCH}_2\text{CH}_2\text{PPh}_2)_2] [\text{BF}_4]_2$  (**5**) ( $\delta = 63.7$ ) and free aminoethyl-diphenylphosphane ( $\delta = -21.0$ ) appear. The resonance of starting **7** disappears and finally, also the acetonitrile complex **5** vanishes. Only the signal of free aminoethyl-diphenylphosphane can be recognized after 420 s (top spectrum).





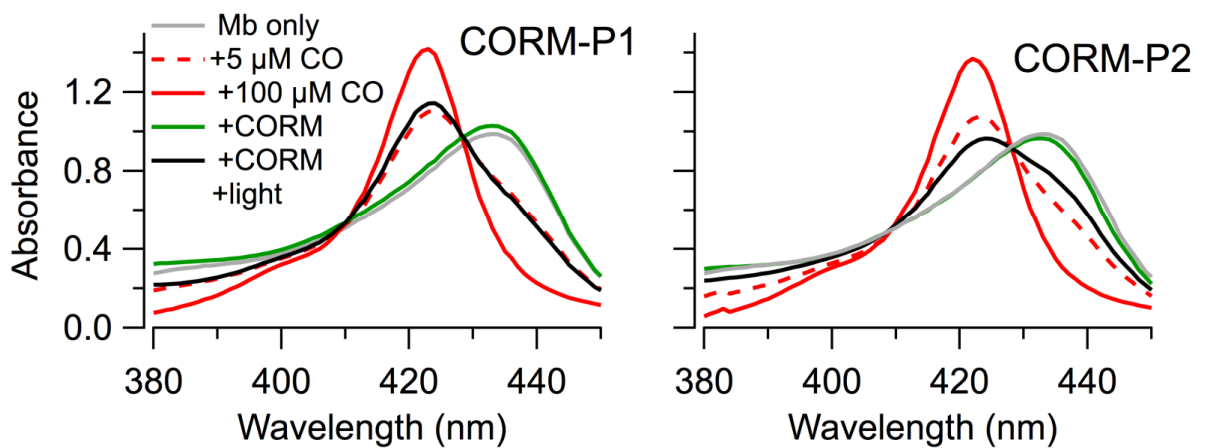
**Fig 2.16:** Light-induced degradation of **7** (circles, CORM-P1) in a 23-mM [D<sub>3</sub>]acetonitrile solution. During the first 20 s, CO is substituted by acetonitrile yielding *trans*-[Fe(NC-Me)<sub>2</sub>(H<sub>2</sub>NCH<sub>2</sub>CH<sub>2</sub>PPh<sub>2</sub>)<sub>2</sub>] [BF<sub>4</sub>]<sub>2</sub> (**5**, squares). Thereafter, the resonance of free aminoethyl-diphenylphosphane (triangles) is detected originating from light-triggered decomposition of complex **5**. Competing formation of **5** from ligand substitution in **7** and light-induced decomposition of **5** implicate a rather constant concentration of **5** after approximately 60 min. Straight lines connect data points for clarity.

We further assayed the properties of the compounds in aqueous solutions. CO release was quantified in a myoglobin-based assay by spectrophotometric measurement of the conversion of deoxymyoglobin (Mb) into the myoglobin-CO complex (Mb-CO). For measurements in the range of 500 to 600 nm a solution was prepared that contained equimolar (100 μM) amounts of deoxymyoglobin and either CORM-P1 or CORM-P2. Myoglobin was reduced with 0.1% sodium dithionite. Both CORMs showed no CO release in the dark but irradiation with white light for 10 minutes led to quantitative (figure 2.17 (left), CORM-P1) or incomplete (figure 2.17 (right), CORM-P2) carbon monoxide liberation.



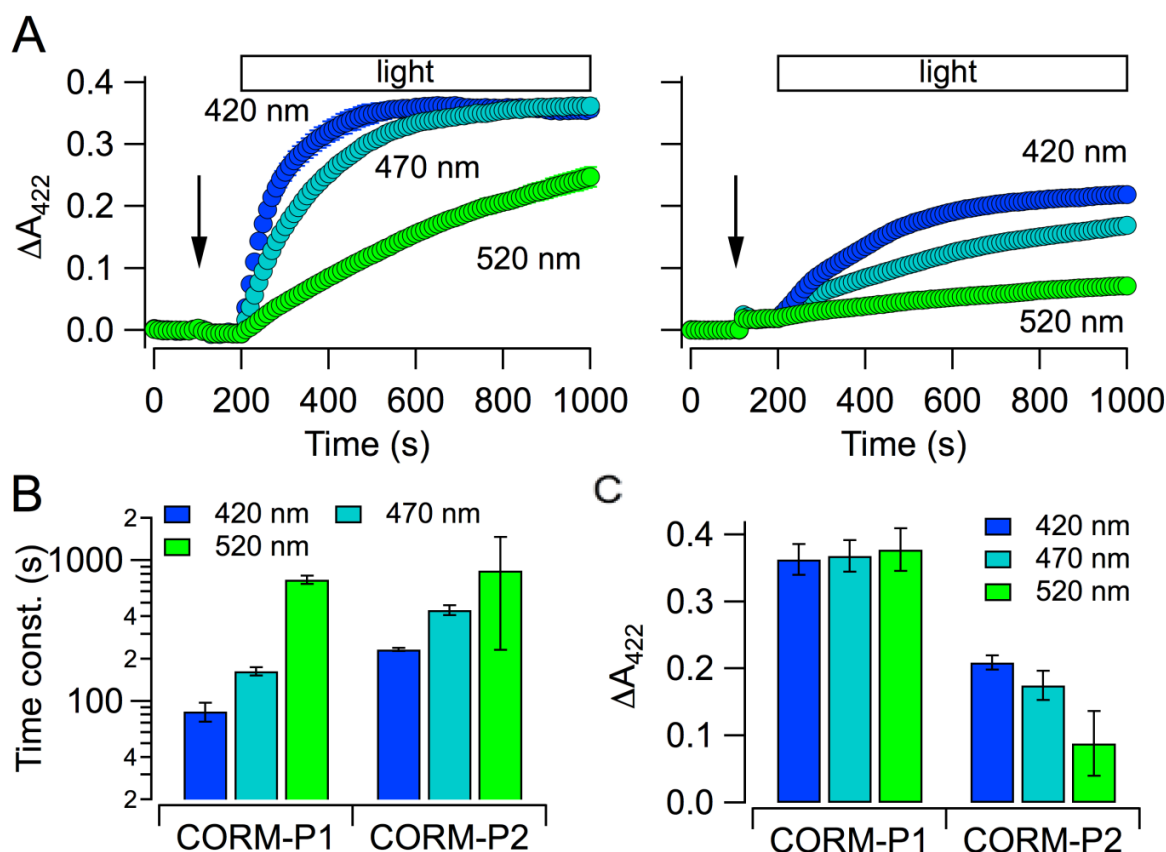
**Fig 2.17:** Absorption spectra for 100  $\mu\text{M}$  CORM-P1 (left) and CORM-P2 (right) irradiated with white light for 10 min in PBS + 0.1% sodium dithionite + 100  $\mu\text{M}$  deoxymyoglobin (Mb) (black line). Absorption spectra for CO-free (gray line) and CO-saturated (red line) Mb are shown for comparison. Also indicated is the self-absorbance of CORM-P2, which precludes the use of this assay for quantitative CO release determination.

However, monitoring of the CO release of CORM-P2 in this wavelength range, which requires a high concentration, was less accurate because of the self-absorbance of this complex. We therefore also investigated the light-dependent CO release at lower concentration (5  $\mu\text{M}$ ) in a spectral range covering the Soret peak (figure 2.18). The CORMs were irradiated for 10 min in a buffered solution, which contained 0.1% of sodium dithionite and a concentration of 10  $\mu\text{M}$  deoxymyoglobin, and the spectra without and with irradiated CORMs were compared (figure 2.18 for irradiation with 420-nm light). While stable in the dark, light completely released CO from CORM-P1. For the benzo derivative CORM-P2, however, the release was incomplete. A comparable observation was also valid for a comparison of  $[(\text{OC})_2\text{Fe}(\text{SCH}_2\text{CH}_2\text{NH}_2)_2]$  (CORM-S1) and  $[(\text{OC})_2\text{Fe}(\text{SC}_6\text{H}_4\text{NH}_2)_2]$  (CORM-S2) [117].



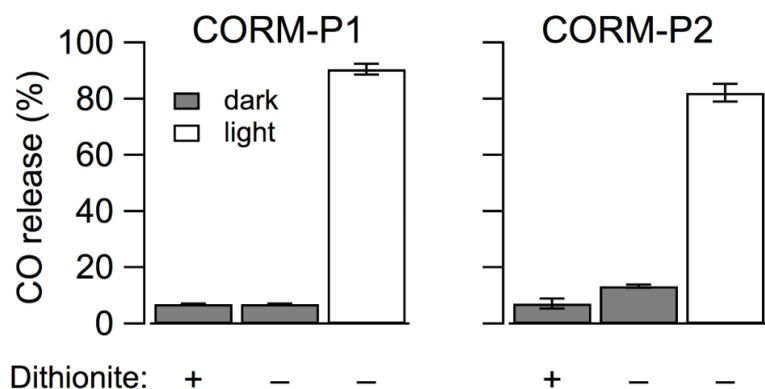
**Fig 2.18:** Absorption spectra in the range of 380-450 nm for 5  $\mu\text{M}$  of the indicated CORMs and 10  $\mu\text{M}$  deoxymyoglobin upon 10-min irradiation with 420-nm light. For controls Mb with 5  $\mu\text{M}$  CO (long dashes red line) and 100  $\mu\text{M}$  CO (red line), as well as Mb with CORMs before irradiation (green line) are shown.

Kinetics of CO release was monitored by measuring the change in absorbance at 422 nm. When exposing the samples to light of 420, 470, or 520 nm, CO release followed a single-exponential time course (figure 2.19, A). The corresponding time constants strongly increased with the wavelength (figure 2.19, B). For CORM-P1, total release of the CO could be obtained for all wavelengths in the chosen experimental setting, while for CORM-P2 only a partial release was observed (figure 2.19, C).



**Fig 2.19:** Absorbance changes at 422 nm ( $\Delta A_{422}$ ) as a function of time for the indicated wavelengths. The arrows indicate addition of 5  $\mu\text{M}$  CORM-P1 (left) or CORM-P2 (right) (A). Samples were illuminated 100 s later, as indicated by the horizontal bar. The instantaneous increase in absorbance upon addition of CORM-P2 originates from the absorbance of the CORM. (B, C) The time courses in (A) were fit with single-exponential functions and the resulting time constants (B) and the maximal absorbance changes (C) are shown for the indicated wavelengths. The bars labeled “CO” show the absorbance change obtained when adding 10  $\mu\text{M}$  Mb to a solution containing 5  $\mu\text{M}$  CO, i.e. they mark the maximal possible release of CO from the CORMs studied. All data shown are means  $\pm$  SEM for  $n = 4-5$ .

As it was reported for CORM-2 and CORM-3 that CO release is strongly facilitated by the reducing agent dithionite [104], we also performed experiments in which CO release was triggered by light in the absence of dithionite. Such experiments (figure 2.20) clearly showed that dithionite itself does not induce release of CO from the compounds studied, which is in agreement with the NMR experiments shown above.



**Fig 2.20:** CO release is not dependent on dithionite. CO release from CORM-P1 and CORM-P2 during 10-min preincubation without Mb in the presence (“+”) or absence (“-”) of dithionite, with (open bars) or without (grey bars) illumination with white light. Spectra were taken right after preincubation and subsequent mixing of the samples with Mb/dithionite. Experimental conditions as in figure 2.17. Data are means  $\pm$  SEM for  $n = 4-5$ .

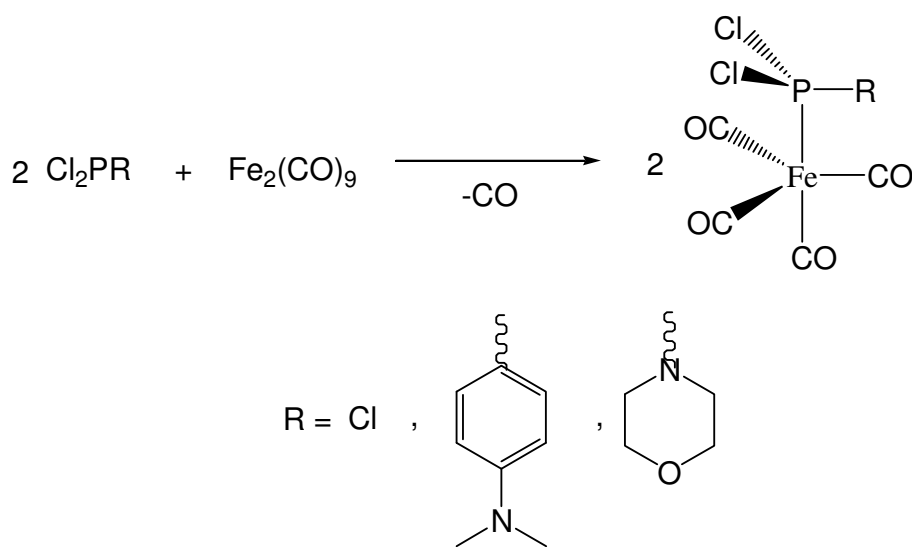
### **2.3 P-iron-based CORMs**

In already known studies on CORMs with iron(0) centers the CO releasing properties (such as half life time) are triggered by the ligands with changes of the ligand backbone leading to different half-lives [61,62,64,70,109,117,125-128]. Unfortunately, systematic studies to get relationships between structural and spectroscopic parameters and the CO releasing characteristics are quite scarce [64,65]. Scapens et al. tried to correlate the half-lives ( $t_{1/2}$ ) of cyclopentadienyl iron carbonyls with their spectroscopic and structural parameters, i.e.  $\nu(\text{CO})$ ,  $\delta(^{13}\text{C})$ ,  $\delta(\text{C}^{17}\text{O})$  as well as  $r(\text{Fe-C})$  [64]. For the spectroscopic parameter they found correlations within a series of compounds but not over all compounds. The correlation of the structural parameter  $r(\text{Fe-C})$  with  $t_{1/2}$  is described as very poor due to the insufficient accuracy of both values.

Based on these investigations we intended to prepare iron(0) based CORMs based on ligands with analogous structural properties to investigate a possible relationship between the spectroscopic and structural parameters and the CO releasing behaviour.

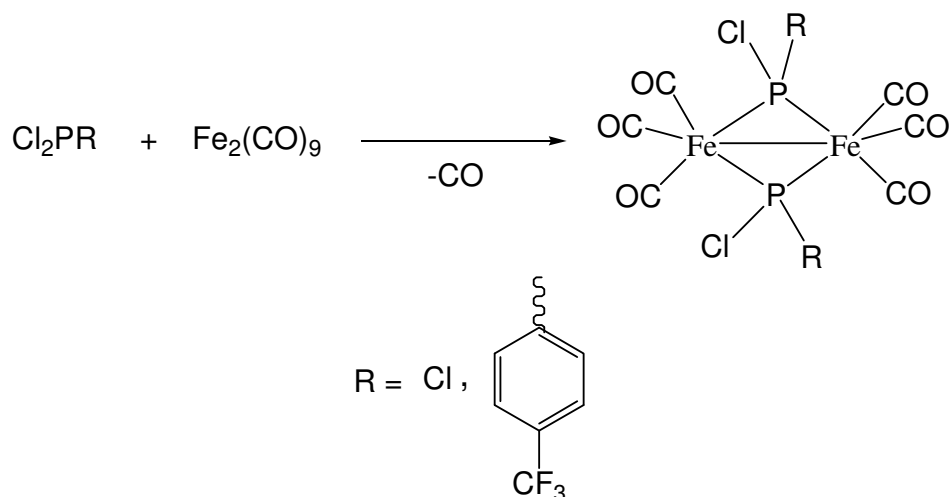
### 2.3.1 Synthesis

The reactions of substituted dichlorophosphanes with diiron nonacarbonyl yield the corresponding tetracarbonylchlorophosphanes as shown in Scheme 2.7. Analogous systems were synthesized earlier by Lang et al. but based on hydrophobic ligands such as alkyl- and aryl-dichlorophosphanes [129]. With tetracarbonyl-[trichlorophosphane]iron(0) (**9**, CORM-P3), tetracarbonyl[dichloro(*p*-*N,N*-dimethylamino-phenyl)phosphine]iron(0) (**10**, CORM-P4) [130], and tetracarbonyl[dichloro-(morpholino)phosphane]iron(0) (**11**, CORM-P5) [130] we present three compounds which should be more hydrophilic.



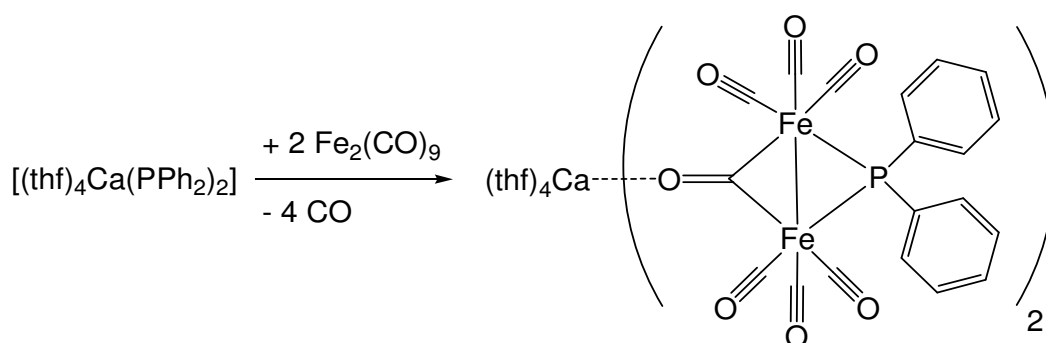
Scheme 2.7: Synthesis of CORM-P3 (9, R =Cl), CORM-P4 (10, R =C<sub>6</sub>H<sub>4</sub>-4-NMe<sub>2</sub>), and CORM-P5 (11, R =N(CH<sub>2</sub>CH<sub>2</sub>)<sub>2</sub>O).

The dinuclear complexes [Fe<sub>2</sub>(CO)<sub>6</sub>(PCl<sub>2</sub>)<sub>2</sub>] (**12**, CORM-P6), and [Fe<sub>2</sub>(CO)<sub>6</sub>{PCl(C<sub>6</sub>H<sub>4</sub>-CF<sub>3</sub>)<sub>2</sub>}<sub>2</sub>] (**13**, CORM-P7) were also prepared *via* the reaction of substituted dichloroarylphosphanes with diironnonacarbonyl (Scheme 2.8).



**Scheme 2.8:** Synthesis of  $[\text{Fe}_2(\text{CO})_6(\text{PCl}_2)_2]$  (**12**, CORM-P4), and  $[\text{Fe}_2(\text{CO})_6(\text{PCl}(\text{C}_6\text{H}_4\text{-CF}_3))_2]$  (**13**, CORM-P5) starting from diironnonacarbonyl.

Complex  $[(\text{thf})_4\text{Ca}\{\text{Fe}_2(\text{CO})_6(\mu\text{-CO})(\mu\text{-PPh}_2)\}_2]$  (**14**, CORM-FC) was prepared by the reaction of  $[(\text{thf})_4\text{Ca}(\text{PPh}_2)_2]$  with excess of iron carbonyls  $\text{Fe}(\text{CO})_5$ ,  $\text{Fe}_2(\text{CO})_9$ , or  $\text{Fe}_3(\text{CO})_{12}$  according to the literature procedure [131] (Scheme 2.9). In the solid state, contact ion pairs were observed whereas in solution solvent-separated ions can be assumed.



**Scheme 2.9:** Synthesis of  $[(\text{thf})_4\text{Ca}\{\text{Fe}_2(\text{CO})_6(\mu\text{-CO})(\mu\text{-PPh}_2)\}_2]$  (**14**, CORM-FC) starting from diironnonacarbonyl.

### 2.3.2 Molecular structures

We will divide these P-iron-based CORMs into two groups according to their molecular structures; the first group contains mono-iron carbonyl complexes such as CORM-P3, CORM-P4, and CORM-P5. The second group consists of dinuclear complexes of iron carbonyl dimers like CORM-P6 and CORM-P7 as well as iron clusters such as CORM-FC.

The IR frequencies of complexes **9** (CORM-P3), **10** (CORM-P4), and **11** (CORM-P5) are summarized in Table 2.2. All these complexes have lower CO vibrations ( $\nu_{\text{CO}}$ ) in comparison to iron pentacarbonyl (2014 and 2034  $\text{cm}^{-1}$ ) [132 (a)]. This behavior results from the fact that the carbonyl ligand is a better  $\pi$ -acceptor compared to the phosphine ligands which comes along with an increased transfer of electron density from the metal center to the antibonding  $\pi^*$ -orbitals of the CO ligands.

**Table 2.2:** Comparison of IR wavenumbers [ $\text{cm}^{-1}$ ] data of the complexes **9** (CORM-P3), **10** (CORM-P4), and **11** (CORM-P5).

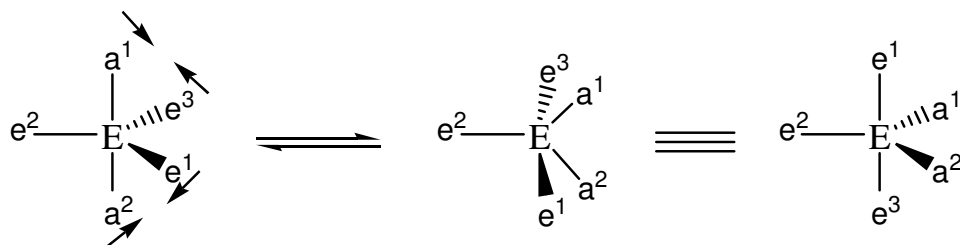
CORMs	( <b>9</b> , CORM-P3)	( <b>10</b> , CORM-P4)	( <b>11</b> , CORM-P5)
$\nu(\text{C-O}) \text{ cm}^{-1}$	2091	2111	2113
	2081	2061	2071
	2020	1997	2000
	1998	1969	1966
	1987	1953	1954

The electron withdrawing effect of chlorine and morpholine is further reflected by a blue shift of the carbonyl IR frequencies of CORM-P3 and CORM-P5 compared to CORM-P4. CORM-P4 and CORM-P5 contain 4 carbonyl and one dichlorophosphine ligands which are trigonal-bipyramidal arranged around the iron center. The Fe-CO bonds of CORM-P4 (1.787(4) Å - 1.802(3) Å) and CORM-P5 (1.797(5) Å - 1.807(5) Å) differs very slightly from the corresponding Fe-CO bonds in pentacarbonyl iron (1.79(4) Å) [132



(b)], while C-O bonds of CORM-P4 (1.141(4) Å - 1.152(4) Å) and CORM-P5 (1.141(5) Å - 1.150(5) Å) are elongated in comparison to iron pentacarbonyl (1.14(8) Å) [132 (b)]. This behavior results from the same fact that shifts CO vibrations ( $\nu_{\text{CO}}$ ) of these CORMs to lower wavenumbers than the CO vibrations ( $\nu_{\text{CO}}$ ) of iron pentacarbonyl. The Fe-P bond in CORM-P4 (2.1727(9) Å) and CORM-P5 (2.1652(12) Å) is stabilized compared to  $[\text{Fe}(\text{CO})_4\text{P}(\text{C}_6\text{H}_5)_3]$  (2.244(1) Å) [133] and  $[\text{Fe}(\text{CO})_4\text{P}(\text{C}_6\text{H}_{11})_3]$  (2.2922(7) Å) [134] due to an increase of the  $\pi$ -acceptor character caused by the electronegativity of the two chlorine atoms.

CORM-P3 contains two different types of carbonyl ligands which are in agreement with the CO stretching frequencies in the IR spectra, whereas only one resonance is observed in the  $^{13}\text{C}$ -NMR spectra. This result can be explained by the pseudorotation phenomenon. It is a kind of stereoisomerisation resulting in a structure that appears to have been produced by rotation of the entire initial molecule and is superposable on the initial one. Different positions are distinguished by substitution, including isotopic substitution. An important example of pseudorotation (Berry pseudorotation) is a polytopal rearrangement that provides an intramolecular mechanism for the isomerisation of trigonal bipyramidal compounds which is shown in Scheme 2.10.

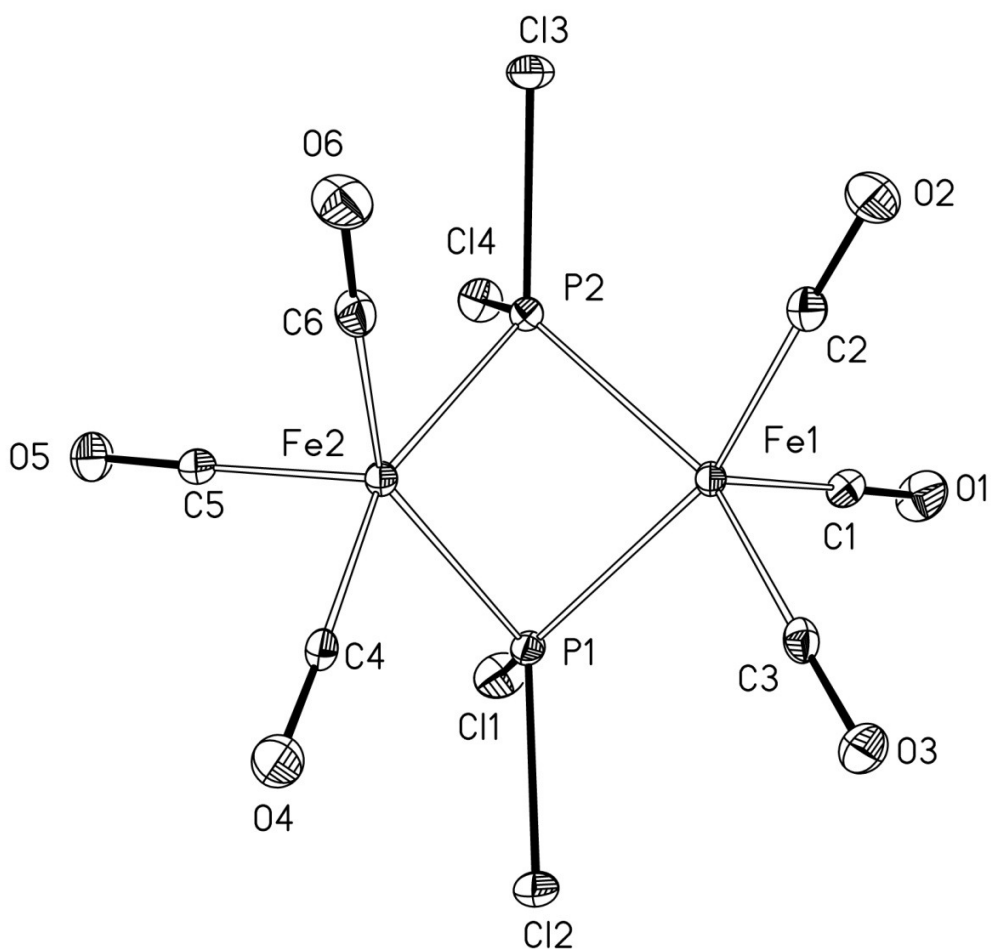


**Scheme 2.10:** Berry pseudorotation of trigonal bipyramidal compounds, the five bonds to the central atom E being represented as  $e^1$ ,  $e^2$ ,  $e^3$ ,  $a^1$  and  $a^2$ . Two equatorial bonds move apart and become apical bonds at the same time as the apical bonds move together to become equatorial.

According to the fact that IR spectroscopy is faster than NMR spectroscopy, IR can detect the pseudorotation stereoisomerisation process in CORM-P3. Thus all CO stretching frequencies of CORM-P3 can be seen in IR spectra. However, we saw in  $^{13}\text{C}$ -NMR spectra only one resonance due to the time scale in the NMR spectroscopy.

The complexes  $[\text{Fe}_2(\text{CO})_6(\text{PCl}_2)_2]$  (**12**, CORM-P6), and  $[\text{Fe}_2(\text{CO})_6\{\text{PCl}(\text{C}_6\text{H}_4\text{-CF}_3)\}_2]$  (**13**, CORM-P7) were prepared as CORMs with high CO content. The molecular structure of complex **12** is shown in figure 2.21.

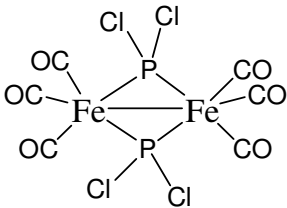
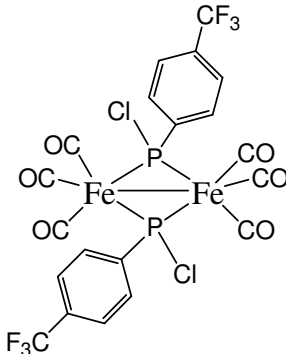
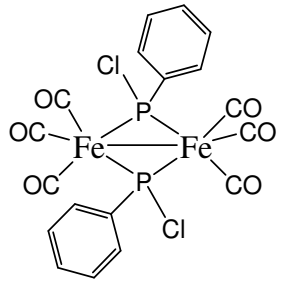
**Fig 2.21:** Molecular structure and numbering scheme of  $[\text{Fe}_2(\text{CO})_6(\text{PCl}_2)_2]$  (**12**, CORM-P6). The ellipsoids represent a probability of 40%. Selected bond lengths (pm): Fe1-C1 180.6(2), Fe1-C2 182.0(2), Fe1-C3 181.8(2), Fe2-C4 183.1(2), Fe2-C5 180.2(2), Fe2-C6 181.1(2), Fe1-P1 217.68(6), Fe1-P2 218.06(6), Fe2-P1 217.17(6), Fe2-P2 217.00(6), Cl1-P1 203.24(8), Cl2-P1 203.57(8), Cl3-P2 203.16(7), Cl4-P2 203.33(8), C1-O1 113.4(3), C2-O2 113.4(3), C3-O3 113.5(3), C4-O4 112.3(3), C5-O5 113.3(3), C6-O6 113.6(3), Fe1-Fe2 269.56(4); selected bond angles [ $^\circ$ ]: C1-Fe1-C3 101.15(10), C1-Fe1-C2 101.10(11), Fe1-P1-Fe2 51.608(16), Fe1-P2-Fe2 51.536(16), Fe1-P1-Cl1 121.41(3), Fe1-P1-Cl2 119.66(3), Fe1-P2-Cl3 120.45(3), Fe1-P2-Cl4 123.76(3), Cl1-P1-Cl2 97.97(3), Cl3-P2-Cl4 98.83(3).



The molecular structures of dinuclear **12** (CORM-P6) and  $[\text{Fe}_2(\text{CO})_6\{\text{PCl}(\text{C}_6\text{H}_5)\}_2]$  [136] both contain six carbonyl and two phosphanide ligands which are octahedrally arranged around the iron(I) centers. Both phosphanides of CORM-P6 carry two highly electronegative chlorine atoms, while in the corresponding phosphanide ligands in  $[\text{Fe}_2(\text{CO})_6\{\text{PCl}(\text{C}_6\text{H}_5)\}_2]$  half of the chlorine atoms are substituted by phenyl groups. The Fe-CO bonds of CORM-P6 (1.802(2) Å-1.831(2) Å) are elongated in comparison to the corresponding Fe-CO bonds in  $[\text{Fe}_2(\text{CO})_6(\text{PC}_6\text{H}_5\text{Cl})_2]$  (1.74(1) Å-1.80(1) Å). This finding results from the higher content of electron withdrawing chlorine atoms in CORM-P6 in comparison to  $[\text{Fe}_2(\text{CO})_6\{\text{PCl}(\text{C}_6\text{H}_5)\}_2]$ , which decreases the transfer of electron density from the iron center to the antibonding  $\pi^*$ -orbitals of the CO ligands.

Furthermore, the IR frequencies of complexes **12** (CORM-P6), **13** (CORM-P7), and  $[\text{Fe}_2(\text{CO})_6\{\text{PCl}(\text{C}_6\text{H}_5)\}_2]$  [136] are shown in table 2.3.

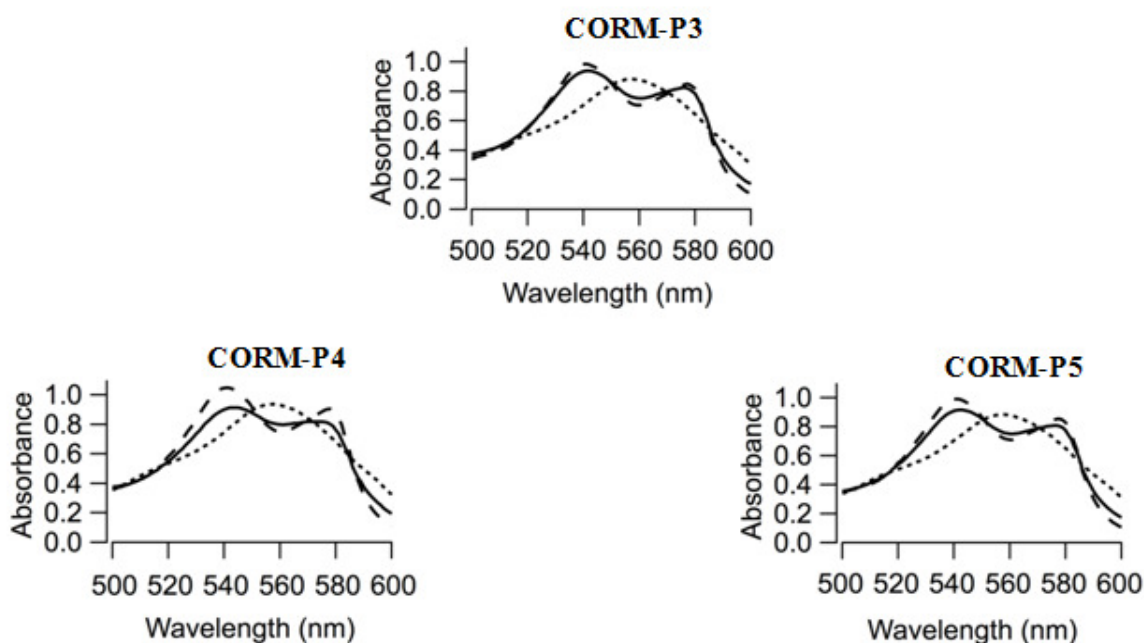
**Table 2.3:** Comparison of and IR frequencies [ $\text{cm}^{-1}$ ] data of the complexes (**12**, CORM-P6), (**13**, CORM-P7), and  $[\text{Fe}_2(\text{CO})_6(\text{PC}_6\text{H}_5\text{Cl})_2]$ .

CORMs	( <b>12</b> , CORM-P6)	( <b>13</b> , CORM-P7)	$[\text{Fe}_2(\text{CO})_6(\text{PC}_6\text{H}_5\text{Cl})_2]$
			
$\nu(\text{C-O}) \text{ cm}^{-1}$	2089	2162	2073
	2060	2078	2036
	2032	2044	2016
	2019	2020	1990

The CO vibrations ( $\nu_{\text{CO}}$ ) of the highest energy are observed for CORM-P7. CORM-P6 and  $[\text{Fe}_2(\text{CO})_6\{\text{PCl}(\text{C}_6\text{H}_5)\}_2]$  exhibit significantly lower energies. This result can be explained by the previous discussion that CORM-P7 contains the extremely strong electron withdrawing trifluoromethyl substituents in para-position of the phenyl rings. This influence decreases the transfer of electron density from the metal center to the antibonding  $\pi^*$ -orbitals of the CO ligands. In addition, the more positive nature of the P atoms by higher contents of chlorine atoms in CORM-P6 leads to a strong blue shift of the carbonyl IR frequencies of CORM-P6 compared to those of  $[\text{Fe}_2(\text{CO})_6\{\text{PCl}(\text{C}_6\text{H}_5)\}_2]$ . Complex  $[(\text{thf})_4\text{Ca}\{\text{Fe}_2(\text{CO})_6(\mu\text{-CO})(\mu\text{-PPh}_2)\}_2]$  (**14**) [131] was investigated as a CORM with a large number of CO ligands. The iron centers in CORM-FC coordinate with different types of carbonyl ligands; the CO bond of the bridging carbonyl ligand is elongated compared to the bond lengths in terminally bound carbonyl groups. This fact is in agreement with the expectation that bridging carbonyl groups should exhibit a C=O bond order of two (comparable to ketones) whereas terminally bound carbonyl groups should show a higher bond order (comparable to isoelectronic cyanide). Moreover within the group of terminally bound carbonyl ligands significant differences can be noticed. The Fe-C bonds in *trans*-position to the bridging carbonyl group show significantly larger Fe-C distances due to the *trans* influence of the bridging carbonyl ligand.

### **2.2.3 CO-release properties**

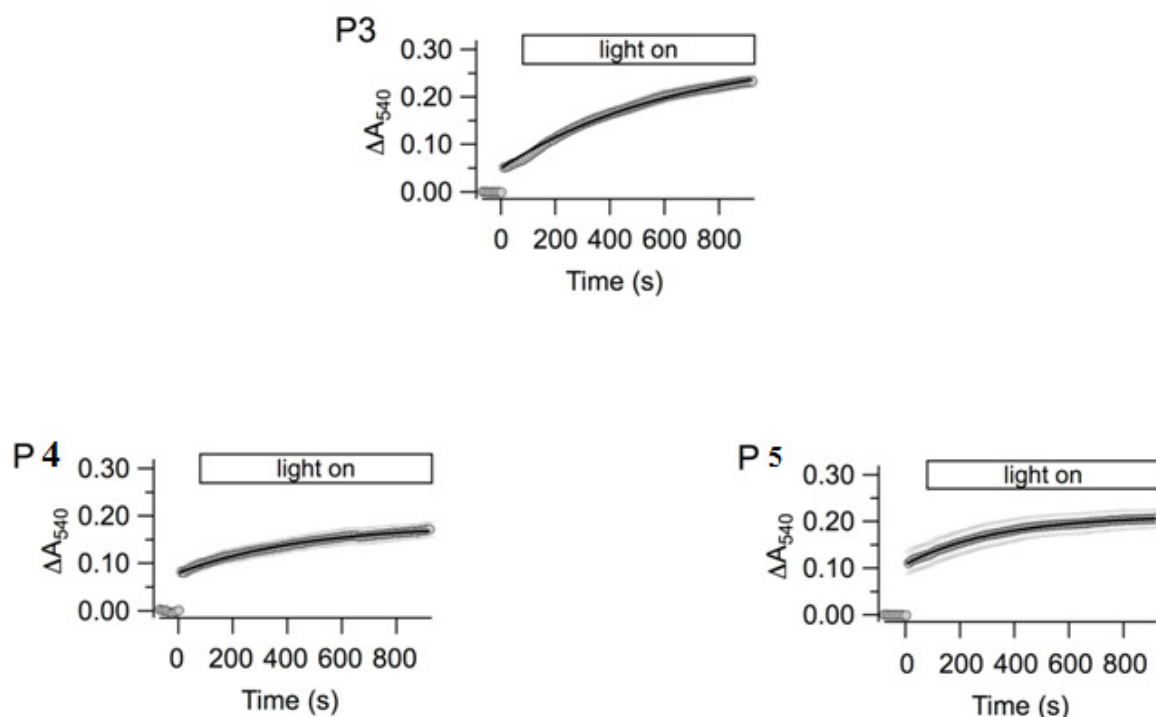
The CO release from all P-iron-based CORMs was quantified in a myoglobin-based assay by measuring the conversion of deoxymyoglobin into the myoglobin-CO complex. As shown in figure 2.22, a spontaneous CO release of  $18.5 \pm 2.3 \mu\text{M}$  ( $n = 6$ ),  $27.4 \pm 3.7 \mu\text{M}$  ( $n = 3$ ), and  $39.2 \pm 8.4 \mu\text{M}$  ( $n = 7$ ) was observed directly after application of  $100 \mu\text{M}$  of **9** (CORM-P3), of **10** (CORM-P4), and of **11** (CORM-P5), respectively, followed by slow additional CO release.



**Fig 2.22:** CO-releasing properties of CORM-P3, CORM-P4, and CORM-P5 (as indicated). Averaged spectra ( $n = 3-7$ ) of the samples (deoxy-myoglobin solutions ( $100 \mu\text{M}$ )) were recorded before CORM application (dotted) and in the presence of CORM after 15 min of illumination (solid). Dashed lines represent spectra of CO-saturated myoglobin solutions.

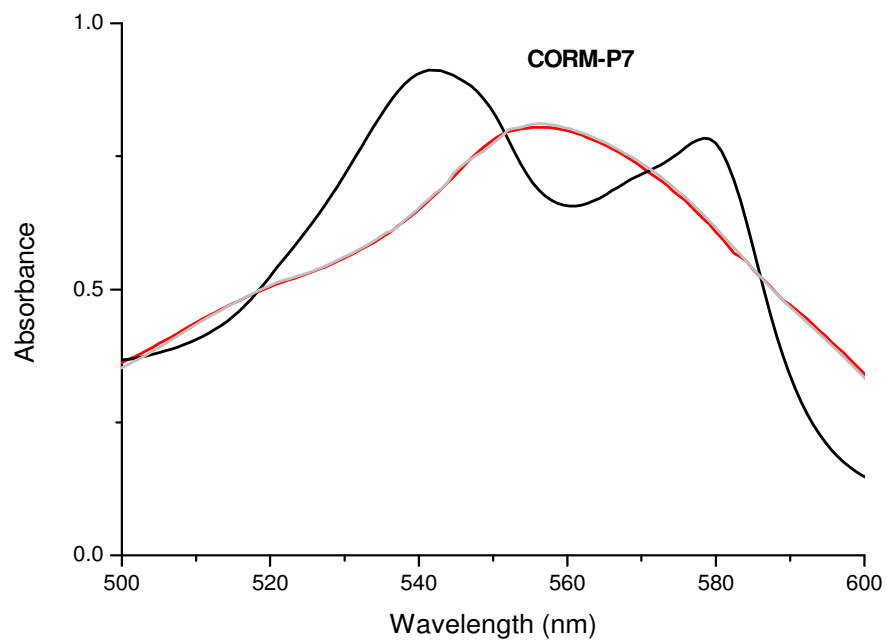
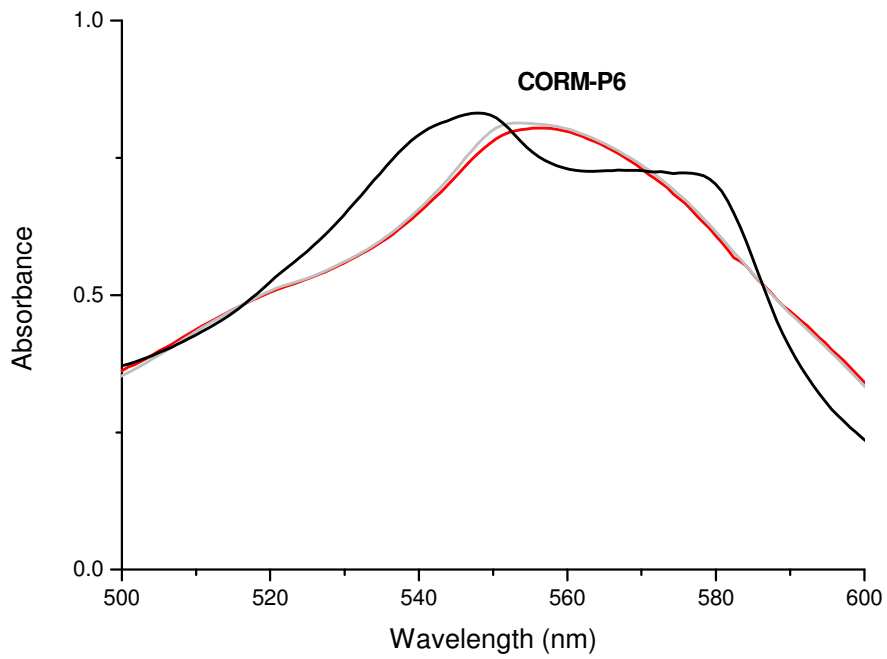
CORM-P3 showed the strongest CO release which is compatible with its highest CO vibrations ( $\nu_{\text{CO}}$ ) in comparison to CORM-P5 and CORM-P4 as a consequence of decreased transfer of electron density from the metal center to the antibonding  $\pi^*$ -orbitals of the CO ligands (figure 2.22). This assay is in agreement with the fact that CORM-P3 contains the weakest Fe-CO bonds of all three tested compounds. In addition, CORM-P5 acts as stronger CO releaser than CORM-P4. Here the weakness of the Fe-CO bond results from the highly electronegative nitrogen atom in CORM-P5 in comparison to CORM-P4 which contains the dimethylaminophenyl substituent as electron donating group causing the weakest CO release behavior in all three mononuclear CORMs.

Time constants for the slow CO release obtained from monoexponential fits (figure 2.23), were 646 s, 468 s, and 341 s for CORM-P3, CORM-P4, and CORM-P5, respectively, with a total CO release of  $82.5 \pm 4.7 \mu\text{M}$ ,  $51.5 \pm 5.3 \mu\text{M}$ , and  $71.9 \pm 6.8 \mu\text{M}$  after 15 min of illumination with white light. For all three CORMs tested, CO release did not require irradiation with light. In this test, CORM-P3 exhibited the strongest CO release of the compounds tested. In addition, only CO release of CORM-P3 was slightly light-stimulated. After start of sample illumination, speed of release was slightly, yet significantly ( $P < 0.005$ ) increased by a factor of 1.56-fold.



**Fig 2.23:** Absorbance of deoxy-myoglobin solutions ( $100 \mu\text{M}$ ) was measured at 540 nm. Relative absorbance changes ( $\Delta A_{540}$ ) compared to starting values are plotted against time. CORM-P3, CORM-P4, and CORM-P5 (as indicated) were applied at time zero. Sample illumination with a cold light source was started at 80 s, as indicated. Data are shown as mean  $\pm$  SEM of 3-7 measurements. The superimposed black curves are single-exponential fits.

Kinetic measurements for **12** (CORM-P6) and **13** (CORM-P7) are based on monitoring the conversion of a buffered aqueous solution of deoxy-myoglobin to carboxy-myoglobin as shown in figure 2.24.

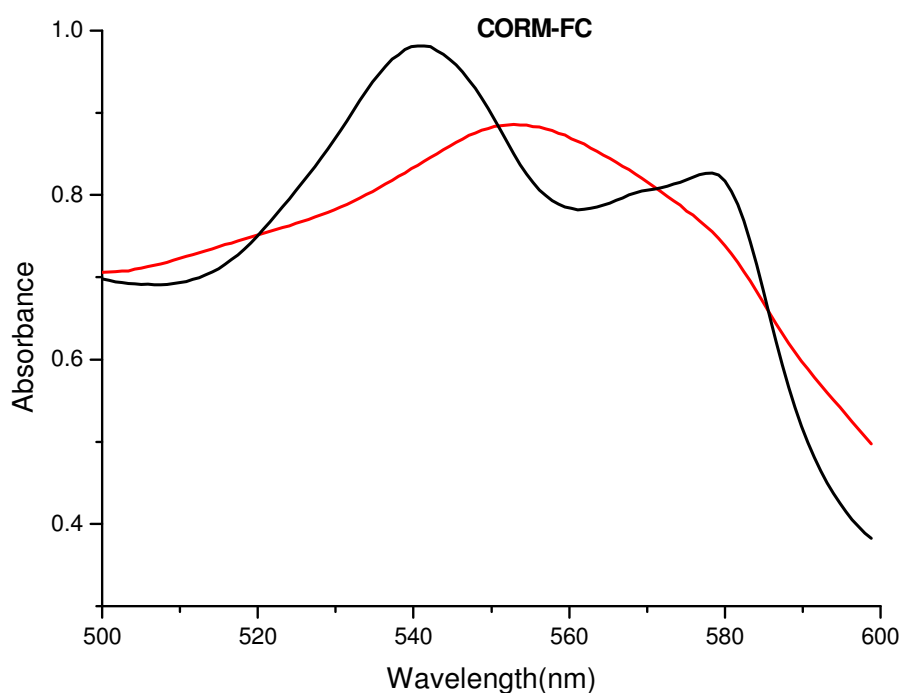


**Fig 2.24:** Myoglobin assay of indicated compounds: Absorbance as a function of wavelength of 100  $\mu\text{M}$  deoxymyoglobin in the absence of CORM (red), as well as myoglobin incubated with 50  $\mu\text{M}$  of CORM after 15min of irradiation at 470 nm (black) or after 15 min in the dark (gray).



CORM-P7 displayed stronger CO release than CORM-P6. This outcome is compatible with the higher CO vibrations ( $\nu_{\text{CO}}$ ) values of CORM-P7 than of CORM-P6. The weaker Fe-CO bond in CORM-P7 is caused by the electron withdrawing effect of the trifluoromethyl group.

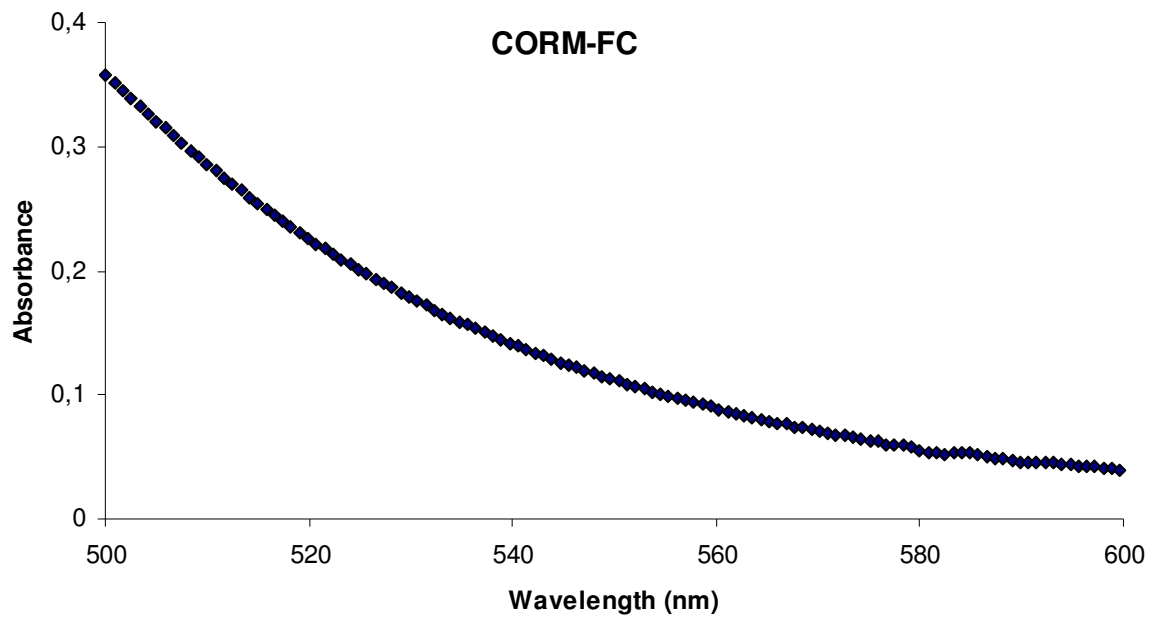
The suitability of complex  $[(\text{thf})_4\text{Ca}\{\text{Fe}_2(\text{CO})_6(\mu\text{-CO})(\mu\text{-PPh}_2)\}_2]$  (**14**) (CORM-FC) [130] as a CORM was investigated by using the myoglobin assay as shown in figure 2.25.



**Fig 2.25:** Myoglobin assay of CORM-FC: Absorbance as a function of wavelength of 100  $\mu\text{M}$  deoxymyoglobin with 50  $\mu\text{M}$  of CORM after 15min of irradiation at 470 nm (black) or after 15 min in the dark (red).

We assayed the properties of complex **14** in aqueous solutions. CO release was quantified in a myoglobin-based assay by spectrophotometric measurement of the conversion of deoxymyoglobin (Mb) into the myoglobin-CO complex (Mb-CO). For measurements in the range of 500 to 600 nm a solution was prepared that contained 50  $\mu\text{M}$  of  $[(\text{thf})_4\text{Ca}\{\text{Fe}_2(\text{CO})_6(\mu\text{-CO})(\mu\text{-PPh}_2)\}_2]$  (**14**) and 100  $\mu\text{M}$  of deoxymyoglobin. Myoglobin was reduced with 0.1% sodium dithionite. CORM-FC showed no CO release

in the dark but irradiation with light for 10 minutes led to carbon monoxide liberation. Furthermore, CORM-FC also absorbs in this wavelength range as shown in figure 2.26, increasing the absorbance in the myoglobin sample with CORM-FC.

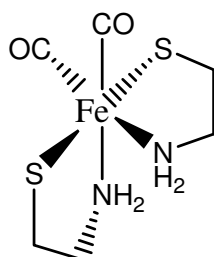


**Fig 2.26:** Absorption spectra in the range of 500-600 nm for 50  $\mu$ M of CORM-FC.

### 3. Experimental

**General remarks** Trirutheniumdodecacarbonyl [Ru<sub>3</sub>(CO)<sub>12</sub>], triirondodecacarbonyl [Fe<sub>3</sub>(CO)<sub>12</sub>], diironnonacarbonyl [Fe<sub>2</sub>(CO)<sub>9</sub>], and iron tetrafluoroborate hexahydrate [Fe(BF<sub>4</sub>)<sub>6</sub>·6H<sub>2</sub>O], myoglobin from equine skeletal muscle, and sodium dithionite were purchased from Sigma-Aldrich Company. Cysteamine HSCH<sub>2</sub>CH<sub>2</sub>NH<sub>2</sub>, cystamine (H<sub>2</sub>NCH<sub>2</sub>CH<sub>2</sub>S)<sub>2</sub>, 2-aminothiophenol HSC<sub>6</sub>H<sub>4</sub>-2-NH<sub>2</sub>, 2-(diphenylphosphino)ethylamine Ph<sub>2</sub>PCH<sub>2</sub>CH<sub>2</sub>NH<sub>2</sub>, o-fluoroaniline NH<sub>2</sub>C<sub>6</sub>H<sub>4</sub>-4-F, potassium diphenylphosphide solution KPPH<sub>2</sub> (.50 M in THF), phosphorus trichloride (PCl<sub>3</sub>), and p-CF<sub>3</sub>C<sub>6</sub>H<sub>4</sub>Br were supplied by Acros Organics. All compounds were prepared and handled in an inert gas atmosphere under anaerobic conditions using Schlenk techniques. Tetrahydrofuran, diethyl ether, hexane, toluene, benzene, pentane, and heptane were distilled from sodium benzophenone, DMF was dried over molecular sieves, acetonitrile and dichloromethane were distilled from calcium hydride. <sup>1</sup>H, <sup>13</sup>C, <sup>31</sup>P, and <sup>19</sup>F NMR spectra were obtained on Bruker Avance 200, 400, and 600 spectrometers. Assignment of NMR data was performed on the basis of <sup>1</sup>H, <sup>13</sup>C, <sup>31</sup>P, <sup>19</sup>F, HSQC, HMBC, and H,H COSY experiments. Mass spectra were obtained on a Finnigan MAT SSQ 710. IR spectra were recorded on the Perkin Elmer FT-IR-Spectrometer System 2000 as Nujol mulls between KBr windows and ATR-IR spectrometer. Elemental analysis on a LECO CHNS-932 apparatus gave values for C, H, N, and S. All UV-visible (UV-VIS) spectra of the myoglobin assay were recorded using an Ultrospec 1100pro spectrophotometer (Amersham Biosciences).

#### 3.1 Synthesis of [Fe(CO)<sub>2</sub>(SCH<sub>2</sub>CH<sub>2</sub>NH<sub>2</sub>)<sub>2</sub>] (CORM-S1) (1):

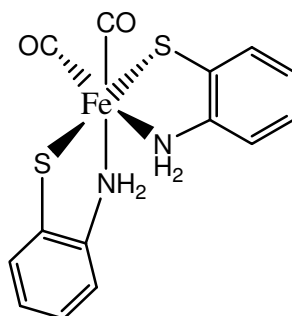


For the synthesis of CORM-S1 (*cis,trans,cis*-dicarbonyl-bis(2-thiolato-κS-ethylamine-κN)iron(II)) a suspension of 510 mg of triirondodecacarbonyl (1.01 mmol) and 463 mg of 2,2'-disulfanediyldiethanamine (cystamine) (3.04 mmol) in 20 ml of THF were stirred under reflux for three hours; during this reaction time an orange suspension was

formed. All solids were collected and the filter cake dried in vacuum giving pure microcrystalline **1**. The filtrate was reduced to 5 ml and stored at -18 °C yielding red-brown single crystals suitable for X-ray diffraction studies. Total yield: 465 mg (1.76 mmol, 58%). The physical data are identical to published ones [125].

**Physical data:** M.p.: 118 °C (dec.). NMR: <sup>1</sup>H NMR ([D<sub>6</sub>]DMSO): 2.08 [t (4.9Hz), 2H]; 2.74 [m (5.0Hz), 4H]. <sup>13</sup>C NMR ([D<sub>6</sub>]DMSO): 28.68; 50.57; 215.08. MS-FAB: 265 [M+H]<sup>+</sup>(16); 237 [M+H-CO]<sup>+</sup> (10); 209 [M+H-2CO]<sup>+</sup> (56); 208 [M-2CO]<sup>+</sup>(88). IR [KBr]: 3436 (m); 3210 (s); 3119 (s); 2952 (m); 2922 (m); 2867(m); 2836 (w); 2364 (w); 2345 (w); 2014 (vs); 1945 (vs); 1584 (m);1454 (w); 1433 (w); 1303 (w); 1269 (m); 1223 (w); 1120 (m); 1094(m); 1042 (m); 971 (w); 918 (w); 848 (w); 805 (w); 648 (w); 591 (s);545 (m); 492 (w). Elemental analysis of THF adduct (C<sub>10</sub>H<sub>20</sub>FeN<sub>2</sub>O<sub>3</sub>S<sub>2</sub>, 336.25 g mol<sup>-1</sup>): calculated: C 27.28; H 4.58; N 10.13; S 24.28; found: C 26.86; H 5.46; N10.13; S 23.18.

### 3.2 Synthesis of [Fe(CO)<sub>2</sub>(SC<sub>6</sub>H<sub>4</sub>-2-NH<sub>2</sub>)<sub>2</sub>] (CORM-S2) (**2**):

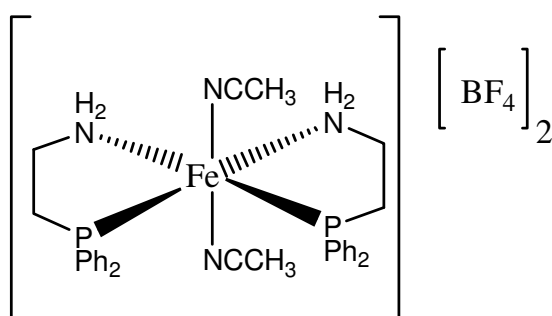


For the preparation of CORM-S2 (*cis,trans,cis*-dicarbonyl-bis(2-thiolato-κS-benzamine-κN)iron(II)·THF) a suspension of 510 mg of triirondodecacarbonyl (1.01 mmol) and 760 mg of 2-aminothiophenol (6.07 mmol) in 15 ml of THF were stirred under reflux for four hours. During this time a red suspension formed. The solids were collected by filtration and the filter cake dried in vacuum giving pure microcrystalline **2**. The solvent of the filtrate was removed in vacuum and the residue dissolved in THF. Slow diffusion of pentane into this solution at -18 °C gave red-brown single crystals within one week suitable for X-ray diffraction experiments. Total yield: 812 mg (1.88 mmol, 62%).

**Physical data:** M.p. 155 °C (dec.). NMR: <sup>1</sup>H NMR ([D<sub>6</sub>]DMSO): δ 1.77 [s, 2H], 3.59 [s, 2H], 5.77 [d (14.1 Hz), 2H], 6.79 [t (7.0 Hz), 2H], 6.84 [d (14.1 Hz), 2H], 6.88 [t (7.1 Hz), 2H], 7.11 [d (7.0 Hz), 2H], 7.21 [d (7.1 Hz), 2H]. <sup>13</sup>C NMR ([D<sub>6</sub>]DMSO): δ 25.1; 67.0,

121.0, 125.7, 125.9, 128.1, 143.4, 147.3, 213.6. MS-FAB: 361  $[M+H]^+$  (16); 333  $[M+H-CO]^+$  (10); 305  $[M+H-2CO]^+$  (56); 304  $[M-2CO]^+$  (88). IR [KBr]: 3227 (w), 3153 (m), 3116 (m), 3055 (m), 2925 (vs), 2854 (vs), 2724(w), 2035 (vs), 1976 (vs), 1609 (w), 1589 (m), 1553 (w), 1465 (vs), 1377 (s), 1294 (w), 1261 (w), 1201 (w), 1162 (w), 1138 (w), 1120 (m), 1063 (w), 1041 (m), 934 (w), 889 (m), 803 (w), 779 (w), 753 (m), 740 (s), 722 (m), 682 (m), 640 (w), 608 (m), 545 (m), 527 (s), 504 (m), 487 (w). Elemental analysis of THF adduct ( $C_{18}H_{20}FeN_2O_3S_2$ , 432.34 g mol<sup>-1</sup>): calculated: C 50.01, H 4.66, N 6.48, S 14.83; found: C 49.86, H 4.52, N 6.57, S 15.18.

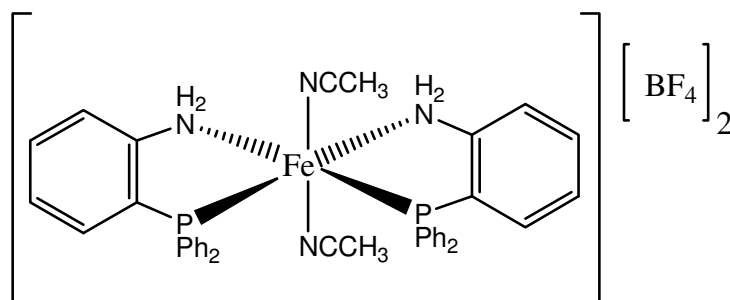
### 3.3 Synthesis of *trans*- $[Fe(NC-Me)_2(H_2NCH_2CH_2PPh_2)_2][BF_4]_2$ (5):



This complex was prepared according to a literature procedure [120]. 2-(diphenylphosphino)ethylamine (136 mg, 0.593 mmol) in  $CH_3CN$  (1 ml) was added dropwise to a stirring solution of  $[Fe(H_2O)_6][BF_4]_2$  (100 mg, 0.296 mmol) and  $CH_3CN$  (5 ml). The mixture turned purple immediately and was stirred for 30 min. Then the solvent was removed in vacuo and the residue was dissolved in 1 ml of  $CH_2Cl_2$ . The addition of 10 ml of diethyl ether yielded a purple solid, which was isolated by filtration and dried in vacuum (212 mg, 0.275 mmol, 93%).

**Physical data:** NMR:  $^{11}B$  NMR ( $[D_6]DMSO$ ):  $\delta$  -1.3.  $^{19}F$  NMR ( $[D_6]DMSO$ ):  $\delta$  -151.9.  $^{31}P\{^1H\}$  NMR ( $CD_3CN$ ):  $\delta$  63.7. IR: 3330 (w); 2163 (s); 1604(s); 1312 (w); 873 (vs); 695 (w); 646(s); 607 (vs); 511(w); 495 (m); 480 (m).

### 3.4 Synthesis of *trans*-[Fe(NC-Me)<sub>2</sub>(H<sub>2</sub>NC<sub>6</sub>H<sub>4</sub>-2-PPh<sub>2</sub>)<sub>2</sub>] [BF<sub>4</sub>]<sub>2</sub> (**6**):



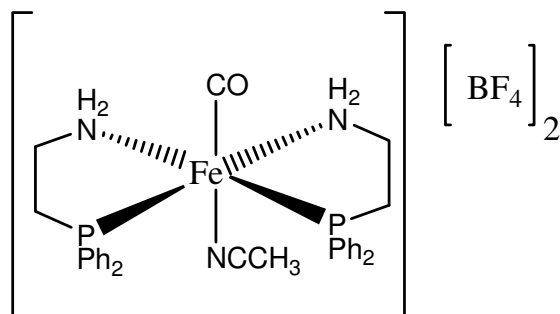
Firstly, the 2-(diphenylphosphino)aniline ligand was prepared as described previously [137]. A microwave vessel was charged with *o*-fluoroaniline (1.1 g, 10 mmol) and KPPH<sub>2</sub> (0.5 M in THF, 20 ml, 10 mmol) under nitrogen. The vessel was closed and heated in a microwave to 180 °C for 15 min (approx. 800 W after the initial temperature ramping). The reaction mixture was quenched with deionized water (15 ml), and the organics were extracted into benzene (2 X 20 ml). The extract was filtered through a short alumina column and recrystallized from boiling EtOH yielding 2-(diphenylphosphino)aniline as a white powder (2.18 g, 79%).

For the synthesis of *trans*-[Fe(NC-Me)<sub>2</sub>(H<sub>2</sub>NC<sub>6</sub>H<sub>4</sub>-2-PPh<sub>2</sub>)<sub>2</sub>] [BF<sub>4</sub>]<sub>2</sub> (**6**) 2-(diphenylphosphino)aniline (164 mg, 0.593 mmol) in CH<sub>3</sub>CN (1 ml) was added dropwise to a stirred solution of [Fe(H<sub>2</sub>O)<sub>6</sub>][BF<sub>4</sub>]<sub>2</sub> (100 mg, 0.296 mmol) in CH<sub>3</sub>CN (5 ml). The reaction mixture turned purple immediately and was stirred for an additional hour. Thereafter, the solvent was removed in vacuo and the residue dissolved in 1 ml of CH<sub>2</sub>Cl<sub>2</sub>. The addition of 10 ml of diethyl ether afforded a purple solid, which was isolated by filtration and dried in vacuum (241 mg, 0.278 mmol, 94%). Recrystallization of a small portion of this solid from CH<sub>3</sub>CN/Et<sub>2</sub>O by using the slow diffusion method gave violet single crystals suitable for X-ray diffraction experiments.

**Physical data:** M.p.: 211-213 °C. NMR: <sup>1</sup>H NMR (CD<sub>3</sub>CN): δ 1.96 (s, 6H), 5.94 (s, 4H), 6.87 (t, 8H), 7.33 (t, 8H), 7.53 (t, 8H), 7.73 (m, 2H), 7.84 (d, 2H). <sup>13</sup>C{<sup>1</sup>H} NMR (CD<sub>3</sub>CN): δ 3.85 (t), 128.00 (t), 128.77 (t), 129.96 (t), 130.85 (m), 131.67 (s), 132.96 (m), 133.36 (t), 133.66 (s), 134.85 (s), 137.95(s), 151.37 (t). <sup>31</sup>P{<sup>1</sup>H} NMR (CD<sub>3</sub>CN): δ 68.1 (s). MS-ESI: 305 [Fe(PPh<sub>2</sub>C<sub>6</sub>H<sub>4</sub>-2-NH<sub>2</sub>)<sub>2</sub>]<sup>2+</sup> (100); 277 [(PPh<sub>2</sub>C<sub>6</sub>H<sub>4</sub>-2-NH<sub>2</sub>)<sub>2</sub>]<sup>2+</sup> (90). IR [KBr]: 3280 (s); 2207(s); 1607(w); 1566 (m); 1478 (s); 1436 (s); 1094 (vs); 1047 (vs); 820 (w); 756

(s); 694 (s); 575 (m); 520 (vs); 485 (m); 471 (vs); 458 (s); 415 (m); 929 (w); 816 (w); 747 (s); 697 (s); 594 (m); 529 (s); 510 (m); 475 (w). Elemental analysis ( $C_{44}H_{44}B_2F_8FeN_6P_2$ , 948.26 g mol<sup>-1</sup>): calculated: C 55.73; H 4.68; N 8.86; found: C 55.62; H 4.68; N 8.76.

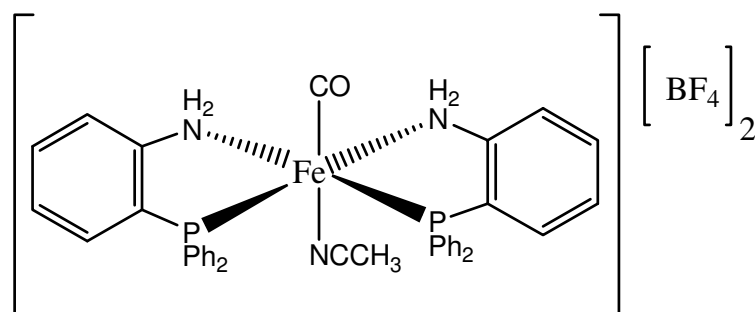
### 3.5 Synthesis of $[Fe(CO)(NC-Me)(H_2NCH_2CH_2PPh_2)_2][BF_4]_2$ (CORM-P1) (7):



For the synthesis of **7** the isolation of complex **5** is not required. Therefore, aminoethyl-diphenylphosphane (136 mg, 0.593 mmol) was added dropwise to a stirred solution of  $[Fe(H_2O)_6][BF_4]_2$  (100 mg, 0.296 mmol) in 5 ml of  $CH_3CN$  yielding a purple reaction mixture. After removal of all volatiles in vacuo and dissolution of the residue with 10 ml of  $CH_2Cl_2$ , this solution was treated with gaseous CO for 16 h. During this time a yellow suspension formed. CORM-P1 was isolated as a yellow solid (190 mg, 0.251 mmol, 91%) by filtration and the filter cake dried in vacuum. Recrystallization of a small portion of this powder from a mixture of  $CH_2Cl_2$  and DMF/ $Et_2O$  by using the slow diffusion method yielded dark orange single crystals suitable for X-ray diffraction experiments.

**Physical data:** M.p.: 202-205 °C. NMR: <sup>1</sup>H NMR ( $[D_6]DMSO$ ):  $\delta$  2.18 (s, 3H), 2.92 (broad, 4H), 4.07 (broad, 4H), 4.8 (broad, 4H), 7.04 (d, 8H), 7.36 (t, 8H), 7.57 (t, 4H). <sup>11</sup>B NMR ( $[D_6]DMSO$ ):  $\delta$  -1.3. <sup>13</sup>C{<sup>1</sup>H} NMR ( $[D_6]DMSO$ ):  $\delta$ : 4.22 (broad), 31.02 (m), 41.46 (broad), 129.22 (d), 131.47 (d), 132.11 (d), 133.30 (broad), 160.63 (broad), 215.20 (broad). <sup>19</sup>F NMR ( $[D_6]DMSO$ ):  $\delta$  -148.7. <sup>31</sup>P{<sup>1</sup>H} NMR ( $[D_6]DMSO$ ):  $\delta$  61.7 (s). MS-ESI: 257  $[Fe(Ph_2PC_2H_4NH_2)_2]^{2+}$  (100); 229  $[(Ph_2PC_2H_4NH_2)_2]^{2+}$  (16); 185  $[(Ph_2P)_2]^{2+}$  (37). IR [Nujol, KBr windows]: 3555 (w); 3307(s); 3269 (s); 3175(m); 3065 (m); 2922 (vs); 2854 (vs); 2303 (m); 1985(vs); 1597 (m); 1460 (s); 1436 (s); 1376(m); 1256 (m); 1094(vs); 1042 (vs); 1011 (s); 996 (s); 929 (w); 816 (w); 747 (s); 697 (s); 594 (m); 529 (s); 510 (m); 475 (w). Elemental analysis ( $C_{31}H_{35}B_2F_8FeN_3OP_2$ , 757.03 g mol<sup>-1</sup>): calculated: C 49.18; H 4.66; N 5.55; found: C 48.93; H 4.35; N 5.35.

### 3.6 Synthesis of $[\text{Fe}(\text{CO})(\text{NC-Me})(\text{H}_2\text{NC}_6\text{H}_4\text{-2-PPH}_2)_2] [\text{BF}_4]_2$ (CORM-P2) (8):

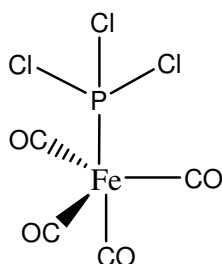


For the synthesis of CORM-P2, **8** (241 mg, 0.278 mmol) was dissolved in 10 ml of  $\text{CH}_2\text{Cl}_2$  and stirred under a CO atmosphere for 16 h. The resulting orange-yellow solution was evaporated to dryness to leave a yellow powder, which was washed with diethyl ether. CORM-P2 was isolated as a yellow powder (218 mg, 0.256 mmol, 92%). Recrystallization of a small portion of this powder from a solvent mixture of  $\text{CH}_2\text{Cl}_2$  and DMF/ $\text{Et}_2\text{O}$  using the slow diffusion method yielded light orange single crystals suitable for X-ray diffraction experiments.

**Physical data:** M.p.: 216-218 °C.  $^1\text{H}$  NMR ( $[\text{D}_6]\text{DMSO}$ ):  $\delta$  2.04 (s, 3H,  $\text{CH}_3$ ), 5.71 (s, 4H,  $\text{H}_2\text{N}$ ), 6.92 (broad 8H), 7.39 (dd, 8H), 7.57 (broad, 8H), 7.76 (broad, 2H), 7.94 (broad, 2H).  $^{13}\text{C}\{^1\text{H}\}$  NMR ( $[\text{D}_6]\text{DMSO}$ ):  $\delta$  3.19 (s), 126.36 (m), 127.20 (m), 128.10 (t), 129.67 (s), 130.86 (d), 131.32 (m), 132.50 (d), 132.88 (d), 133.11 (m), 134.99 (d), 162.12 (broad), 206.35 (broad).  $^{31}\text{P}\{^1\text{H}\}$  ( $\text{CD}_3\text{CN}$ ):  $\delta$  58.2 (s). MS-ESI: 305  $[\text{Fe}(\text{PPh}_2\text{C}_6\text{H}_4\text{-2-NH}_2)_2]^{2+}$  (100); 277  $[(\text{PPh}_2\text{C}_6\text{H}_4\text{-2-NH}_2)_2]^{2+}$  (90); 201  $[(\text{PPh}_2\text{-NH}_2)_2]^{2+}$  (7). IR [Nujol, KBr windows]: 3280 (s); 2290 (m); 2001 (vs); 1590 (w); 1480(s); 1437 (s); 1096 (w); 1056 (vs); 751 (s); 696 (vs); 578 (m); 516 (vs); 464 (vs); 448 (m); 411 (w). Elemental analysis ( $\text{C}_{40}\text{H}_{37}\text{B}_2\text{Cl}_2\text{F}_8\text{FeN}_3\text{OP}_2$ , 938.04 g mol $^{-1}$ ): calculated: C 51.22; H 3.98; N 4.48; found: C 50.76; H 4.03; N 4.65.



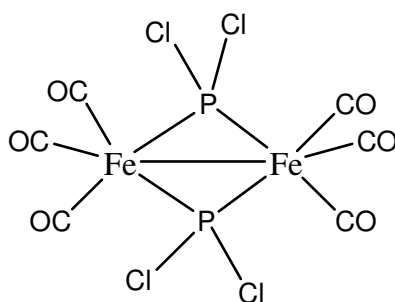
### 3.7 Synthesis of $[\text{Fe}(\text{CO})_4(\text{PCl}_3)]$ (CORM-P3) (**9**):



CORM-P3, (**9**, tetracarbonyl[trichlorophosphine]iron(0)) was prepared according to a literature procedure [138]. A suspension of 1.0 g (2.75 mmol) of diironnonacarbonyl and 757 mg (5.51 mmol) of phosphorus trichloride in 70 ml of toluene were stirred at 90 °C for two hours. During the reaction time the color changed to deep red. Then the solvent was removed by cold distillation and the residue was suspended in 20 ml of n-pentane and poured over silica gel with n-pentane as eluent for column chromatography (40 x 3 cm), the first band is a broad yellow zone which was collected. The solvent was reduced to 5 ml and stored the solution at -18 °C. After two days, complex **9** precipitated as a pure bright yellow powder. Yield: 1.11 g (3.63 mmol, 66%).

**Physical data:** M.p.: 165 (dec.). NMR:  $^{13}\text{C}$  NMR ( $\text{CDCl}_3$ ):  $\delta$  207.64.  $^{31}\text{P}$  NMR ( $\text{CDCl}_3$ ):  $\delta$  183.10(s). MS-FAB: 305  $[\text{M}]^+$  (16); 277  $[\text{M}-\text{CO}]^+$  (54); 270  $[\text{M}-\text{Cl}]^+$  (37); 249  $[\text{M}-2\text{CO}]^+$  (15); 242  $[\text{M}-\text{CO}-\text{Cl}]^+$  (11); 221  $[\text{M}-3\text{CO}]^+$  (16); 213  $[\text{M}-2\text{CO}-\text{Cl}]^+$  (30); 193  $[\text{M}-4\text{CO}]^+$  (100). IR [KBr]: 3413 (vs); 2966 (m); 2470 (w); 2091 (m); 2081 (m); 2020 (vs); 1998(s); 1987(s); 1602 (s); 1405(w); 1266 (s); 1077 (vs); 935 (m); 818 (m); 579 (vs). Elemental analysis ( $\text{C}_4\text{Cl}_3\text{FeO}_4\text{P}$ , 305.22  $\text{g mol}^{-1}$ ): calculated: C 15.74; found: C 14.82.

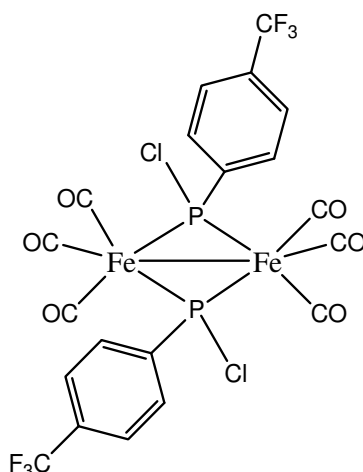
### 3.8 Synthesis of $[\text{Fe}_2(\text{CO})_6(\text{PCl}_2)_2]$ (CORM-P6) (12):



This complex was prepared as by-product during the synthesis of complex **9**. Separation of the reaction mixture by column chromatography (40 x 3 cm) initially gave a bright yellow zone, which was complex **9** as described above. Then an orange zone was collected, the solution was reduced to 3 ml and stored at -18 °C leading to the formation of complex **12** as pure dark yellow single crystals after one week suitable for X-ray diffraction experiments. Yield: 62 mg (127  $\mu\text{mol}$ , 4.6%).

**Physical data:** M.p.: 220 (dec.). NMR:  $^{13}\text{C}$  NMR ( $\text{CDCl}_3$ ):  $\delta$  206.12.  $^{31}\text{P}$  NMR ( $\text{CDCl}_3$ ):  $\delta$  304 (s). MS-FAB: 484  $[\text{M}]^+$  (11); 456  $[\text{M}-\text{CO}]^+$  (31); 428  $[\text{M}-2\text{CO}]^+$  (23); 400  $[\text{M}-3\text{CO}]^+$  (8); 372  $[\text{M}-4\text{CO}]^+$  (12); 344  $[\text{M}-5\text{CO}]^+$  (26); 316  $[\text{M}-6\text{CO}]^+$  (51); 281  $[\text{M}-6\text{CO}-\text{Cl}]^+$  (39); 244  $[\text{M}-6\text{CO}-2\text{Cl}]^+$  (9); 213  $[\text{M}-6\text{CO}-2\text{Cl}-\text{P}]^+$  (17); 178  $[\text{M}-6\text{CO}-3\text{Cl}-\text{P}]^+$  (11); 143  $[\text{M}-6\text{CO}-4\text{Cl}-\text{P}]^+$  (37); 112  $[\text{M}-6\text{CO}-4\text{Cl}-2\text{P}]^+$  (43); 56  $[\text{M}-6\text{CO}-4\text{Cl}-2\text{P}-\text{Fe}]^+$  (100). IR [KBr]: 3413 (vs); 2966 (m); 2470 (w); 2089 (m); 2060 (vs); 2032 (vs); 2019 (s); 1602 (s); 1402 (w); 1259 (m); 1070 (s); 927 (m); 812 (s); 577 (vs). Elemental analysis ( $\text{C}_6\text{Cl}_4\text{Fe}_2\text{O}_6\text{P}_2$ , 483.50  $\text{g mol}^{-1}$ ): calculated: C 14.90; found: C 14.78.

### 3.9 Synthesis of $[\text{Fe}_2(\text{CO})_6\{\text{PCl}(\text{C}_6\text{H}_4\text{-CF}_3)\}_2]$ (CORM-P7) (13):



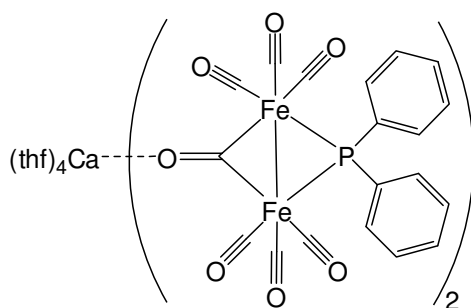
Firstly (p-CF<sub>3</sub>C<sub>6</sub>H<sub>4</sub>)PCl<sub>2</sub> was prepared according to the literature procedure [139]. (Et<sub>2</sub>N)<sub>2</sub>PCl required for this experiment was synthesized as described previously [140], n-Butyllithium (34.5 ml of 1.6 M solution in hexane, 55 mmol) was slowly added to a solution of p-CF<sub>3</sub>C<sub>6</sub>H<sub>4</sub>Br (12.5 g, 55 mmol) in diethyl ether (500 ml) at 5 °C. The mixture was stirred for one hour and (Et<sub>2</sub>N)<sub>2</sub>PCl (11.6 g, 55 mmol) was slowly added to the mixture at 5°C. The contents of the flask were warmed to room temperature and the mixture was stirred for two hours. (p-CF<sub>3</sub>C<sub>6</sub>H<sub>4</sub>)P(NEt<sub>2</sub>)<sub>2</sub> was not isolated but used in situ. HCl (137.5 ml of a 2 M solution in diethyl ether, 275 mmol) was added to the reaction mixture at -78 °C containing (p-CF<sub>3</sub>C<sub>6</sub>H<sub>4</sub>)P(NEt<sub>2</sub>)<sub>2</sub>. The mixture was allowed to warm to room temperature and stirred for 12 hours. The solvent was removed in vacuo, the solid dissolved in hexane (250 ml) and then filtered. The filtrate was concentrated and the remaining oil was distilled (85 °C, 11 mm Hg) to yield (p-CF<sub>3</sub>C<sub>6</sub>H<sub>4</sub>)PCl<sub>2</sub> as colorless liquid (10.45 g, 77%).

For the synthesis of  $[\text{Fe}_2(\text{CO})_6\{\text{PCl}(\text{C}_6\text{H}_4\text{-CF}_3)\}_2]$  (**13**), a mixture of  $[\text{Fe}_2(\text{CO})_9]$  (3 g, 8.25 mmol), [(p-CF<sub>3</sub>C<sub>6</sub>H<sub>4</sub>)PCl<sub>2</sub>] (4.08 g, 16.5 mmol), and 60 ml of toluene was heated slowly to 90 °C and stirred for four hours. Then it was filtered at room temperature to remove undissolved materials, and the filtrate was chromatographed on a silica gel column (40 x 3 cm).  $[\text{Fe}_2(\text{CO})_6\{\text{PCl}(\text{C}_6\text{H}_4\text{-CF}_3)\}_2]$  obtained by eluting with 10/1 pentane/toluene and recrystallization from the same solvent mixture gave complex **11** as a yellow powder. Yield: 640 mg (0.91 mmol, 11%).

**Physical data:** M.p.: 245 (dec.). NMR: <sup>1</sup>H NMR (CDCl<sub>3</sub>): δ 7.34 (broad). <sup>13</sup>C NMR (CDCl<sub>3</sub>): δ 122.67, 125.04, 130.25, 132.38, 209.59. <sup>19</sup>F NMR (CDCl<sub>3</sub>): δ 63.75. <sup>31</sup>P NMR

(CDCl<sub>3</sub>): δ 240.21 (s). MS-FAB: 702 [M]<sup>+</sup> (32); 674 [M-CO]<sup>+</sup> (48); 646 [M-2CO]<sup>+</sup> (7); 618 [M-3CO]<sup>+</sup> (5); 438 [M-3CO-Cl-Ph-CF<sub>3</sub>]<sup>+</sup> (3); 407 [M--3CO-Cl-Ph-CF<sub>3</sub>-P]<sup>+</sup> (21); 350 [M-3CO-Cl-Ph-CF<sub>3</sub>-P-Fe]<sup>+</sup> (11); 316 [M-3CO-2Cl-Ph-CF<sub>3</sub>-P-Fe]<sup>+</sup> (100); 260 [M-5CO-2Cl-Ph-CF<sub>3</sub>-P-Fe]<sup>+</sup> (53); 232 [M-6CO-2Cl-Ph-CF<sub>3</sub>-P-Fe]<sup>+</sup> (13); 201 [M-6CO-2Cl-Ph-CF<sub>3</sub>-2P-Fe]<sup>+</sup> (37). IR [KBr]: 3423 (w); 2962 (w); 2324 (w); 2295 (w); 2162 (s); 2078 (s); 2044 (vs); 2020 (vs); 1606 (m); 1396 (s); 1323 (s); 1181 (m); 1106 (s); 1063 (w); 954 (w); 829 (m); 705 (m); 573 (s); 468 (m); 447 (w). Elemental analysis (C<sub>20</sub>H<sub>8</sub>Cl<sub>2</sub>F<sub>6</sub>Fe<sub>2</sub>O<sub>6</sub>P<sub>2</sub>, 702.81 g mol<sup>-1</sup>): calculated: C 34.18; H 1.15; found: C 33.86; H 1.06.

### 3.10 Synthesis of [(thf)<sub>4</sub>Ca{Fe<sub>2</sub>(CO)<sub>6</sub>(μ-CO)(μ-PPh<sub>2</sub>)<sub>2</sub>}] (CORM-CF) **14**:



The complex **14** was prepared in a manner similar to the literature procedure [131].

**Method A:** A solution of 0.16 g of [(thf)<sub>4</sub>Ca(PPh<sub>2</sub>)<sub>2</sub>] (0.229 mmol), which was prepared according to the literature procedure [141], in 15 ml of THF was added dropwise at 0 °C to a solution of 0.17 g of Fe<sub>2</sub>(CO)<sub>9</sub> (0.458 mmol) in 35 ml of THF. The color of the solution changed from yellow to red. After complete addition, the solution was warmed to room temperature and stirred for several hours. After reduction of the volume and storage at -25 °C, 0.23 g of red crystals of **14** (0.17 mmol, 77%) precipitated.

**Method B:** A solution of 0.21 g of [(thf)<sub>4</sub>Ca(PPh<sub>2</sub>)<sub>2</sub>] (0.30 mmol) [141] in 15 ml of THF was added dropwise at 0 °C to a solution of Fe<sub>3</sub>(CO)<sub>12</sub> (0.30 g, 0.60 mmol) in 35 ml of THF. The color of the solution changed from yellow to red. After complete addition, the solution was warmed to room temperature and stirred for several hours. In order to complete the reaction, the solution was heated under reflux for 4 h. After reduction of the volume and storage at -25 °C, 0.29 g of red crystals of **14** (0.22 mmol, 73%) precipitated.

### **3.11 Myoglobin Assay:**

The amount of CO released from the complexes prepared in this study was evaluated in a spectrophotometric assay by measuring the conversion of deoxy-myoglobin (deoxy-Mb) to the carbon monoxide myoglobin complex (Mb-CO). Reduced myoglobin solutions (100  $\mu\text{mol/L}$ ) were prepared immediately before the experiments by dissolving the protein in phosphate buffered saline (PBS, pH 7.4) with freshly added 0.1% sodium dithionite. Carbonyl complexes were added from 10-mmol/L DMSO stock solutions to a final concentration of 50-200  $\mu\text{mol/L}$ . The light-dependent CO release from all CORMs in this study was measured by recording spectra in the range of 500-600 nm before the carbonyl complexes were added to the deoxy-myoglobin solution and 15 min after exposing these solutions to light from a cold light source (20 W halogen lamp, Osram GZX4, with 2 W output power at the end of the light guide; the light guide was placed at the top of a 1-mL cuvette at a distance of 20 mm.). However, because of the strong self-absorbance of CORM-P2 further experiments were performed at lower concentration (5  $\mu\text{M}$  CORM and 10  $\mu\text{M}$  Mb) in a spectral range covering the Soret region (380-450 nm). Spectra in the absence of CO and in CO-saturated solution were recorded to calculate the maximal absorbance difference, required to convert absorbance changes to relative CO release. The time course of CO release was monitored by measuring the changes in absorbance at 540 nm for CORM-S1, CORM-S2, CORM-P3, CORM-P4, and CORM-P5. For CORM-S2, absorption of the compound itself was corrected for by performing equivalent experiments in the absence of myoglobin. Variations of this assay are critically reviewed by Atkin et al. [142]. For CORM-P1 and CORM-P2 the time course of CO release was monitored by measuring absorbance at 422 nm, 470 nm, and 520 nm every 10 s. To test for dependence of CO release from light, myoglobin, or dithionite, samples were preincubated for 10 min under different conditions. Spectra in the Soret region were recorded immediately after addition of myoglobin and sodium dithionite at their final concentrations of 10  $\mu\text{M}$  and 0.1%, respectively.

### **3.12 X-Ray Structure Determinations:**

The intensity data for the compounds were collected on a Nonius KappaCCD diffractometer using graphite-monochromated Mo-K $\alpha$  radiation. Data were corrected for Lorentz and polarization effects but not for absorption effects [143,144]. The structures for all complexes in this study were solved by direct methods (SHELXS [145]) and refined by full-matrix least squares techniques against  $F_o^2$  (SHELXL-97[145]). All hydrogen atoms for compound **6**, the amine hydrogen atoms of **2** (CORM-S2), **4**, **7** (CORM-P1), and **8** (CORM-P2), additional to the acetonitrile hydrogen atoms of **7** (CORM-P1), were located by difference Fourier synthesis and refined isotropically [145]. All other hydrogen atoms were included at calculated positions with fixed thermal parameters. All non-hydrogen atoms were refined anisotropically [145]. A disorder has been observed for the coordinated DMF molecule of **4**. Three alternative sites were refined that resulted in equal occupancies of 33.33%. The non-coordinated DMF molecule was refined in two alternative sites with occupancies of 69(2) and 31(2)% for atoms C1DA–C3DA and C1DF–C3DF, respectively. All non-disordered non-hydrogen atoms were refined anisotropically [145]. Crystallographic data for all compounds in this study and refinement details are summarized in Tables 1, 2, and 3 (SIEMENS Analytical X-ray Instruments, Inc.) was used for structure representations.

## Summary

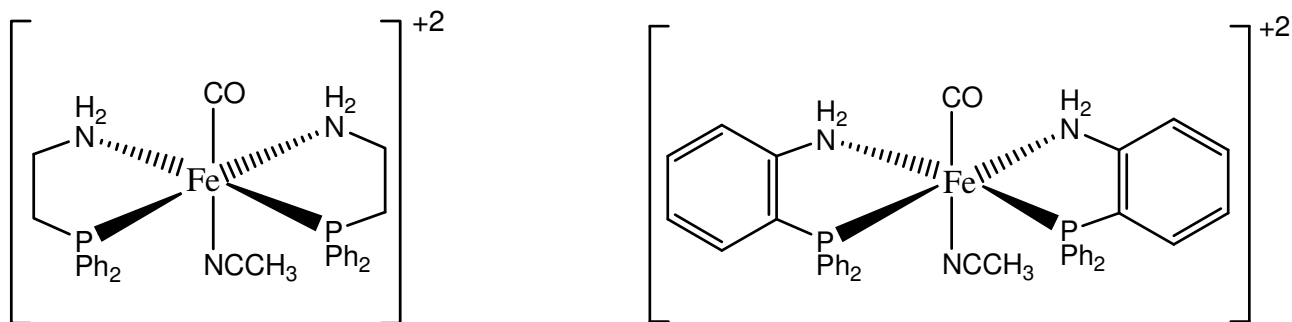
Carbon monoxide (CO) is a highly toxic gas; nevertheless, it is increasingly being accepted as a cytoprotective and homeostatic molecule with important signalling capabilities in physiological and pathophysiological situations [7-12]. Due to the high toxicity of CO if inhaled sophisticated strategies have to be developed in order to use these gaseous messenger molecules in cellular tissues. The most promising strategies include the use of carbonyl complexes of transition metals (CO-releasing molecules, CORMs) including water-insoluble  $[\text{Mn}_2(\text{CO})_{10}]$  as CORM-1 and  $[\text{Ru}_2(\text{CO})_6\text{Cl}_2(\mu\text{-Cl})_2]$  as CORM-2, water soluble  $[\text{RuCl}(\text{CO})_3(\text{H}_2\text{NCH}_2\text{COO})]$  as CORM-3 (CO-release *via* ligand exchange reactions) and  $\text{Na}_2[\text{H}_3\text{B-COO}]$  as CORM-A1 (pH-dependent CO release) [50,77,94].

Iron-based CO-releasing complexes represent a promising target because iron is a non-toxic 3d metal whose concentration is tightly regulated in biological systems [60]. We prepared CORM-S1 (figure 3.1 (left)) and CORM-S2 (figure 3.1 (right)) with good yields *via* the oxidative addition of cystamine to iron carbonyls and *via* the direct metalation of iron carbonyls with the appropriate thiol, respectively [117].



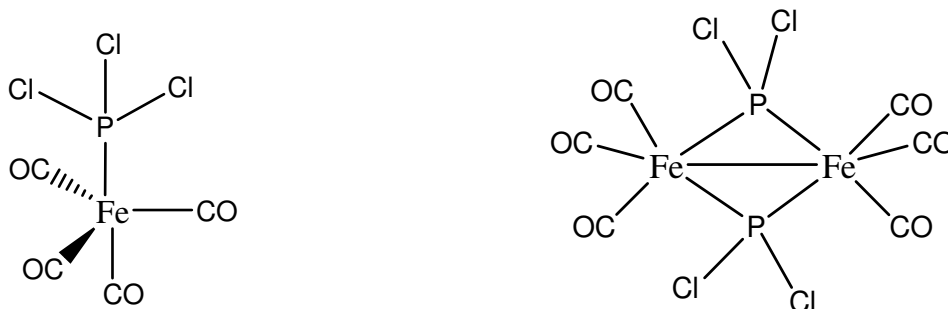
**Fig 3.1:** Molecular Structures of (left)  $[\text{Fe}(\text{CO})_2(\text{SCH}_2\text{CH}_2\text{NH}_2)_2]$  (CORM-S1) and (right)  $[\text{Fe}(\text{CO})_2(\text{SC}_6\text{H}_4\text{-2-NH}_2)_2]$  (CORM-S2) [117].

In addition, CORM-P1 (figure 3.2 (left)) and CORM-P2 (figure 3.2 (right)) were synthesized with very good yields in order to investigate the CO liberation kinetics [119]. The largest advantage for these CORMs is based on the phosphorus-containing ligands which give one sharp resonance in the  $^{31}\text{P}$  NMR spectrum. Therefore, the release kinetics of carbon monoxide during irradiation with visible light can be studied by using  $^{31}\text{P}$  NMR techniques.



**Fig 3.2:** Molecular structures of  $[\text{Fe}(\text{CO})(\text{CH}_3\text{CN})(\text{Ph}_2\text{PCH}_2\text{CH}_2\text{NH}_2)_2][\text{BF}_4]_2$  (CORM-P1, left) and  $[\text{Fe}(\text{CO})(\text{CH}_3\text{CN})(\text{Ph}_2\text{P}-\text{C}_6\text{H}_4-2-\text{NH}_2)_2][\text{BF}_4]_2$  (CORM-P2, right) [119].

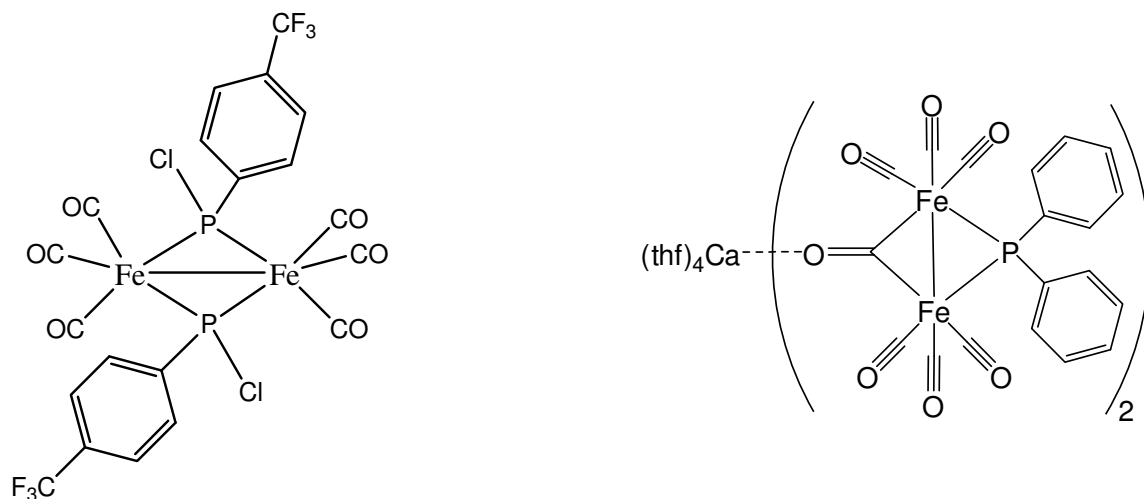
We extend the presented work in the synthesis of CORMs with higher CO contents. Accordingly CORM-P3 (figure 3.3 (left)) and CORM-P4 (figure 3.3 (right)) were prepared *via* the reaction of diironnonacarbonyl  $[\text{Fe}_2(\text{CO})_9]$  with phosphorus trichloride ( $\text{PCl}_3$ ).



**Fig 3.3:** Molecular structures of  $[\text{Fe}(\text{CO})_4(\text{PCl}_3)]$  (CORM-P3, left) and  $[\text{Fe}_2(\text{CO})_6(\text{PCl}_2)_2]$  (CORM-P4, right).

Also as CORMs with high CO contents CORM-P4 (figure 3.4 (left)) and CORM-FC (figure 3.4 (right)) [131] were synthesized *via* the reaction of diironnonacarbonyl  $[\text{Fe}_2(\text{CO})_9]$  with [4-(Trifluoromethyl)phenyl]phosphonous dichloride in CORM-P4 and the reaction of diironnonacarbonyl  $[\text{Fe}_2(\text{CO})_9]$  or triiron dodecacarbonyl  $[\text{Fe}_3(\text{CO})_{12}]$  with calcium bis(diphenylphosphanide) in CORM-FC.





**Fig 3.4:** Molecular structures of  $[\text{Fe}_2(\text{CO})_6\{\text{PCl}(\text{C}_6\text{H}_4\text{-CF}_3)\}_2]$  (CORM-P4, left) and  $[(\text{thf})_4\text{Ca}\{\text{Fe}_2(\text{CO})_6(\mu\text{-CO})(\mu\text{-PPh}_2)\}_2]$  (CORM-FC, right) [131].

The main target for synthesis of these complexes is to improve the CO releasing properties by addition of an electron withdrawing group in a *trans* position to the carbonyl ligands, such as trifluoromethyl in CORM-P4 and the bridging carbonyl in CORM-CF. These terminal carbonyl ligands which are in a *trans* position to the electron withdrawing group have higher stretching frequencies in the IR spectra than the other terminal carbonyls. This fact indicates that the M-CO bond is weaker due to a lower back donation of charge from the metal to the  $\pi^*(\text{CO})$  ligand orbitals which eases the liberation of CO from these CORMs.

## Zusammenfassung

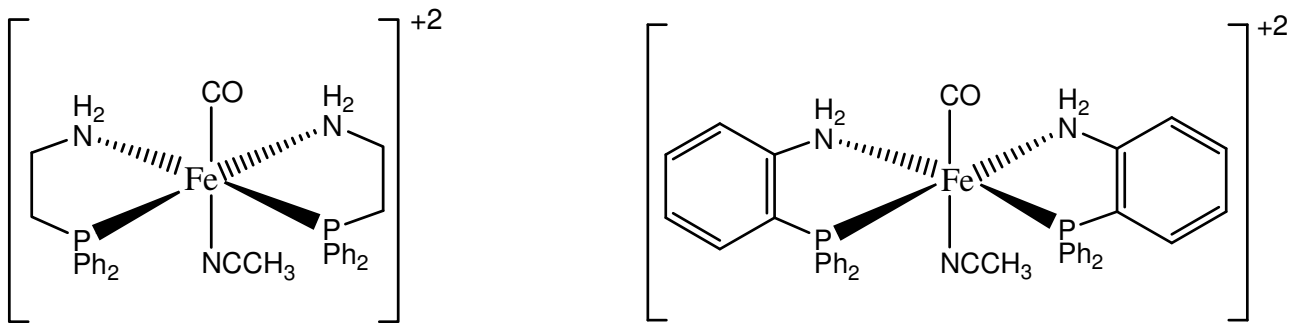
Kohlenstoffmonoxid (CO) ist ein sehr toxisches Gas und wird trotzdem zunehmend als zytoprotektives und homöostatisches Molekül sowie als physiologischer und pathophysiologischer Botenstoff erkannt [7-12]. Durch die hohe Giftigkeit, die CO beim Einatmen besitzt, müssen wohl durchdachte Strategien entwickelt werden, um den gasförmigen Botenstoff in zellulärem Gewebe einzusetzen. Die vielversprechendsten Ansätze umfassen den Einsatz von Übergangsmetall-Carbonylkomplexen (CO-releasing molecules, CORMs), wie die wasserunlöslichen Verbindungen  $[\text{Mn}_2(\text{CO})_{10}]$  (CORM-1) und  $[\text{Ru}_2(\text{CO})_6\text{Cl}_2(\mu\text{-Cl})_2]$  (CORM-2), sowie die wasserlöslichen Komplexe  $[\text{RuCl}(\text{CO})_3(\text{H}_2\text{NCH}_2\text{COO})]$  (CORM-3, CO-Freisetzung durch eine Ligandenaustauschreaktion) und  $\text{Na}_2[\text{H}_3\text{B-COO}]$  (CORM-A1, pH-abhängige CO-Freisetzung) [50,77,94]. Eisenbasierte, CO-freisetzende Komplexe sind vielversprechend, da Eisen ein ungiftiges 3d-Metall ist, dessen Konzentration in biologischen Systemen in engen Grenzen reguliert wird [60]. CORM-S1 (Abb. 3.1 (links)) und CORM-S2 (Abb. 3.1 (rechts)) konnte mit guten Ausbeuten, mittels oxidativer Addition von Cystamin an Eisencarbonyle sowie durch direkte Metallierung geeigneter Thiole durch Eisencarbonyle, dargestellt werden [117].



**Abb. 3.1:** Molekülstrukturen von (links)  $[\text{Fe}(\text{CO})_2(\text{SCH}_2\text{CH}_2\text{NH}_2)_2]$  (CORM-S1) und (rechts)  $[\text{Fe}(\text{CO})_2(\text{SC}_6\text{H}_4\text{-2-NH}_2)_2]$  (CORM-S2) [117].

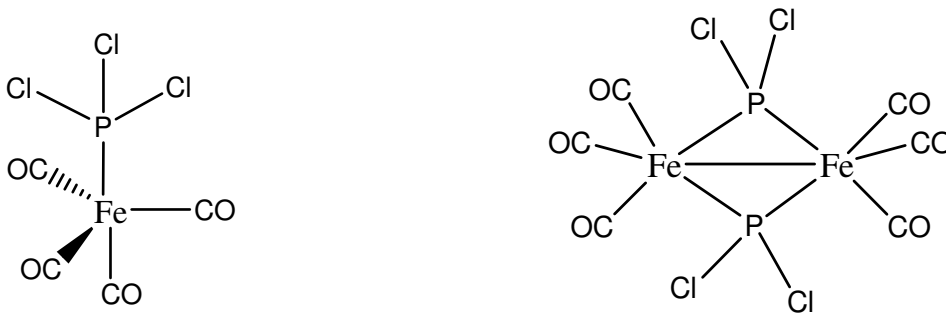
Darüber hinaus wurden CORM-P1 (Abb. 3.2 (links)) und CORM-P2 (Abb. 3.2 (rechts)) mit sehr guten Ausbeuten dargestellt, um die CO-Freisetzungskinetik zu untersuchen [119]. Der größte Vorteil dieser CORMs liegt in den phosphorhaltigen Liganden, welche ein scharfes Signal im  $^{31}\text{P}$  NMR spektrum zeigen. Damit kann die Kohlenstoffmonoxid

freisetzungskinetik, während der Bestrahlung mit sichtbarem Licht, mit NMR-Techniken untersucht werden.



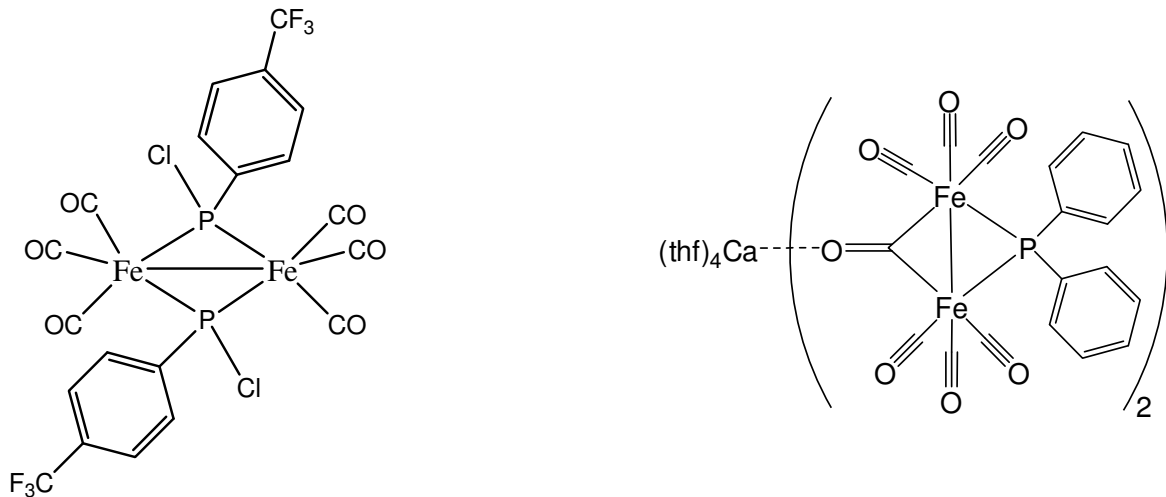
**Abb. 3.2:** Molekülstrukturen von  $[\text{Fe}(\text{CO})(\text{CH}_3\text{CN})(\text{Ph}_2\text{PCH}_2\text{CH}_2\text{NH}_2)_2] [\text{BF}_4]_2$  (CORM-P1, links) und  $[\text{Fe}(\text{CO})(\text{CH}_3\text{CN})(\text{Ph}_2\text{P}-\text{C}_6\text{H}_4-2-\text{NH}_2)_2] [\text{BF}_4]_2$  (CORM-P2, rechts) [119].

Außerdem wurden CORMs mit höherem CO-Gehalt dargestellt. CORM-P3 (Abb. 3.3 (links)) und CORM-P4 (Abb. 3.3 (rechts)) konnten durch die Umsetzung von Dieisennonacarbonyl  $[\text{Fe}_2(\text{CO})_9]$  mit Phosphortrichlorid ( $\text{PCl}_3$ ) erhalten werden.



**Abb 3.3:** Molekülstrukturen von  $[\text{Fe}(\text{CO})_4(\text{PCl}_3)]$  (CORM-P3, links) und  $[\text{Fe}_2(\text{CO})_6(\text{PCl}_2)_2]$  (CORM-P4, rechts).

Ebenso wurden CORM-P4 (Abb. 3.4 (links)) und CORM-FC (Abb. 3.4 (rechts)) [131] als CORMs mit hohem CO-Gehalt, durch Reaktion von Dieisennonacarbonyl  $[\text{Fe}_2(\text{CO})_9]$  mit [4-(Trifluormethyl)phenyl]phosphordichlorid (CORM-P4) und Dieisennonacarbonyl  $[\text{Fe}_2(\text{CO})_9]$  oder Trieisendodecacarbonyl  $[\text{Fe}_3(\text{CO})_{12}]$  mit Calcium bis(diphenylphosphanid) (CORM-FC), dargestellt.



**Fig 3.4:** Molekülstrukturen von  $[\text{Fe}_2(\text{CO})_6\{\text{PCl}(\text{C}_6\text{H}_4\text{-CF}_3)\}_2]$  (CORM-P4, links) und  $[(\text{thf})_4\text{Ca}\{\text{Fe}_2(\text{CO})_6(\mu\text{-CO})(\mu\text{-PPh}_2)\}_2]$  (CORM-FC, rechts) [131].

Das Hauptaugenmerk bei der Synthese lag auf der Verbesserung der CO-Freisetzungseigenschaften durch Einführung von elektronenziehenden Liganden in *trans*-Position zum Carbonylliganden, z.B. Trifluormethyl in CORM-P4 oder das verbrückende Carbonyl CORM-FC. Die terminalen Carbonylliganden, die *trans*-ständig zu einem elektronenziehenden Liganden sitzen, haben größere Streckenschwingungsfrequenzen im IR als andere terminale Carbonyle. Dies zeigt eine Schwächung der M-CO-Bindung durch verminderte Metall-Ligandrückbindung an, welche die CO-Freisetzung der CORMs erleichtert.

## References

- [1] See *Carbon Monoxide-Molecule of the Month*, Dr Mike Thompson. Winchester College, UK.
- [2] See *Crossing the Energy Divide: Moving from Fossil Fuel Dependence to a Clean-Energy Future*, Robert U. Ayres, Edward H. Wharton School Publishing. p. 36.
- [3] Weinstock, B.; Niki, H, *Science*. **1972**, 176, 290-292.
- [4] See textbooks of biochemistry, e.g.: D. Nelson, M. Cox: *Lehninger Biochemie*, Springer-Verlag: Berlin Heidelberg, **2009**.
- [5] S. Hou, M. F. Reynolds, F. T. Horrigan, S. H. Heinemann, T. Hoshi, *Acc. Chem. Res.* **2006**, 39, 918-924.
- [6] L. D. Prockop, R. I. Chichkova, *Journal of the Neurological Sciences*. **2007**, 262, 122-130.
- [7] B. E. Mann, Top, *Organomet. Chem.* **2010**, 32, 247-285.
- [8] A. Hermann, G. F. Sitdikova, T. M. Weiger, *Biol. Unserer Zeit*. **2010**, 40, 185-193.
- [9] W. J. Wilkinson, P. J. Kemp, *J. Physiol.* **2011**, 589, 3055-3062.
- [10] C. C. Romão, W. A. Blättler, J. D. Seixas, G. J. L. Bernardes, *Chem. Soc. Rev.* **2012**, 41, 3571-3583.
- [11] R. Foresti, M. G. Bani-Hani, R. Motterlini, *Intensive Care Med.* **2008**, 34, 649-658.
- [12] R. Motterlini, L. E. Otterbein, *Nature Rev. Drug Discovery*. **2010**, 9, 728-743.
- [13] See textbooks of organometallic, e.g.: C. Elschenbroich: *Organometallic*, WILEY-VCH: Weinheim, **2006**.
- [14] W. E. J. Trout, *Journal of Chemical Education*. **1937**, 14, 453-462.
- [15] W. A. Herrmann, *Chemie in unserer Zeit*. **1988**, 22, 113-122.
- [16] P. Schützenberger, *Bulletin de la Société Chimique de Paris*. **1868**, 10, 188-192.
- [17] de Gruyter. J. Huheey, E. Keiter, R. Keiter, *Anorganische Chemie, 2nd ed*: Berlin-New York, **1995**.
- [18] R. B. King, *Transition-Metal Compounds*: New York, Academic Press, **1965**.
- [19] E. H. Braye, W. Hübel, M. D. Rausch, T. M. Wallace, *Inorganic Syntheses*. **1966**, 8, 178-181.
- [20] See A. F. Holleman, E. Wiberg, N. Wiberg, *Lehrbuch der Anorganischen Chemie, 2nd ed*: Berlin-de Gruyter, **2007**.

- [21] R. D. Pike, *Encyclopedia of Reagents for Organic Synthesis*, **2001**.
- [22] Q. Xu, Y. Imamura, M. Fujiwara, Y. Souma, *Journal of Organic Chemistry*. **1997**, **62**, 1594-1598.
- [23] Weinheim, C. Elschenbroich, *Organometallics*: Wiley-VCH, **2006**.
- [24] H. H. Ohst, J. K. Kochi, *Journal of the American Chemical Society*. **1986**, **108**, 2897-2908.
- [25] P. J. Dyson, McIndoe, J. S. Amsterdam, *Transition Metal Carbonyl Cluster Chemistry*. : Gordon & Breach, **2000**.
- [26] P. S. Braterman, *Metal Carbonyl Spectra*: Academic Press, **1975**.
- [27] F. A. Cotton, *Chemical Applications of Group Theory* , 3rd ed: Wiley Interscience, **1990**.
- [28] R. L. Carter, *Molecular Symmetry and Group Theory*: Wiley, **1997**.
- [29] D. C. Harris, M. D. Bertolucci, *Symmetry and Spectroscopy: Introduction to Vibrational and Electronic Spectroscopy*: Oxford University Press, **1980**.
- [30] U. Schatzschneider, *Inorganica Chimica Acta*, **2011**, **374**, 19-23.
- [31] U. Schatzschneider, *European Journal of Inorganic Chemistry*. **2010**, 1451-1467.
- [32] M. J. Alcaraz, M. I. Guillen, M. L. Ferrandiz, J. Megias, R. Motterlini, *Current Pharmaceutical Design*. **2008**, **14**, 465-472.
- [33] T. R. Johnson, B. E. Mann, T. I. P. easdale, H. Adams, R. Foresti, C. J. Green, R. Motterlini, *Dalton Transactions*. **2007**, 1500-1508.
- [34] R. Alberto, R. Motterlini, *Dalton Transactions*. **2007**, 1651-1660.
- [35] B. E. Mann, R. Motterlini, *Chem. Commun.* **2007**, 4197-4208.
- [36] R. Motterlini, *Biochem. Soc. Trans.* **2007**, **35**, 1142-1146.
- [37] J. Boczkowski, J. J. Poderoso, R. Motterlini, *Trends in Biochemical Sciences*. **2006**, **31**, 614-621.
- [38] B. Mann, R. Motterlini, *Chemistry & Industry*. **2005**, **16**, 16-18.
- [39] R. Motterlini, R. Foresti, in L. E. Otterbein, B. S. (eds.) Zuckerbraun,: *Heme Oxygenase*, Nova Science Publishers: Hauppauge, NY. **2005**, pp. 191-210.
- [40] B. E. Mann, T. R. Johnson, J. E. Clark, R. Foresti, C. Green, R. Motterlini, *J. Inorg. Biochem.* **2003**, **96**, 40-46.
- [41] A. J. Atkin, S. Williams, P. Sawle, R. Motterlini, J. M. Lynam, I. J. S. Fairlamb, *Dalton Trans.* **2009**, 3653-3656.

- [42] C. C. Romão, S. S. Rodrigues, J. D. Seixas, Pina, A. R. M. B. Royo, A. C. Fernandes, I. Goncalves, W. Haas, *Method using CO releasing molybdenum carbonyl complexes for the treatment of inflammatory diseases*. **2007**, WO 2007/073226, 20061220.
- [43] A. F. N. Tavares, Miguel Teixeira, C. C. Romão, J. D. Seixas, L. S. Nobre, L. M. Saraiva, *Journal of Biological Chemistry*. **2011**, 286, 26708-26717.
- [44] I. J. S. Fairlamb, J. M. Lynam, I. E. Taylor, A. C. Whitwood, *Organometallics*. **2004**, 21, 4964.
- [45] B. E. Mann, Signalling molecule delivery (CO). In *Comprehensive Inorganic Chemistry II*, Hambley, T., Ed., Elsevier: Oxford, U.K., **2013**; Vol. 3, press.
- [46] L. S. Nobre, J. D. Seixas, C. C. Romão, L. M. Saraiva, *Treatment of infections by carbon monoxide*. **2008**, WO 2008130261, 20080424.
- [47] S. S. Rodrigues, J. D. Seixas, B. Guerreiro, N. M. P. Pereira, C. C. Romao, W. E. Haas, I. M. D. S. Goncalves, *Prevention of gastric ulcers by carbon monoxide*. **2009**, WO 2009/013612, 20080724.
- [48] D. Achatz, M. Lang, A. Volkl, W. Fehlhammer, W. Z. Beck, *Anorg. Allg. Chem.* **2005**, 631, 2339-2346.
- [49] A. R. Marques, L. Kromer, D. J. Gallo, N. Penacho, S. S. Rodrigues, J. D. Seixas, G. J. L. Bernardes, P. M. Reis, S. L. Otterbein, R. A. Ruggieri, A. S. G. Gonçalves, A. M. L. Gonçalves, M. N. DeMatos, I. Bento, L. E. Otterbein, W. A. Blättler, C. C. Romão, *Organometallics*. **2012**, 31, 5810-5822.
- [50] R. Motterlini, J. E. Clark, R. Foresti, P. Sarathchandra, B. E. Mann, C. J. Green, *Circ. Res.* **2002**, 90, 17-24.
- [51] R. Motterlini, B. E. Mann, D. A. Scapens, *Therapeutic delivery of carbon monoxide*. **2008**, WO 2008/003953, 20070704.
- [52] R. Motterlini, B. E. Mann, D. A. Scapens, *Therapeutic delivery of carbon monoxide*. **2010**, WO 2010/ 0105770.
- [53] S. V. C. Vummaleti, D. Branduardi, M. Masetti, M. D. Vivo, R. Motterlini, A. Cavalli, *Chem. Eur. J.* **2012**, 18, 9267- 9275.
- [54] M. A. Gonzalez, M. A. Yim, S. Cheng, A. Moyes, A. J. Hobbs, P. K. Mascharak, *Inorg. Chem.* **2012**, 51, 601-608.
- [55] M. A. Gonzalez, S. J. Carrington, N. L. Fry, J. L. Martinez, P. K. Mascharak, *Inorg. Chem.* **2012**, 51, 11930-11940.

- [56] J. Niesel, A. Pinto, H. W. P. N'Dongo, K. Merz, I. Ott, R. Gustb, U. Schatzschneider, *Chem. Commun.* **2008**, 1798-1800.
- [57] P. C. Kunz, W. Huber, A. Rojas, U. Schatzschneider, B. Spingler, *Eur. J. Inorg. Chem.* **2009**, 5358-5366.
- [58] A. E. Pierri, A. Pallaoro, G. Wu, P. C. Ford, *J. Am. Chem. Soc.* **2012**, 134, 18197-18200.
- [59] F. Zobi, O. Blacque, R. A. Jacobs, M. C. Schaubc, A. Yu. Bogdanovab, *Dalton Trans.* **2012**, 41, 370-378.
- [60] T. Matsui, M. Iwasaki, R. Sugiyama, M. Unno, M. Ikeda-Saito, *Inorg. Chem.* **2010**, 49, 3602-3609.
- [61] I. J. S. Fairlamb, A. K. Duhme-Klair, J. M. Lynam, B. E. Moulton, C. T. O. Brien, P. Sawle, J. Hammadb, R. Motterlinib, *Bioorg. Med. Chem. Lett.* **2006**, 16, 995-998.
- [62] P. Sawle, J. Hammad, I. J. S. Fairlamb, B. Moulton, C. T. O'Brien, J. M. Lynam, A. K. Duhme-Klair, R. Foresti, R. Motterlini, *The Journal of Pharmacology and Experimental Therapeutics.* **2006**, 318, 403-410.
- [63] I. J. S. Fairlamb, S. M. Syv'anne, A. C. Whitwood, *Synlett.* **2003**, 1693.
- [64] D. Scapens, H. Adams, T. R. Johnson, B. E. Mann, P. Sawle, R. Aqil, T. Perriorc, R. Motterlini, *Dalton Trans.* **2007**, 4962-4973.
- [65] W. Q. Zhang, A. J. Atkin, R. J. Thatcher, A. C. Whitwood, I. J. S. Fairlamb, J. M. Lynam, *Dalton Trans.* **2009**, 4351-4358.
- [66] L. Hewison, S. H. Crook, T. R. Johnson, B. E. Mann, H. Adams, S. E. Plant, P. Sawle, R. Motterlinic, *Dalton Trans.* **2010**, 39, 8967-8975.
- [67] C. S. Jackson, S. Schmitt, Q. P. Dou, J. J. Kodanko, *Inorg. Chem.* **2011**, 50, 5336-5338.
- [68] R. K. Afshar, A. K. Patra, E. Bill, M. M. Olmstead, P. K. Mascharak, *Inorg. Chem.* **2006**, 45, 3774-3781.
- [69] M. A. Gonzalez, N. L. Fry, R. Burt, R. Davda, A. Hobbs, P. K. Mascharak, *Inorg. Chem.* **2011**, 50, 3127-3134.
- [70] S. Romanski, B. Kraus, U. Schatzschneider, J. M. Neud, S. Amslinger, H. G. Schmalz, *Angew. Chem. Int. Ed.* **2011**, 50, 2392-2396.
- [71] S. Romanski, H. Rücker, E. Stamellou, M. Guttentag, J. M. Neudörfel, R. Alberto, S. Amslinger, B. Yard, H. G. Schmalz, *Organometallics.* **2012**, 31, 5800-5809.



- [72] T. Okauchi, T. Teshima, K. Hayashi, N. Suetsugu, T. Minami, *J. Am. Chem. Soc.* **2001**, 123, 12117-12118.
- [73] T. Okauchi, T. Teshima, M. Sadoshima, H. Kawakubo, K. Kagimoto, Y. Sugahara, M. Kitamura, *Chem. Commun.* **2010**, 46, 5015-5017.
- [74] L. Hewison, S. H. Crook, B. E. Mann, A. J. H. M. Meijer, H. Adams, P. Sawle, R. A. Motterlini, *Organometallics*. **2012**, 31, 5823-5834.
- [75] J. Takács, L. Markó, *Transition Met. Chem.* **1984**, 9, 10-12.
- [76] R. Motterlini, P. Sawle, J. Hammad, B. E. Mann, T. R. Johnson, C. J. Green, R. Foresti, *Pharmacological Research*. **2013**, 68, 108-117.
- [77] J. E. Clark, P. Naughton, S. Shurey, C. J. Green, T. R. Johnson, B. E. Mann, R. Foresti, *Circ. Res.* **2003**, 93, 2–8.
- [78] B. E. Mann, *Organometallics*. **2012**, 31, 5728–5735.
- [79] R. A. Motterlini, B. E. Mann, *Preparation of metal complexes for therapeutic delivery of carbon monoxide as vasodilator*. **2002**, WO 2002/092075, 20020515.
- [80] T. J. M. de Bruin, A. Milet, F. Robert, Y. Gimbert, A. E. Greene, *J. Am. Chem. Soc.* **2001**, 123, 7184.
- [81] K. Schmidt, M. Jung, R. Keilitz, B. Schnurr, R. Gust, *Inorg.Chim. Acta.* **2000**, 306, 6
- [82] I. Ott, B. Kircher, R. Gust, *J. Inorg. Biochem.* **2004**, 98, 485
- [83] S. Top, H. El Hafa, A. Vessieres, M. Huche, J. Vaissermann, G. Jaouen, *Chem. Eur. J.* **2002**, 8, 5241
- [84] I. Ott, B. Kircher, P. Schumacher, K. Schmidt, R. Gust, *J. Med. Chem.* **2005**, 48, 622
- [85] C. D. Sergeant, I. Ott, A. Sniady, S. Meneni, R. Gust, A. L. Rheingold, R. Dembinski, *Org. Biomol. Chem.* **2008**, 6, 73.
- [86] M. A. Neukamm, A. Pinto, N. Metzler-Nolte, *Chem. Commun.* **2008**, 232.
- [87] D. E. Bikiel, E. G. Solveyra, F. D. Salvo, H. M. S. Milagre, M. N. Eberlin, R. S. Correa, J. Ellena, D. A. Estrin, F. Doctorovich, *Inorg. Chem.* **2011**, 50, 2334–2345.
- [88] F. Di. Salvo, D. A. Estrin, G. Leitus, F. Doctorovich, *Organometallics*. **2008**, 27, 1985–1995.
- [89] N. Escola, A. Llebaría, G. Leitus, F. Doctorovich, *Organometallics*. **2006**, 25, 3799–3801.
- [90] F. Doctorovich, F. Di. Salvo, *Acc. Chem. Res.* **2007**, 40, 985–993.

- [91] N. Escola, F. Di. Salvo, R. Haddad, L. Perissinotti, M. N. Eberlin, F. Doctorovich, *Inorg. Chem.* **2007**, 46, 4827–4834.
- [92] L. L. Perissinotti, G. Leitus, L. Shimon, D. Estrin, F. Doctorovich, *Inorg. Chem.* **2008**, 47, 4723–4733.
- [93] L. L. Perissinotti, D. A. Estrin, G. Leitus, F. Doctorovich, *J. Am. Chem. Soc.* **2006**, 128, 2512–2513.
- [94] R. Motterlini, P. Sawle, J. Hammad, S. Bains, R. Alberto, R. Foresti, C. J. Green, *FASEB J.* **2005**, 19, 284–286.
- [95] R. A. Motterlini, R. A. Alberto, *Use of boranocarbonates for the therapeutic delivery of carbon monoxide.* **2005**, WO 2005/013691,20040804.
- [96] T. S. Pitchumony, B. Spingler, R. Motterlini, R. Alberto, *Org. Biomol. Chem.* **2010**, 8, 4849–4854.
- [97] R. Alberto, K. Ortner, N. Wheatley, R. Schibli, A. P. Schubiger, *J. Am. Chem. Soc.* **2001**, 123, 3135–3136.
- [98] D. Christodoulou, S. Kudo, J. A. Cook, M. C. Krishna, A. Miles, M. B. Grisham, R. Murugesan, P. C. Ford, D. A. Wink, *Methods Enzymol.* **1996**, 268, 69.
- [99] S. Kudo, J. L. Bourassa, S. E. Boggs, Y. Sato, P. C. Ford, *Anal. Biochem.* **1997**, 247, 193.
- [100] I. Horvath, L. E. Donnelly, A. Kiss, P. Paredi, S. A. Kharitonov, P. J. Barnes, *Thorax.* **1999**, 53, 668.
- [101] P. Paredi, W. Biernacki, G. Invernizzi, S. A. Kharitonov, P. J. Barnes, *Chest.* **1999**, 116, 1007.
- [102] A. J. Atkin, J. M. Lynam, B. E. Moulton, P. Sawle, R. Motterlini, N. M. Boyle, M. T. Pryce, I. J. S. Fairlamb, *Dalton Trans.* **2011**, 40, 5755.
- [103] R. D. Rimmer, H. Richter, P. C. Ford, *Inorg. Chem.* **2010**, 49, 1180.
- [104] S. McLean, B. E. Mann, R. K. Poole, *Anal. Biochem.* **2012**, 427, 36-40.
- [105] W. Cremer, *Biochem. Z.* **1928**, 194, 231-232.
- [106] W. Cremer, *Biochem. Z.* **1929**, 206, 228-239.
- [107] F. Ferrier, G. Terzian, J. Mossoyan, D. Benlian, *J. Mol. Struct.* **1995**, 344, 189-193.
- [108] J. Takács, E. Soós, Z. Nagy-Magos, L. Markó, G. Gervasio, T. Hoffmann, *Inorg. Chim. Acta.* **1989**, 166, 39-46.

- [109] L. Hewison, T. R. Johnson, B. E. Mann, A. J. H. M. Meijer, P. Sawle, R. Motterlini, *Dalton Trans.* **2011**, 40, 8328-8334.
- [110] W. F. Liaw, J. H. Lee, H. B. Gau, C. H. Chen, G. H. Lee, *Inorg. Chim. Acta.* **2001**, 322, 99-105.
- [111] J. V. Kingston, J. W. S. Jamieson, G. Wilkinson, *J. Inorg. Nucl. Chem.* **1967**, 29, 133-138.
- [112] D. Sellmann, U. Reineke, G. Huttner, L. Zsolnai, *J. Organomet. Chem.* **1986**, 310, 83-93.
- [113] D. Sellmann, O. K ppler, F. Knoch, *J. Organomet. Chem.* **1989**, 367, 161-174.
- [114] D. Sellmann, R. Ruf, F. Knoch, M. Moll, *Z. Naturforsch.* **1995**, 50b, 791-801.
- [115] D. Sellmann, R. Ruf, F. Knoch, M. Moll, *Inorg. Chem.* **1995**, 34, 4745-4755.
- [116] D. Sellmann, U. Reineke, *J. Organomet. Chem.* **1986**, 314, 91-103.
- [117] V. P. L. Vel squez, T. M. A. Jazzazi, A. Malassa, H. G rls, G. Gessner, S. H. Heinemann, M. Westerhausen, *Eur. J. Inorg. Chem.* **2012**, 1072-1078.
- [118] B. E. Mann, T. R. Johnson, J. E. Clark, R. Foresti, C. Green, R. Motterlini, *Angew. Chem. Int. Ed.* **2003**, 42, 3722-3729.
- [119] T. M. A. Jazzazi, H. G rls, G. Gessner, S. H. Heinemann, M. Westerhausen, *J. Organomet. Chem.* **2013**, 733, 63-70.
- [120] P. O. Lagaditis, A. A. Mikhailine, A. J. Lough, R. H. Morris, *Inorg. Chem.* **2010**, 49, 1094-1102.
- [121] C. H. Chen, Y. S. Chang, C. Y. Yang, T. N. Chen, C. M. Lee, W. F. Liaw, *Dalton Trans.* **2004**, 137-143.
- [122] J. Weidlein, U. M ller, K. Dehnicke: Schwingungsfrequenzen I: Hauptgruppenelemente, Georg Thieme: Stuttgart, **1981**.
- [123] K. Nakamoto: Infrared and Raman Spectra of Inorganic and Coordination Compounds, 4<sup>th</sup> ed., John Wiley: New York, **1986**.
- [124] J. A. S. Howell, J. Y. Saillard, A. de Beuze, G. Jaouen, *J. Chem. Soc. Dalton Trans.* **1982**, 2533-2537.
- [125] I. J. Fairlamb, J. M. Lynam, B. E. Moulton, I. E. Taylor, A. K. Duhme-Klair, P. Sawle and R. Motterlini, *Dalton Trans.* **2007**, 3603-3605.
- [126] R. Kretschmer, G. Gessner, H. G rls, S. H. Heinemann and M. Westerhausen, *J. Inorg. Biochem.* **2011**, 105, 6-9.

- [127] B. Pathak, D. Majumdar and J. Leszczynski, *Int. J. Quant. Chem.* **2009**, 109, 2263-2272.
- [128] M. Melník, J. Valentová and F. Devínsky, *Rev. Inorg. Chem.* **2011**, 31, 57-82.
- [129] H. Lang, L. Zsolnai and G. Huttner, *J. Orgmet. Chem.* **1985**, 282, 23-51.
- [130] Robert Kretschmer, Synthese von lichtinduziert Kohlenmonoxid freisetzenden Metallkomplexen. *Diplomarbeit*, Jena, **2010**.
- [131] T. M. A. Al-Shboul, H. Görls, M. Westerhausen, *Jordan Journal of Chemistry.* **2009**, 4(2), 111-118.
- [132] a) J. Donohue, A. Caron, *Acta Cryst.* **1964**, 17, 663-667. b) W. F. Edgell, M. P. Dunkle, *The Journal of Physical Chemistry.* **1964**, 68, 452-456.
- [133] W. Imhof and D. Berger, *Acta Cryst.* **2006**, 62, 1376-1377.
- [134] P. E. Riley and R. E. Davis, *Inorg. Chem.* **1980**, 19, 159-165.
- [136] S. A. E. Sequoia, *J. Orgmet. Chem.* **1983**, 243, 331-337.
- [137] K. R. Seipel, Z. H. Platt, M. Nguyen, A. W. Holland, *J. Org. Chem.* **2008**, 73, 4291-4294.
- [138] J. B. P. Tripathi, M. Bigorgne, *J. Organomet. Chem.* **1967**, 9, 307.
- [139] T. J. Clark, J. M. Rodezno, S. B. Clendenning, S. Aouba, P. M. Brodersen, A. J. Lough, H. E. Ruda, I. Manners, *Chem. Eur. J.* **2005**, 11, 4526-4534.
- [140] R. B. King, P. M. Sundaram, *J. Org. Chem.* **1984**, 49, 1784.
- [141] J. T. Lin, Y. C. Chou, Y. E. Shih, F. E. Hong, Y. S. Wen, S. C. Lin, M. M. Chen, *J. Chem. Soc., Chem. Commun.* **1995**, 1791-1798.
- [142] A. J. Atkin, J. M. Lynam, B. E. Moulton, P. Sawle, R. Motterlini, N. M. Boyle, M. T. Pryce, I. J. S. Fairlamb, *Dalton Trans.* **2011**, 40, 5755-5761
- [143] COLLECT, Data Collection Software; Nonius B.V., Netherlands, **1998**.
- [144] Processing of X-Ray Diffraction Data Collected in Oscillation Mode: Z. Otwinowski, W. Minor, in C. W. Carter, R. M. Sweet (eds.): *Methods in Enzymology, Vol. 276, Macromolecular Crystallography, Part A*, pp. 307-326, Academic Press, New York **1997**.
- [145] G. M. Sheldrick, *Acta Cryst.* **2008**, A64, 112-122.

**Table 1:** Crystal data and refinement details for the X-ray structure determinations of the compounds **1** (CORM-S1), **2** (CORM-S2), **3**, and **4**.

Compound	<b>1</b> (CORM-S1)	<b>2</b> (CORM-S2)	<b>3</b>	<b>4</b>
Formula	C <sub>6</sub> H <sub>12</sub> FeN <sub>2</sub> O <sub>2</sub> S <sub>2</sub> , C <sub>4</sub> H <sub>8</sub> O	C <sub>14</sub> H <sub>12</sub> FeN <sub>2</sub> O <sub>2</sub> S <sub>2</sub> , C <sub>4</sub> H <sub>8</sub> O	C <sub>6</sub> H <sub>8</sub> N <sub>2</sub> O <sub>2</sub> RuS <sub>2</sub> , C <sub>4</sub> H <sub>8</sub> O	C <sub>14</sub> H <sub>12</sub> N <sub>2</sub> O <sub>2</sub> Ru S <sub>2</sub> , 2 C <sub>3</sub> H <sub>7</sub> NO
fw (g·mol <sup>-1</sup> )	336.25	432.33	377.44	551.64
<i>T</i> /K	-140(2)	-140(2)	-140(2)	-140(2)
crystal system	monoclinic	triclinic	monoclinic	monoclinic
space group	P 2 <sub>1</sub> /n	<i>P</i> 1̄	P 2 <sub>1</sub> /n	P 2 <sub>1</sub> /n
<i>a</i> /Å	16.3227(3)	5.6236(1)	16.5181(6)	5.6470(1)
<i>b</i> /Å	9.7721(2)	8.8547(2)	9.7343(3)	20.4208(3)
<i>c</i> /Å	20.0057(4)	10.5982(2)	20.1750(8)	22.3020(3)
<i>α</i> /°	90	106.325(1)	90	90
<i>β</i> /°	111.759(1)	103.221(1)	111.248(2)	90.743(2)
<i>γ</i> /°	90	94.462(1)	90	90
<i>V</i> /Å <sup>3</sup>	2963.69(10)	487.304(17)	3023.46(19)	2571.57(7)
<i>Z</i>	8	1	8	4
<i>ρ</i> (g·cm <sup>-3</sup> )	1.507	1.473	1.658	1.519
<i>μ</i> (mm <sup>-1</sup> )	13.01	10.08	13.14	8.09
measured data	17902	12952	17299	13093
data with <i>I</i> > 2σ( <i>I</i> )	5868	4148	5362	5004
unique data ( <i>R</i> <sub>int</sub> )	6762/0.0338	4232/0.0453	6854/0.0588	5584/0.0256
w <i>R</i> <sub>2</sub> (all data, on <i>F</i> <sup>2</sup> ) <sup>a)</sup>	0.0888	0.0598	0.1172	0.1342
<i>R</i> <sub>1</sub> ( <i>I</i> > 2σ( <i>I</i> )) <sup>a)</sup>	0.0404	0.0238	0.0559	0.0615
<i>s</i> <sup>b)</sup>	1.185	1.050	1.117	1.301
res. dens./e·Å <sup>-3</sup>	0.466/-0.505	0.297/-0.333	0.956/-0.639	1.761/-0.629
CCDC No.	848989	848990	848991	848992

<sup>a)</sup> Definition of the *R* indices:  $R_1 = (\sum ||F_o| - F_c||) / \sum F_o$ ;

$wR_2 = \{\sum[w(F_o^2 - F_c^2)^2] / \sum[w(F_o^2)^2]\}^{1/2}$  with  $w^{-1} = s^2(F_o^2) + (aP)^2 + bP$ ;  $P = [2F_c^2 + \max(F_o^2)]/3$ ;

<sup>b)</sup>  $s = \{\sum[w(F_o^2 - F_c^2)^2] / (N_o - N_p)\}^{1/2}$ .

**Table 2:** Crystal data and refinement details for the X-ray structure determinations of the compounds **6**, **7** (CORM-P1), and **8** (CORM-P2).

Compound	<b>6</b>	<b>7</b> (CORM-P1)	<b>8</b> (CORM-P2)
formula	[C <sub>40</sub> H <sub>36</sub> FeN <sub>4</sub> P <sub>2</sub> ] <sup>2+</sup> , 2[BF <sub>4</sub> ], 2(C <sub>2</sub> H <sub>3</sub> N)	[C <sub>31</sub> H <sub>35</sub> FeN <sub>3</sub> OP <sub>2</sub> ] <sup>2+</sup> , 2[BF <sub>4</sub> ]	[C <sub>39</sub> H <sub>35</sub> FeN <sub>3</sub> OP <sub>2</sub> ] <sup>2+</sup> , 2[BF <sub>4</sub> ], CH <sub>2</sub> Cl <sub>2</sub>
fw (g·mol <sup>-1</sup> )	948.26	757.03	938.04
T/°C	-140(2)	-140(2)	-140(2)
crystal system	triclinic	triclinic	monoclinic
space group	<i>P</i> $\bar{1}$	<i>P</i> $\bar{1}$	<i>P</i> 2 <sub>1</sub> / <i>n</i>
<i>a</i> /Å	11.3798(2)	9.8383(1)	13.4610(3)
<i>b</i> /Å	12.4188(2)	11.7972(3)	23.0816(4)
<i>c</i> /Å	17.8206(3)	14.4190(3)	13.5722(3)
<i>α</i> /°	74.966(1)	98.138(1)	90
<i>β</i> /°	85.178(1)	92.800(1)	100.427(1)
<i>γ</i> /°	68.964(1)	95.042(1)	90
<i>V</i> /Å <sup>3</sup>	2270.05(7)	1647.08(6)	4147.26(15)
<i>Z</i>	2	2	4
<i>ρ</i> (g·cm <sup>-3</sup> )	1.387	1.526	1.502
<i>μ</i> (cm <sup>-1</sup> )	4.75	6.32	6.43
measured data	14722	9907	23878
data with <i>I</i> > 2σ( <i>I</i> )	9507	6869	7781
unique data ( <i>R</i> <sub>int</sub> )	10305/0.0197	7443/0.0151	9451/0.0390
<i>wR</i> <sub>2</sub> (all data, on <i>F</i> <sup>2</sup> ) <sup>a)</sup>	0.0986	0.0828	0.1347
<i>R</i> <sub>1</sub> ( <i>I</i> > 2σ( <i>I</i> )) <sup>a)</sup>	0.0390	0.0380	0.0547
<i>s</i> <sup>b)</sup>	1.057	1.070	1.054
Res. dens./e·Å <sup>-3</sup>	0.589/-0.469	0.822/-0.441	0.843/-0.979
CCDC No.	905061	905062	905063

<sup>a)</sup> Definition of the *R* indices:  $R_1 = (\sum ||F_o| - F_c||) / \sum F_o$ ;

$wR_2 = \{\sum [w(F_o^2 - F_c^2)^2] / \sum [w(F_o^2)^2]\}^{1/2}$  with  $w^{-1} = \sigma^2(F_o^2) + (aP)^2 + bP$ ;  $P = [2F_c^2 + \text{Max}(F_o^2)]/3$ ;

<sup>b)</sup>  $s = \{\sum [w(F_o^2 - F_c^2)^2] / (N_o - N_p)\}^{1/2}$ .

**Table 3:** Crystal data and refinement details for the X-ray structure determinations of the compound **12** (CORM-P6).

Compound	<b>12 (CORM-P6)</b>
formula	C <sub>6</sub> Cl <sub>4</sub> Fe <sub>2</sub> O <sub>6</sub> P <sub>2</sub>
fw (g·mol <sup>-1</sup> )	483.50
T/°C	-140(2)
crystal system	trilinic
space group	<i>P</i> $\bar{1}$
<i>a</i> /Å	7.8114(2)
<i>b</i> /Å	8.2118(2)
<i>c</i> /Å	12.5477(3)
$\alpha$ /°	83.767(1)
$\beta$ /°	81.531(1)
$\gamma$ /°	69.899(1)
<i>V</i> /Å <sup>3</sup>	746.16(3)
<i>Z</i>	2
$\rho$ (g·cm <sup>-3</sup> )	2.152
$\mu$ (cm <sup>-1</sup> )	28.88
measured data	4564
parameters	181
data with $I > 2\sigma(I)$	3490
unique data / $R_{int}$	3384/0.0171
$wR_2$ (all data, on $F^2$ ) <sup>a)</sup>	0.0641
$R_1$ ( $I > 2\sigma(I)$ ) <sup>a)</sup>	0.0258
$s$ <sup>b)</sup>	1.060
Res. dens./e·Å <sup>-3</sup>	0.916/-0.429

<sup>a)</sup> Definition of the *R* indices:  $R_1 = (\sum || F_o | - | F_c ||) / \sum | F_o |$ ;

$wR_2 = \{\sum [w(F_o^2 - F_c^2)^2] / \sum [w(F_o^2)^2]\}^{1/2}$  with  $w^{-1} = \sigma^2(F_o^2) + (aP)^2 + bP$ ;  $P = [2F_c^2 + \text{Max}(F_o^2)]/3$ ;

<sup>b)</sup>  $s = \{\sum [w(F_o^2 - F_c^2)^2] / (N_o - N_p)\}^{1/2}$ .

## ACKNOWLEDGEMENTS

First of all, I would like to express my thanks, obedience, and gratitude to Allah the great from whom I receive guidance and help.

It is difficult to overstate my gratitude to my supervisor, **Prof. Dr. Matthias Westerhausen**. With his enthusiasm, his inspiration, and his great efforts to explain things clearly and simply, he helped to make chemistry fun for me. Throughout my thesis-writing period, he provided encouragement, sound advice, good teaching, good company, and lots of good ideas. I would have been lost without him.

I wish to extend my appreciation to my second referee **Prof. Dr. Beckert** and to all members of my committee, also for the staff of the Institut für Anorganische und Analytische Chemie, Friedrich-Schiller-Universität Jena.

I offer my regards and blessings to all of those who supported me in any respect during the completion of the thesis, Dr. Guido Gessner and Dr. Helmar Görls.

I thank all technical assistants of the Institut für Anorganische und Analytische Chemie (**IAAC**), namely IR, NMR, MS, EA and X-Ray for analyses of the samples.

The staff of **IAAC** took care for the daily workflow, such as mail orders, the dispense of chemicals and glassware, dealing with applications, reparations, waste disposal, a welcome atmosphere and much more. Thus, I want to thank Heike Müller, Sarah Jamski, Christine Agthe, Martina Gase, Veronika Lenzner, Karin Landrock, Renate Grunert, Jens Rückoldt, Alexander Müller and Gerhard Wilke. For all additional support I wish to express my gratitude to the groups of Prof. Weigand, Prof. Imhof, Prof. Schiller, Prof. Robl, and Prof. Plass.

I am indebted to my many colleagues for providing a stimulating and pleasant environment for learning and growing. I am especially grateful to Fadi Younis, Silvio Preußner, Vaneza Lorret, Claas Loh, Dr. Martin Schulz, Dr. Tobias Kloubert, Maurice Klopffleisch, Dr. Dirk Olbert, Gritt Volland, Dr. Marcel Kahnes, Dr. Christian Koch, Dr.



Astrid Malassa, Dr. Carsten Glock, Katja Wimmer, Dr. Jens Langer, Dr. Sven Kriek and Dr. Heike Schreer.

I wish to thank the Carl Zeiss Foundation/Stuttgart (Germany) for financially supporting me with a Ph.D. grant. I also gratefully acknowledge the German Research Foundation (DFG, Bonn-Bad Godesberg/Germany) for generous financial support within the collaborative research group FOR 1738.

Also I wish to thank Yarmouk University/Jordan, which I will go back to it as assistant Professor after I get my PhD degree.

I wish to thank my entire extended family for providing a loving environment for me. My brother, my sisters for their encouragement and love through my life and for everything.

Lastly, and most importantly, I wish to thank my beloved husband Tareq, who always supported me during the completion of the thesis, and my parents. They bore me, raised me, supported me, taught me, and loved me. To them I dedicate this thesis with proud.

## **Declaration of Originality**

I certify that the work presented here is, to the best of my knowledge and belief, original and the result of my own investigations, except as acknowledged, and has not been submitted, either in part or whole, for a degree at this or any other university.

Ich erkläre, dass ich die vorliegende Arbeit selbstständig und nur unter Verwendung der angegebenen Hilfsmittel, persönlichen Mitteilungen und Quellen angefertigt habe und dass ich nicht die gleiche, eine in wesentlichen Teilen ähnliche oder eine andere Abhandlung bei einer anderen Hochschule als Dissertation eingereicht habe.

Taghreed Jazzazi

Jena, den 26.04.2013

# Curriculum Vitae

## **Taghreed Marwan Ali Jazzazi** **Bio-inorganic Chemistry**

**Tel:** +49 -176-64125857

**E-mail:** tjazazi85@gmail.com

---

### Personal:

**Place & date of birth:** - Amman, Jordan, 16<sup>th</sup> of July 1985

**Marital status:** - Married

**Gender:** - Female

**Nationality:** - Jordanian

### Educational history: -

- Sep/2009-2013 PhD student at Friedrich-Schiller-Universität Jena under supervisor Prof. Dr. Matthias Westerhausen
- 2007-2009 Jordan University of Science and Technology  
M.Sc., Applied Chemistry, GPA: 80.0% (Very good)  
date of graduation: August 2009.
- 2003- 2007 Tafila Technical University  
B.Sc., Applied Chemistry, GPA: 82.37% (V. Good).
- 2003 Gandaweel Secondary School, General secondary  
Education Certificate, Jordan, percentage average 72.9%

### M.Sc research: -

Synthesis and Characterization of Cyclopentadienyl  
Ruthenium Thiocarboxylate Complexes

### Experience: -

- *Research assistant and teaching assistance*, Jordan University of  
Science and Technology → (2007- August/2009).

**Scholarships:-**

- Teaching and research assistant (FSU University 1/09/2009- 30/05/2010)
- Carl-Zeis Scholarship (1/06/2010-30/05/2013)

**Languages: -**

- Arabic: native language.
- English: very good command of both spoken and written.
- German: good

**Additional information: -**

- teaching assistant/I have taught: -

*General chemistry Lab (Chem. 107)*

*Organic chemistry Lab (Chem. 213)*

*Organic chemistry lab (chem.218)*

Taghreed Jazzazi

Jena, den 26.04.2013

## List of publications

- 1- Mohammad El-khateeb, **Taghreed M. A. Jazzazi**, Helmar Görls, Tareq M. A. Al-Shboul, Matthias Westerhausen. Synthesis and Characterization of Ruthenium heterocyclic-thiocarboxylate complexes. *Trans. Met. Chem.* (2011), 36, 29-33.
- 2- Vaneza P. Lorett Velasquez, **Taghreed M. A. Jazzazi**, Malassa, Astrid; Goerls, Helmar; Gessner, Guido; Heinemann, Stefan H.; Westerhausen, Matthias. Derivatives of Photosensitive CORM-S1 - CO Complexes of Iron and Ruthenium with the  $(OC)_2M(SCH_2CH_2NH_2)_2$  Fragment. *Eur. J. Inorg. Chem.* (2012), 7, 1072-1078.
- 3- **Taghreed M. A. Jazzazi**, Helmar Görls, Guido Gessner, Stefan H. Heinemann, M. Westerhausen. Photosensitive iron(II)-based CO releasing molecules (CORMs) with vicinal amino and diphenylphosphino substituted chelating ligands. *J. Organomet. Chem.* (2013), 733, 63-70.

## List of Oral presentation and Posters

- 1- Sixth Jordanian International Conference of Chemistry, *April-2011 (Poster)*.
- 2- Proposal meeting of the DFG research unit FOR 1738, *September-2011 (Poster)*.
- 3- Kick-off meeting of the P7 and P8 in the DFG research unit FOR 1738, *April-2012 (Oral presentation)*.
- 4- Symposium of Hem and Haemoglobin Degradation Products (HHDP), *May-2012 (Oral presentation)*.
- 5- Conference of MANS-10, *September-2012 (Oral presentation)*.
- 6- Symposium of Hem and Haemoglobin Degradation Products (HHDP), *May-2013 (Oral presentation)*.